

Zeolite encapsulated metal complexes as heterogeneous catalysts for oxidation reactions

By

Gavin Von Willingh

M.Sc. thesis submitted in fulfilment of the requirements for the degree of

Magister Scientiae,

In the Department of Chemistry, Catalysis Group,

University of Western Cape

UNIVERSITY *of the*
WESTERN CAPE

Supervisor: Dr. Salam Titinchi

Department of Chemistry

DECLARATION

I declare that the “Zeolite encapsulated metal complexes as heterogeneous catalysts for oxidation reactions”, is my own work, that it has not been submitted for any degree or examination in any other University and that all sources I have used or quoted have been indicated and acknowledged by complete references.

Full name ...**Gavin Von Willingh** Date

Signed



Copyright © University of Western Cape
All right reserved

ABSTRACT

This study describes the synthesis and characterisation of Cu(II) and V(IV) complexes of tri- and quadridentate ligands L1 and L2 formed by condensation of ethylenediamine with acetylacetonate in 1:1 and 1:2 molar ratio, respectively. Encapsulation of these metal complexes in the nanocage of zeolite-Y generates new heterogeneous catalysts. These catalysts were synthesized employing the flexible ligand method encapsulation technique. The structures of these encapsulated complexes were established on the basis of various physico-chemical and spectroscopic studies. The results indicated that the complexes did not hinder or modify the framework or structure of the zeolite, confirming successful immobilization of Schiff-bases through the voids of zeolite Y.

These encapsulated complexes were screened as heterogeneous catalysts for various oxidation reactions such as phenol, benzene, styrene and cyclohexene using a green oxidant (H_2O_2).

For comparison, the corresponding neat complexes were screened as potential homogeneous catalysts for these oxidation reactions. The results proved that the corresponding homogeneous systems described here represent an efficient and inexpensive method for oxidation of phenol, benzene, styrene and cyclohexene, having advantages over heterogeneous catalysis are its high activity and selectivity and short reaction times. Its major problem is its industrial application regarding principally the separation of the catalyst from the products.

The size of the substrate has a significant effect on the conversion by encapsulated complexes such as in styrene oxidation. Therefore, it was established that steric effects of the substrates play a critical role in the poor reactive nature of the encapsulated complexes. In general, the percentage conversion decreased upon encapsulation of complexes in zeolite Y. All catalysts studied proved to be potential catalysts for the various oxidation reactions.

It has been shown in this study that encapsulation can effectively improve product selectivity but requires a longer reaction time in most cases for maximum activity. Furthermore, oxovanadium complexes were more reactive than copper-based catalysts in all oxidation reactions tested in this study.

A reaction mechanism study revealed that the activity of the encapsulated and neat complexes occurs through either formation of peroxovanadium (V) or hydroperoxide-copper(II) intermediate species.

The studies in this thesis, therefore, conclude that the Cu(II) and V(IV) complexes encapsulated in Y-zeolite are active heterogeneous catalysts for the selective oxidation of various substrates. Encapsulation of the metal complexes in the super cages (α -cages) of the zeolite matrix has the advantages of solid heterogeneous catalysts of easy separation and handling, ruggedness, thermostability, reusability (regeneration of the deactivated catalysts) as well as share many advantageous features of homogeneous catalysts.



ACKNOWLEDGMENTS

First off all, I would like to thank God for giving me the strength and courage through all my years of studying through good and bad times.

Thank you very much to my supervisor Dr. Salam Titinchi for guiding me through this process of understanding zeolite encapsulated metal complexes and their applications in catalysis. Thank you also for your patience and friendliness.

I particularly thank Dr. H Abbo for scientific discussions, practical assistance on the electronic spectroscopy analysis and for her support in the final stages of this thesis.

I would also like to thank my parents for standing by me through all these years of my studies and for their support. Mom and dad, I really appreciate for what you have done to me and I can't think of a better mom and dad than you.

To all the teachers from Rocklands senior secondary school from 1999 to 2003, thank you for your advice and giving me a proper education. I especially would like to thank my science teacher in 2000 Mr. A. Adams, for his advice. I would also like to thank my matric class from 2003 for being so awesome to me.

A special thanks to Prof. E. Iwuoha and National Research Foundation for financial assistance.

Thank you Mr.T Lesch for always assisting me with the gas chromatography.

To my colleagues from the University of the Western Cape, thank you for the good times we shared together. Lastly, I would like to thank the Chemistry staff of UWC for helping me in doing research and for their expertise.

Dedicated to my mother Brenda and my father, Norman

Poster Presentations at Conference

1. Post graduate research open day, New Life Science Building, University of Western Cape, Bellville, Cape Town, South Africa, November 2011.
2. SACI Young Chemist Symposium, New Life Science Building, University of Western, Cape, Bellville, Cape Town, South Africa, 24 November 2011.
3. Post graduate research open day, New Life Science Building, University of Western Cape, Bellville, Cape Town, South Africa, 31 October 2012.



Table of Contents

Glossary	v
List of Figures	vi
List of Scheme	viii
List of Tables	ix
CHAPTER 1	1
1. INTRODUCTION AND OBJECTIVES	1
1.1 Introduction	1
1.2 Objectives	3
1.3 Thesis Outline	4
References	5
CHAPTER 2	8
2. LITERATURE REVIEW	8
2.1 Introduction	8
2.2 Concept of heterogenization of homogeneous catalysts	8
2.3 Methodologies for heterogenization of homogeneous catalysts	9
2.3.1 Liquid-liquid two-phase system	9
2.3.2 Supported liquid-phase catalysis	9
2.3.3 Fixation on/in solid supports	10
2.3.3.1 Covalent bonding	10
2.3.3.2 Non-covalent interactions	11
2.3.3.3 Encapsulation/entrapment	13
2.3.3.3.1 Entrapment in sol-gel	13
2.3.3.3.2 Ship-in-the-bottle	15
2.3.3.3.3 Entrapment in silicate layers	17
2.4 Types of support used in heterogenization of homogeneous catalysts	18
2.4.1 Inorganic Supports	18
2.5 Zeolites as supports for immobilization of homogeneous catalysts	20
2.5.1 Structure	20
2.5.2 Supported materials in catalysis	21



2.6	Encapsulation strategies	23
2.6.1	Flexible Ligand method	23
2.6.2	Zeolite synthesis method	24
2.6.3	Template (Ship-in-the-bottle) synthesis method	24
2.6.4	Adsorption method	24
2.6.5	Ion-exchange strategy	24
2.7	Schiff-bases and their complexes	25
2.7.1	General Overview	25
	References	27

CHAPTER 3 44

3.	EXPERIMENTAL	44
3.1	Materials	44
3.2	Synthesis of Schiff-base ligands (L1 – L2)	44
3.2.1	7-Amino-5-aza-4-methyl-hept-3-en-one, L1	44
3.2.1	Bis(acetylaceton-ethylene) diamine, L2	44
3.3	Synthesis of Cu(II) and VO(IV) complexes	45
3.3.1	Preparation of Cu(II) complexes (1 – 2)	45
3.3.1.1	Cu(L1)Cl, (1)	45
3.3.1.2	Cu(L2), (2)	45
3.3.2	Preparation of VO(IV) complexes (5 - 6)	45
3.4	Preparation of Zeolite Encapsulated Cu(II) and VO(IV) complexes	47
3.4.1	Preparation of Metal Exchanged Zeolite, M-Y (M = Cu(II) or VO(IV))	47
3.4.2	Synthesis of Zeolite-Y Encapsulated Metal Complexes	47
3.5	Analytical techniques and instruments used	49
3.5.1	Nuclear Magnetic Resonance (NMR) spectroscopy	49
3.5.2	Fourier - Transform Infrared (FT-IR) spectroscopy	49
3.5.3	Inductively Coupled Plasma–Optical Emission Spectrometry (ICP – OES)	49
3.5.4	Scanning Electron Microscopy (SEM)	50
3.5.5	Ultraviolet-visible spectroscopy (UV-Vis)	50
3.5.6	Gas Chromatography (GC)	50
3.5.7	X-ray powder diffraction (XRPD)	51

3.5.8 BET Analysis	51
References	52

CHAPTER 4 53

4. Characterization 53

4.1. Characterization of ligands 53

4.1.1. ^1H and ^{13}C NMR spectroscopic studies of Schiff-base ligands 53

4.1.2. FT-IR spectroscopic studies of Schiff-base ligands 59

4.1.3. UV/Vis spectroscopic of Schiff-base ligands 59

4.2. Characterization of Cu(II) complexes 60

4.2.1 FT-IR spectroscopy 60

4.2.2 UV/Vis spectroscopy 63

4.3. Characterization of VO(IV) complexes 64

4.3.1. FT-IR spectroscopy 64

4.3.2. UV/Vis spectroscopy 67

4.4. X- Ray Powder diffraction of Cu (II) and VO(IV) encapsulated complexes 70

4.5. Scanning electron microscopy of Cu(II) and OV(VI) encapsulated complexes 72

4.6. Surface textural studies of Cu(II) and OV(VI) encapsulated complexes 72

4.7. Possible reaction pathway of catalysts 75

4.7.1. Cu(II) system 75

4.7.2. VO(IV) systems 78

References 81

CHAPTER 5 85

5. Catalytic activity studies of Cu(II) catalysts for oxidation reactions 85

5.1. Introduction 85

5.2. Oxidation reactions 86

5.2.1. Hydroxylation of phenol 86

5.2.1.1 Effect of H_2O_2 /phenol molar ratio 87

5.2.1.2 Effect of reaction temperature 88

5.2.1.3 Effect of solvents 89

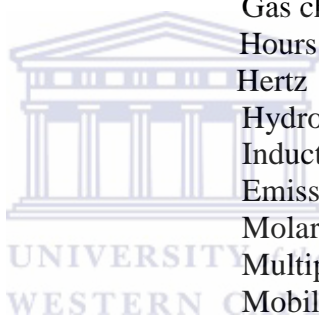
5.2.1.4 Effect of volume of solvent	91
5.2.1.5 Effect of amount of catalyst	93
5.2.1.6 Comparison studies of different copper catalysts	94
5.2.2. Hydroxylation of benzene	96
5.2.3. Oxidation of styrene	98
5.2.4. Oxidation of cyclohexene	101
References	105
CHAPTER 6	110
6. Catalytic activity studies of OV(IV) catalysts for oxidation reactions	110
6.1 Hydroxylation of phenol	110
6.2 Hydroxylation of benzene	112
6.3 Oxidation of styrene	114
6.4 Oxidation of cyclohexene	116
References	118
CHAPTER 7	120
7. Conclusion and recommendations	120
7.1 Conclusion	120
7.2 Future work and recommendations	121



Glossary

Abbreviations

Å	Angstrom
Acac	Acetylacetone
Bal	Benzaldehyde
CAT	Catechol
CDCl ₃	Deuterated chloroform
CyO	Cyclohexene oxide
CyOl	Cyclohex-2-ene-1-ol
CyONE	Cyclohex-2-ene-1-one
CydiOl	Cyclohexane-1,2-diol
d	Doublet
DCM	Dichloromethane
EtOH	Ethanol
FT-IR	Fourier transform infrared spectroscopy
g	Gram
GC	Gas chromatography
h	Hours
Hz	Hertz
HQ	Hydroquinone
ICP-OES	Inductive coupled plasma optical Emission spectroscopy
M	Molar
m	Multiplet
MCM-41	Mobile crystalline material
MeCN	Acetonitrile
ml	Millilitres
nm	Nanometre
NMR	Nuclear magnetic resonance
PhOH	Phenol
ppm	Parts per million
SEM	Scanning electron microscope
Sto	Styrene oxide
s	Singlet
sh	Shoulder
Sto	Styrene oxide
str	Strong
%T	Percentage transmission
t	Triplet
UV/Vis	Ultraviolet-visible spectroscopy
w	Weak
% wt	Weight percentage of metal
XRPD	X - Ray powder diffraction
ZEMC	Zeolite encapsulated metal complexes
°C	Degrees celcius
v	Vibrational frequency



List of Figures

CHAPTER 2

Figure 2.1 Manganese Schiff-base complex physically entrapped in zeolite-Y	15
Figure 2.2 A model structure of intercalated catalysts (i) the catalyst is located between sheets of clay or between interlayer spaces of (ii) Mg/Al layered double hydroxide	18
Figure 2.3 Illustrating immobilization of catalysts on various mesoporous silica supports, MCM-41, SBA-15 and FSM-16	20
Figure 2. 4 (a) Different types of zeolites (b) various units Faujasite zeolite	22
Figure 2.5 A schematic model for illustrating how the pores of zeolites controls shape selectivity	23
Figure 2.6 Examples of different types of Schiff-base ligands with its characteristic C=N group	27

CHAPTER 4

Figure 4.1 ^1H NMR of 7-amino-5-aza-4-methyl-hept-3-en-one, L1	56
Figure 4.2 ^{13}C NMR spectra of 7-amino-5-aza-4-methyl-hept-3-en-one, L1	57
Figure 4.3 ^1H NMR data of bis(acetylacetonate ethylene diamine), L2	58
Figure 4.4 ^{13}C NMR spectra of bis(acetylacetonate ethylene diamine), L2	59
Figure 4.5 Electronic spectra in methanol of (a) L1 and (b) L2	60
Figure 4.6 FT-IR spectra of L1, Cu(L1)Cl, L2 and Cu(L2)	62
Figure 4.7 FT-IR spectra of L1, Cu(L1)Cl and Cu(L2)	62
Figure 4.8 FT-IR spectra of H-Y, Cu-exchanged zeolite and their zeolite encapsulated metal complexes	63
Figure 4.9 Electronic spectra of (a) Cu(L1)Cl and (b) Cu(L2)	64
Figure 4.10 Electronic spectra of (a) Cu(L1)Cl-Y and (b) Cu(L2)-Y	65
Figure 4.11 FT-IR spectra of VO(L1)(acac)-Y, VO(L2)-Y and their parent compound in the range $380 - 1800 \text{ cm}^{-1}$	67
Figure 4.12 Electronic spectra: UV (top) and vis. region (bottom) of (a) VO(L1)(acac) and (b) VO(L2)	69
Figure 4.13 Electronic spectra: UV (top) and vis. region (bottom) of VO(L1)(acac)-Y and VO(L2)-Y	70
Figure 4.14 XRD patterns of (a) H-Y, (b) Cu-H-Y, (c) Cu(L2)-Y and (d) Cu(L1)(Cl)-Y	72

Figure 4.15 XRD of (a) H-Y, (b) VO-H-Y, (c) VO(L2)-Y and (d) VO(L1)(acac)-Y	72
Figure 4.16 Scanning electron micrograph of Cu-Y (left) and Cu(L2)-Y (right)	73
Figure 4.17 N ₂ adsorption/desorption isotherms of Cu-H-Y, Cu(L1)Cl-Y and Cu(L2)-Y	74
Figure 4.18 N ₂ adsorption/desorption isotherms VO-H-Y, VO(L1)(acac)-Y and VO(L2)-Y	74
Figure 4.19 Pore size distribution of VO-H-Y, VO(L1)(acac)-Y and VO(L2)-Y	75
Figure 4.20 Kinetic studies of Cu(L1)Cl in (a) UV and (b) visible region	77
Figure 4.21 Kinetic studies of Cu(L2) in (a) UV and (b) visible region	78
Figure 4.22 Kinetic studies of VO(L1)(acac) in (a) UV and (b) visible	80
Figure 4.23 Kinetic studies of VO(L2) in (a) UV and (b) visible region	81
 CHAPTER 5	
Figure 5.1 % Phenol conversion using different H ₂ O ₂ /PhOH molar ratios	88
Figure 5.2 Effect of reaction temperature on % phenol conversion over time	90
Figure 5.3 Effect of different solvents on the % phenol conversion over time	91
Figure 5.4 Catalytic performance under different volumes of solvent for phenol oxidation	93
Figure 5.5 % Phenol conversion with increasing the amount of catalyst	94
Figure 5.6 % Phenol conversion for catalysts over time	96
Figure 5.7 Benzene conversion for catalysts over time.	98
Figure 5.8 Styrene conversion for catalysts over time	100
Figure 5.9 Cyclohexene conversion for catalysts over time	104
 CHAPTER 6	
Figure 6.1 % Phenol conversion for catalysts over time	112
Figure 6.2 % Benzene conversion for catalysts over time	114
Figure 6.3 Styrene conversion for catalysts over time	116
Figure 6.4 Cyclohexene conversion for catalysts over time	118

List of Schemes

CHAPTER 2

Scheme 2.1 Rhodium complex covalently anchored to mesoporous silica, SBA-15	11
Scheme 2.2 Schematic illustration of electrostatic immobilisation of a copper(I)pybox catalyst on silica	12
Scheme 2.3 Illustrating cyclodextrins immobilized proline catalysts via hydrophobic interactions	12
Scheme 2.4 The condensation steps in non-aqueous sol-gel process, alkyl halide elimination (Eq.1), ether elimination (Eq.2), ester elimination (Eq.3), and aldol-like condensation (Eq.4)	14
Scheme 2.5 Illustrating the hydrolysis (Eq.1) and condensation (Eq. 2 and 3) steps in aqueous sol-gel process	14
Scheme 2.6 The pathway of intrazeolitic complexes when the complex size is smaller than zeolite pores leading to the complex leaching out of the zeolite	16
Scheme 2.7 Methods for encapsulating metal complexes within zeolites: Ion exchange (A), flexible ligand (B), ligand adsorption (C), 'ship in a bottle' (D) and zeolite synthesis methods (E)	23

CHAPTER 3

Scheme 3.1 Structures of Ligands and Cu(II) and OV(IV) complexes.	46
Scheme 3.2 A schematic description for the synthesis of neat and encapsulated copper(II) and oxovanadium(IV) complexes	48

CHAPTER 5

Scheme 5.1 Oxidized products for the hydroxylation of phenol	86
Scheme 5.2 Oxidized products for the oxidation of benzene	96
Scheme 5.3 The oxidized products for the oxidation of styrene	99
Scheme 5.4 Mechanism for the formation of benzaldehyde from styrene oxide	100
Scheme 5.5 The oxidized products for the oxidation of cyclohexene	102

List of Tables

CHAPTER 4

Table 4.1 ¹ H NMR data of 7-amino-5-aza-4-methyl-hept-3-en-one, L1	55
Table 4.2 ¹³ C NMR data of 7-amino-5-aza-4-methyl-hept-3-en-one, L1	56
Table 4.3 ¹ H NMR data of bis(acetylacetonate ethylene diamine), L2	57
Table 4.4 ¹³ C NMR data of bis(acetylacetonate ethylene diamine), L2	58
Table 4.5 FT-IR vibrations of the ligands and Cu(II) complexes	60
Table 4.6 Electronic spectral data of the ligands (L1-L2) and Cu(II) complexes.	64
Table 4.7 FT-IR vibrations of the ligands and VO(IV) complexes	65
Table 4.8 Electronic spectral data of ligands and VO(VI) complexes	70
Table 4.9 Physical, analytical data and surface area and pore volume data for the catalysts	74

CHAPTER 5

Table 5.1 Effect of H ₂ O ₂ /PhOH molar ratio on phenol hydroxylation and product selectivity	88
Table 5.2 Effect of reaction temperature on phenol conversion and product selectivity	89
Table 5.3 Effect of solvents on phenol hydroxylation, and product selectivity	91
Table 5.4 Effect of volume of solvent on phenol conversion and product selectivity	92
Table 5.5 Effect of amount of catalyst on % phenol conversion and selectivity	94
Table 5.6 % phenol conversion and product selectivity	96
Table 5.7 % Benzene conversion and product selectivity	97
Table 5.8 The styrene conversion and product selectivity	101
Table 5.9 The cyclohexene conversion and product selectivity	104

CHAPTER 6

Table 6.1 % phenol conversion and product selectivity	112
Table 6.2 The % benzene conversion and product selectivity	113
Table 6.3 % Styrene conversion and product selectivity	115
Table 6.4 Cyclohexene conversion and product selectivity	117

CHAPTER 1

1. INTRODUCTION AND OBJECTIVES

1.1 Introduction

Over the years many researchers have devoted intensive attention to the studies of various reactions and different catalytic complexes, especially transition metals or complexes encapsulated inside a solid matrix such as mesoporous materials and zeolites [1, 2].

The attractiveness of encapsulating metal complexes in nanoporous materials such as zeolite-Y and MCM-41 are important for the petroleum industry because they are good heterogeneous and redox catalysts and are also used for the production of chemicals for various types of shape selective conversion and separation reactions [3]. The advantages of using these materials are that they are cheaper, more efficient and more environment friendly for carrying out chemical reactions.

These materials have recently attracted considerable attention as they have a wide variety of applications because of their potential use in shape or size-selective catalysis [4], photo [5, 6] and/ or electrocatalysis [7] and electroanalysis [8 - 10]. The main focus of transition metal complexes encapsulated in molecular sieves with aluminosilicate frameworks *viz.*, zeolites is their catalytic ability in industrially important reactions, which will be investigated in this study. These materials display potential catalytic activity in a wide variety of synthetically useful oxidative transformation reactions using different oxidants under mild reaction conditions. They have more advantages over their homogeneous liquid phase catalysts [11 – 16].

In this work, the encapsulated complexes were Schiff-base ligands as these systems can be easily prepared and form complexes with almost any metal ion. There have been many reports on their applications in homogeneous and heterogeneous catalysts. An advantage of Schiff-base complexes is that most of these complexes show excellent catalytic activity in various reactions such as polymerization reactions, oxidation, decomposition of hydrogen peroxide, carbonylation reactions, Heck reactions, Diels-Alder reactions and Lewis acid assisted organic transformations even at high temperatures above 100 °C [17].

The chemical industry has a strong demand for phenolic compounds. In recent years, this has led to the need for development of improved catalysts for selective and efficient

Chapter 1: Introduction

conversion of phenol. The hydroxylation of phenol to commercially important products *viz.*, hydroquinone and catechol has wide applications in many fields [18].

The selective one-step hydroxylation of phenol using oxidants such as H_2O_2 is a research topic of high industrial importance [19] from an economical and environmental point of view. The products, catechol and hydroquinone are important for manufacturing petrochemicals, agrochemicals and plastics [20]. They are also used as photographic chemicals, antioxidants, pesticides, flavouring agents and medicine. Catechol was also used for organic synthesis in the photoelectrochemical cell [21].

Phenol is normally produced from benzene employing the cumene-process but this method is rather undesirable from an economic and environmental point of view [22].

The reason is that in the cumene method, one of the most common industrial methods, consists of three-steps and although each step gives high selectivity, it is energy intensive, producing considerable waste and leads to a 1:1 mixture of phenol and acetone [23 - 26].

A one-step process would require less energy and produce only phenol. This represents an attractive method not only for its economic advantage but also from a chemical transformation point of view. Therefore in this research topic, benzene oxidation was studied under a direct-one step protocol to produce phenol in a manner that serves to be economically favourable.

Two other industrially important reactions investigated were styrene and cyclohexene oxidation. The products of these respective reactions were studied due to their potential use in commercial products [27, 28].

The oxidation of styrene draws interest from academics and industry, mainly in the production of fine chemicals such as benzaldehyde [29]. Benzaldehyde is important for cosmetics as it is used as denaturant, flavouring agent and as a fragrance [30]. Another important product of this reaction, phenylacetaldehyde, is practically useful for the production of drugs, perfumes, artificial sweeteners, and agricultural chemicals such as insecticides, fungicides and herbicides [31].

The catalytic oxidation of cyclohexene has been investigated with the view of obtaining high yields of industrially important products such as cyclohexene oxide and cyclohexenol. Catalytic oxidation of cyclohexene is attracting attention because its oxidation products (e.g., 2-cyclohexen-1-one, 2-cyclohexen-1-ol, epoxide) are very useful synthetic intermediates [32]. Cyclohexenol is an important raw material for the production

cyclohexadiene which finds application in nylon and perfumery industries, respectively [33]. Cyclohexene oxide is a highly reactive and selective organic intermediate widely used in the synthesis of enantioselective drugs, epoxy paints and rubber promoters [33].

The aim for this research programme is to synthesize catalysts that display both high catalytic activity and good selectivity for industrially important oxidations that will be of benefit to the industry.

1.2 Objectives

The objectives of this study were as follows:

- 1.2.1 To prepare two Schiff-base ligands derived from β -diketones and ethylene diamine using different molar ratios and thereafter synthesizing transition metal Cu(II) and OV(IV) complexes of these ligands respectively.
- 1.2.2 To heterogenize the homogeneous Cu(II) and OV(IV) Schiff-base complexes by encapsulation inside the supercages of Y-type zeolite using the flexible ligand encapsulation technique.
- 1.2.3 Investigating the catalyst's activity for the liquid-phase hydroxylation of phenol, benzene, styrene and cyclohexene using H_2O_2 as oxidant. Thereafter, determining the selectivity of each catalyst for the products of their respective oxidation reactions.
- 1.2.4 To test the optimized reaction conditions at which maximum % conversion will be obtained by varying the reactions conditions only for phenol hydroxylation.
- 1.2.5 To compare the activity of the "neat" versus the encapsulated complexes.
- 1.2.6 To establish the possible reaction pathway of the catalysts using UV/Vis.

1.3 Thesis Outline

Chapter 1 serves as a summary regarding the problem identification for the various oxidation reactions, heterogenization of homogeneous catalysts studied and gives the aims and objectives for this research topic.

Chapter 2 gives a very detailed description of the historical and theoretical background for this research topic and focuses on the role of zeolites in catalysis, heterogenization of homogeneous catalysts and the application of Schiff-base complex systems especially in oxidation reactions. The applications of encapsulated complexes as catalysts are also discussed.

Chapter 3 is the experimental section and details the synthesis and of the series of zeolite encapsulated Cu(II) and OV(IV) complexes, their “neat” analogues and the series of Schiff-base ligands.

Chapter 4 represents the characterization of all the Schiff-base ligands synthesized, their respective Cu(II) and OV(IV) transition metal complexes and their encapsulated analogues.

The results for the possible reaction pathway of the catalysts are also discussed in this chapter.

Chapter 5, describes the catalytic activity of both the encapsulated and neat copper catalysts for the oxidation of phenol, benzene, styrene and cyclohexene. The optimized reaction conditions are also described in this chapter.

Chapter 6 describes the catalytic activity of the neat and encapsulated oxovanadium complexes as potential catalysts in the oxidation of phenol, benzene, styrene and cyclohexene. The results for these catalysts were discussed.

A final conclusion is given regarding the results and findings and is summarized in the final chapter, **Chapter 7** regarding this thesis and recommendations for future work on this research topic are also discussed in this chapter.

Reference

- [1] Fan B., Fan W., Li R., Fe-containing Y as a host for the preparation of a ship-in-a-bottle catalyst, *J Mol Catal A: Chem* 201 (2003) 137.
- [2] Basset J.M, Psaro R., Roberto D., R. Ugo, *Modern Surface Organometallic Chemistry*, Wiley-VCH, (2009) 209.
- [3] Cheetham A.K., Ferey G., Loiseau T., *Open-Framework Inorganic Materials*, *Angew Chem, Int Ed* 38 (1999) 3268.
- [4] Okuhara T., *Microporous heteropoly compounds and their shape selective catalysis*, *Appl Catal A: Gen* 256 (2003) 213-224.
- [5] Zhang G., Choi W., Kim S. H, Hong S. B, *Selective photocatalytic degradation of aquatic pollutants by titania encapsulated into FAU-type zeolites*, *J Hazard Mat* 188 (2011) 198-205.
- [6] Kim Y., Yoon M., *TiO₂/Y-Zeolite encapsulating intramolecular charge transfer molecules: a new photocatalyst for photoreduction of methyl orange in aqueous medium*, *J Mol Catal A: Chem*, 168 (2001) 257-263.
- [7] Bessel C. A., Rolison D. R, *Electrocatalytic Reactivity of Zeolite-Encapsulated Co(salen) with Benzyl Chloride*, *J Am Chem Soc* 119 (1997) 12673-12674.
- [8] Walcarius A., Barbaise T., Bessiere J., *Factors affecting the analytical applications of zeolite-modified electrodes preconcentration of electroactive species*, *Anal Chim Acta* 340 (1997) 61.
- [9] Chen B., Ngoh-Khang G., Lian-Sai C., *Determination of copper by zeolite molecular sieve modified electrode*, *Electrochim Acta* 42 (1997) 595.
- [10] Briot E., Bediou F., Balkus Jr. K. J., *Electrochemistry of zeolite-encapsulated complexes: new observations*, *J Electroanal Chem* 454 (1998) 83.
- [11] Kaucky D., Vondrova A., Dedecek J., Wichterlova B., *Activity of Co Ion Sites in ZSM-5, Ferrierite, and Mordenite in Selective Catalytic Reduction of NO with Methane*, *J Catal* 194 (2000) 318.
- [12] Silva M., Freire C., de Castro B., Figueiredo J.L., *Styrene oxidation by manganese Schiff base complexes in zeolite structures*, *J Mol Catal A: Chem* 258 (2006) 327.
- [13] Połtowicz J., Pamin K., Tabor E., Haber J., Adamski A., Sojka Z., *Metallosalen complexes immobilized in zeolite NaX as catalysts of aerobic oxidation of cyclooctane*, *Appl Catal A: Gen.* 299 (2006) 235.

- [14] Drechsel S.M., Kaminski R.C.K., Nakagaki S., Wypych F., Encapsulation of Fe(III) and Cu(II) complexes in NaY zeolite, *J Coll Inter Sci* 277 (2004) 138.
- [15] Hensen E.J.M., van Veen J.A.R., Encapsulation of transition metal sulfides in faujasite zeolite for hydroprocessing applications, *Catal. Today* 86 (2003) 87.
- [16] Salavati-Niasari M., Nanodimensional Microreactor-encapsulation of 18-Membered Decaaza Macrocyclic Copper(II) Complexes, *Chem Lett* 34 (2005) 244.
- [17] (a) Gupta K.C., Abdulkadir H.K., Chand S., Synthesis of polymer anchored N,N'-bis(3-allyl salicylidene)-o-phenylenediamine cobalt(II) Schiff base complex and its catalytic activity for decomposition of hydrogen peroxide, *J Mol Catal A: Chem.* 202 (2003) 253-268; (b) Gupta K.C., Sutar A.K., Catalytic activities of Schiff base transition metal Complexes, *Coord Chem Rev* 252 (2008) 1420-1450; (c) Li-Juan C., Jie B., Fu-Ming M., Xing L.G., Oxidative carbonylation of aniline to N,N'-diphenyl urea catalyzed by cobalt(II)-Schiff base complex/pyridine catalytic system *Catal Commun* 9 (2008) 658-663; (d) Gupta K.C., Sutar A.K., Lin C.C., Polymer-supported Schiff base complexes in oxidation reactions, *Coord Chem Rev* 253 (2009) 1926-1946.
- [18] Zhao W., Luo Y.F., Deng P., Li Q.Z., Synthesis of Fe-MCM-48 and its catalytic performance in phenol hydroxylation, *Catal Lett* 73 (2001) 199.
- [19] Park J., Wang J., Choi K.Y., Dong W., Hong S., Lee C. W., Hydroxylation of phenol with H₂O₂ over Fe²⁺ and/or Co²⁺ ion-exchanged NaY catalyst in the fixed-bed flow reactor, *J Mol Catal A: Chem* 247 (2006) 73.
- [20] Sheldon R.A., Santen R.A., *Catalytic Oxidation: Principles and Applications*, World Scientific, Singapore (1995).
- [21] Kianfar A.H, Mohebbi S., Synthesis and electrochemistry of vanadium (IV) Schiff base complexes *J Iranian Chem Soc* 4 (2007) 215-220.
- [22] Panov G.I., Kharitonov A.S., Sobolev V.I., Oxidative hydroxylation using dinitrogen monoxide: a possible route for organic synthesis over zeolites, *Appl Catal* 98 (1992) 1-20.
- [23] Cavani F., Trifiro F., Some innovative aspects in the production of monomers via catalyzed oxidation processes, *Appl Catal A: Gen* 88 (1992) 115.
- [24] Sheldon R.A., J.K. Kochi, *Metal-Catalyzed Oxidations of Organic Compounds*, Academic Press, (1981), (Chapter 10).

Chapter 1: Introduction

- [25] Centi G., Cavani F., Trifiro F., *Selective Oxidation by Heterogeneous Catalysis*, Kluwer Academic Publishers/Plenum Press, Dordrecht/New York (2001)
- [26] H. Nur, H. Hamid, S. Endud, H. Hamdan, Z. Ramli, Iron-porphyrin encapsulated in poly(methacrylic acid) and mesoporous Al-MCM-41 as catalysts in the oxidation of benzene to phenol, *Mat Chem Phys* 96 (2006) 338.
- [27] Lee S.O., Raja R., Harris K.D.M., Thomas J.M., Johnson B.F.G., Sankar G., Mechanistic insights into the conversion of cyclohexene to adipic acid by H₂O₂ in the presence of a TAPO-5 catalyst, *Angew Chem Int Ed* 42 (2003) 1520-1523.
- [28] Liu J., Wang F., Gu Z., Xu X., Vanadium phosphorus oxide catalyst modified by silver doping for mild oxidation of styrene to benzaldehyde, *Chem Eng J* 151 (2009) 319.
- [29] Adam F., Iqbal A., The oxidation of styrene by chromium–silica heterogeneous catalyst prepared from rice husk, *Chem Eng J* 160 (2010) 742-750.
- [30] Andersen A. Final Report on the Safety Assessment of benzaldehyde, *Int J Toxicology* 25 (2006) 11-27
- [31] Sheldon R.A, van Bekkum H., *Fine Chemicals through Heterogeneous Catalysis* Wiley-VCH (2001) 217-231.
- [32] Bohstrom Z., Rico-Lattes I., Holmberg K., Oxidation of cyclohexene into adipic acid in aqueous dispersions of mesoporous oxides with built-in catalytical sites, *Green Chem* 12 (2010) 1861
- [33] Cohen S., Kozuch S., Hazan C., Shaik S., Does Substrate Oxidation Determine the Regioselectivity of Cyclohexene and Propene Oxidation by Cytochrome P450, *J Am Chem Soc* 128 (2006) 11028.

CHAPTER 2

2. LITERATURE REVIEW

2.1 Introduction

This section will review the literature describing encapsulation of metal complexes using zeolites as supports, their selectivity in catalytic reactions and methods of encapsulating metal complexes inside zeolites.

The problem areas normally identified in homogeneous catalytic systems are introduced and how these problems are solved by “heterogenizing” the homogeneous catalyst on solid supports. A very detailed description and purpose for the heterogenizing of homogeneous catalysts and different methods of immobilizing are also presented.

2.2 Concept of heterogenization of homogeneous catalysts

Over the past decades, various transition metal complexes of Schiff base ligands have been employed in homogeneous catalysis [1-3]. The reason is, these catalytic systems enjoy success in various oxidation reactions offering high activity, homogeneity, reproducibility, selectivity under mild conditions and thus affirms their usage in organic synthesis [4, 5]. Unfortunately, homogeneous catalytic systems are plagued by various difficulties. Firstly, the catalyst, reactants and products are in one phase, making catalyst-product separation, catalyst recovery, recycling and reuse difficult [6-11]. Another drawback is leaching of the active metal into the solvent and the insufficient stability of the catalyst. This is because during the workup of the reaction to obtain the reaction products, the catalyst are normally destroyed making its recovery difficult [12]. Moreover, formation of oxo-dimers and other polymeric species are always possible in homogeneous catalytic systems and will lead to irreversible catalyst deactivation [13]. Solvent and catalyst losses that occur during separation can lead to unacceptable amounts of wastage [14]. Thus, heterogeneous catalysts [15-21] were developed to overcome these drawbacks and environmental hazards and have become an important active field of research. Notably, the advantages of immobilized catalysts are their high activity, selectivity and recoverability, but also to simplify the separation and purification processes, and thus, decrease the formed impurities. Recovery and reuse of a catalyst is especially desired when expensive or toxic catalysts are involved.

Recyclable catalysts offer higher total turnover numbers and less (toxic) waste, which is essential, both from an environmental and commercial point of view. Development of recyclable catalysts has, therefore, become a key issue in the field of homogeneous catalysis [21-23].

This can provide the ideal method for combining the advantages and also avoid the disadvantages of homogeneous and heterogeneous catalysts [24-26]. The aim of these catalysts, clearly, is to improve the stability of the transition metal complex under the reaction conditions by preventing the catalytic species from dimerizing or aggregation and to tune the selectivity of the reaction using the walls of the pores of the solid via steric effects [27].

The process of immobilization of homogeneous catalysts on a solid support is termed “heterogenization”.

2.3 Methodologies for heterogenization of homogeneous catalysts

In general, three concepts for the heterogenization of homogeneous metal complexes can be distinguished:

2.3.1 Liquid-liquid two-phase system

The first immobilization technique does not require a solid support, but involves use of a liquid–liquid (biphasic) two-phase system [28, 29]. In the biphasic system, the catalyst is soluble in one solvent, whilst the substrates and products are soluble in the other solvents, which are immiscible with each other. This methodology allows the separation of reaction products from homogeneous catalyst phase usually by simple phase separation after the reaction is complete in order to recycle the catalyst. The reaction products are extracted into non-polar solvent leaving behind the catalyst [30]. An example is the Ruhrchemie/ Rhone-Poulenc oxo-process [30] and Shell Higher Energy Olefin Process (SHOP) [31].

2.3.2 Supported liquid-phase catalysis

The idea of using supported liquid-phase catalysis (SLPC) was proposed by Davis and his co-workers [32]. In their work, they prepared a thin aqueous phase containing rhodium complexes over the surface of porous silica and its good performance was proven for hydroformylation, as reviewed by Davis. The liquid (solvent and dissolved catalyst) is

dispersed in a porous solid support to produce a large gas–liquid interface. SLPCs are, therefore, particularly suited for catalysts with a low diffusion rate in the liquid phase. The reaction takes place throughout the liquid phase in a homogeneous SLPC. The distribution of the liquid inside the porous support is of great importance [33]. The SLPC is used in a solvent that does not dissolve the film liquid and could easily separate by simple filtration and recycle. A disadvantage of SLPC catalysts is that they are usually restricted to the synthesis of low boiling compounds [34]. Another specific problem usually occurring in SLPC is the loss of liquid phase by conveyance of vapour with the reaction gas flow due to the small, but still perceptible, vapour pressure of the liquid [35].

After a certain time, the solvent in which the catalyst is dissolved vapourises. This causes anchoring of the catalyst onto the solid surface resulting in a tremendous loss in yield and reduction in selectivity [33].

2.3.3 Fixation on/in solid supports

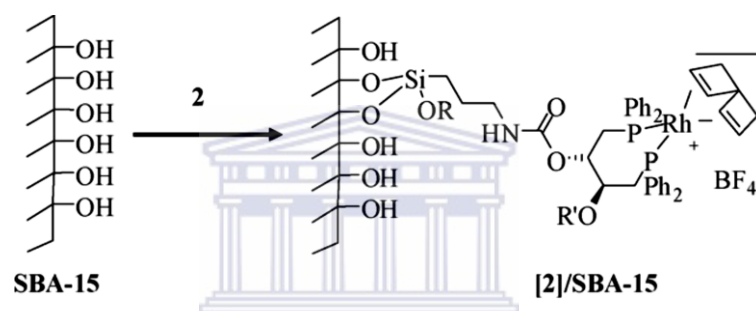
The most common and used method of heterogenization of homogeneous catalysts is the fixation of complexes to solid supports in various ways, e.g. on polymers, on metal oxides, by covalent or co-ordinative linkage or electrostatic attraction, via functionalized ligands, by adsorption on porous supports or by inclusion of metal complexes into molecular sieves, sol–gel matrices or other materials [36 - 39]. This is the type of heterogenization which will be discussed in more detail as this method will be the encapsulation of complexes in inorganic supports. The immobilization methods discussed here are only fixation of catalysts on/in solid supports. There are different approaches to immobilize metal complexes onto solid supports. The most common way to classify them is the type of interaction between the molecular species and support. Three different groups can according to support-molecule interactions be identified as: (a) covalent bonding, (b) non-covalent interactions and (c) encapsulation [40, 41].

2.3.3.1 Covalent bonding

In covalently supported catalysts, the ligand or catalyst is covalently anchored or immobilized to a soluble or insoluble support. The immobilization involves either reaction of a functional resin with a suitably functionalized catalytic species or copolymerization of a derivative of the organocatalyst with other monomers [42].

It can be accomplished, either directly by reaction of the metal complex with the support surface groups or mediated through a spacer previously grafted to the support or reacted with the support.

One of the most important advantages of this technique is that the molecular species are linked to the support via chemical bonds and experience almost no leaching as far as all bonds are stable in the reaction media [43 – 45]. The drawback of this method, however, is the large preparative effort which involves a multi-step procedure and not only the functionalization of the ligands coordinate to the metal, but also the grafting of the spacers onto the support [46]. Scheme 2.1 is an example of covalent bonding between an inorganic support and a metal complex.



Scheme 2.1: Rhodium complex covalently anchored to mesoporous silica, SBA-15 [47].

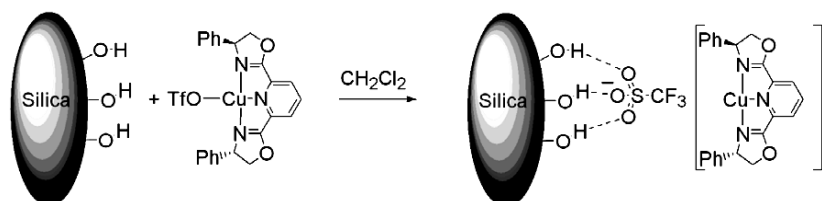
Furthermore, covalent bonding of metal complexes, directly or via spacers, can alter, to different extents, the electronic density within the metal which in turn can modify the performance of the catalyst in a way that may be difficult to foresee [41].

2.3.3.2 Non-covalent interactions

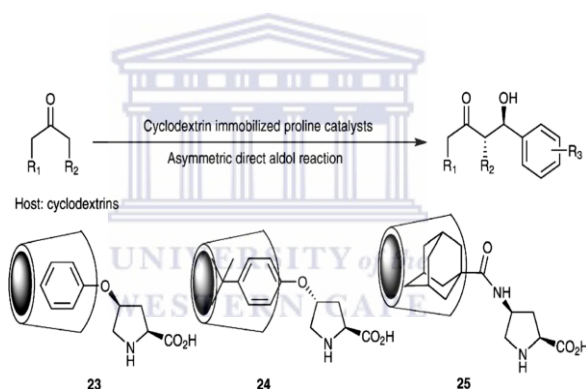
Alternatively, transition metal complexes can also be immobilized by non-covalent bonding through hydrogen bridges, hydrophobic, fluorine interactions, electrostatic interaction (e.g. ion-exchange material) via functionalised ligands or by adsorption on porous supports to combine the good activities and selectivities of the homogeneous catalysts and the simplicity of recycling and recovery of the heterogeneous ones or entrapment within several supports such as sol-gel matrices [47 - 49].

Non-covalent interactions between the support and metal complex include two methodologies, for complex immobilization, namely, physical adsorption [50] and electrostatic interaction [51, 52]. Physical adsorption involves π - π , Van der Waals

interactions, hydrogen bonds, hydrophobic-hydrophilic interactions between the support and the complex. The second approach consists of electrostatic interactions between the support and the complex, and therefore, charges of opposite signals are required between them (Scheme 2.2). These catalysts are created by first synthesizing the solid support and then contacting it with the catalytic complex. An example of hydrophobic interactions between support and catalyst is presented in Scheme 2.3.



Scheme 2.2: Schematic illustration of electrostatic immobilisation of a copper(I)pybox catalyst on silica [53].



Scheme 2.3: Cyclodextrins immobilized proline catalysts via hydrophobic interactions [54].

The catalyst can be weakly bound via physisorption or more strongly electrostatic interaction or through metal coordination [40]. The non-covalent interaction can also occur between the support and complex, or through spacers, in the latter case, interaction between the spacer and the complex can be of a different nature, covalent or non-covalent. The major advantage over non-covalent interactions is their easy separation.

A disadvantage rather, is their sensitivity to solvents which are an important weakness as this may cause leaching of the active phase by simple manipulation of the experimental conditions used in the preparations of the immobilized complexes or during the catalytic reactions, therefore, these catalysts may be relegated for use involving mild reaction conditions [41].

2.3.3.3 Encapsulation/entrapment

A special type of immobilization of homogeneous catalysts involves an encapsulation principle and characterized as ‘host guest’ structures, ‘ship-in-the-bottle’ constructions in zeolites or by entrapment in sol–gel structures.

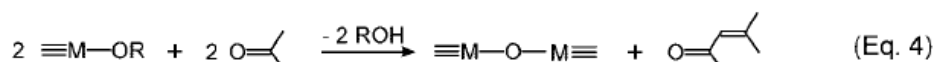
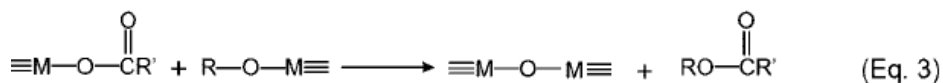
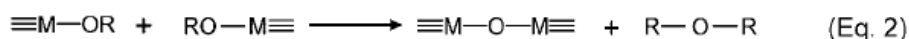
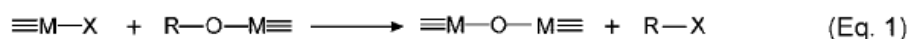
Generally, there are two different types of encapsulated complexes. The first methodology of encapsulation involves the synthesis of the support with the catalyst present in the reaction mixture. Two well-known examples are sol-gel and polymeric materials. In both cases, the polymerizable unit (usually alkoxysilanes or sodium silicates with sol-gels or olefins or other polymerizable monomers in the polymers) are mixed together in one-pot while the solid support forms which will be discussed in more detail in this section [56]. Another method to entrap metal complex catalysts is the intercalation of metal complexes into layered structures.

2.3.3.3.1 Entrapment in sol-gel

One of the most recent methods for encapsulation of homogeneous catalysts was described by Gelman *et al* involving entrapment of rhodium and ruthenium complexes in sol gel [56].

The sol-gel process consists of the following general steps: sol formation, gelation, drying and densification. The preparation starts with an appropriate metal alkoxide which is mixed with a suitable solvent. Firstly, a colloidal sol forms from hydrolysis and condensation of the metal alkoxide precursor. The liquid sol then becomes a gel as hydrolysis and condensation proceeds and the solid phase forms a network that extends throughout the container having nanosized pores. The liquid phase is removed causing the aged gels to become xerogels [57]. Two different types of sol-gel processes can be distinguished, namely, non-aqueous and aqueous.

In non-aqueous sol-gel, the transformation of the precursor to an inorganic solid takes place in the organic solvent in the absence of water. The list of potential precursors involved is longer in non-aqueous systems and includes in addition to inorganic metal salts and metal oxides, metal acetates and metal acetylacetonates. The condensation steps in the non-aqueous process are presented in Scheme 2.4.



Scheme 2.4: The condensation steps in non-aqueous sol-gel process, alkyl halide elimination (Eq.1), ether elimination (Eq.2), ester elimination (Eq.3), and aldol-like condensation (Eq.4) [58].

Aqueous sol-gel process involves the conversion of a precursor solution into an inorganic solid via inorganic polymerization reactions which are induced by water. The precursor is normally an inorganic, metal salt or an organic metal compound such as alkoxide. In most cases, metal alkoxide precursors are widely used. Unfortunately, this process is quite complex, due to the high reactivity of metal precursors towards water and the double role of water as both ligand and solvent and due to a large number of parameters *viz.*, hydrolysis and condensation rate of the metal oxide precursors, pH, temperature, method of mixing and rate of oxidation. The parameters have to be strictly controlled in order to provide good reproducibility of the synthesis protocol [59]. Scheme 2.5 illustrates the condensation and hydrolysis steps in aqueous sol-gel process.



Scheme 2.5: Hydrolysis (Eq.1) and condensation (Eq. 2 and 3) steps in aqueous sol-gel process [60].

Overall, studies on heterogenization of homogeneous transition metal catalysts revealed that physical entrapment of a wide range of mono- and homobimetallic complexes in SiO_2 sol-gel matrices does not only permit facile recycling of the entrapped catalysts, but also increases their stability and enhances their catalytic properties [61]. The sol-gel method is particularly useful for the synthesis of binary and multinary metal oxides and for ceramic composite materials [62].

On the other hand, this type of encapsulation of complexes suffers from various difficulties. A drawback is the active catalyst may diffuse out of the swollen solid support, reducing recyclability and also leading to product contamination. These materials are also prone to leaching as the sol-gel and polymer may be subject to swelling in certain solvents. This swelling could also cause problems in fixed volume reactors, leading to increase pressure differentials across the reactor [56].

2.3.3.3.2 Ship-in-the-bottle

The second strategy is the encapsulation process which involves heterogenization of transition metal complexes having potential catalytic activity in porous materials such as zeolites, MCM - 41 or any other molecular sieves and requires no bonding between the catalyst and support [63 – 66]. In other words, it involves physical entrapment of the metal complex within the pores of the support and it is assumed that no other interaction should exist besides the physical confinement. This methodology depends on the size of the complex and therefore, the catalyst should be larger than the pore of the zeolite. This smaller pore keeps the metal complex encapsulated in the zeolite framework in order to prevent the metal complex from leaching out of the zeolite (Fig.2.1) [67]. In the molecular sieve host, the metal complex should be free to move within the confines of the cavities but be prevented from leaching by restrictive pore openings. Therefore, the term zeolite “ship-in-the-bottle” complex may be applied [68]. Scheme 2.6 demonstrates how leaching occurs when the encapsulated complex is smaller than the zeolites pores resulting in leaching out of the zeolite.

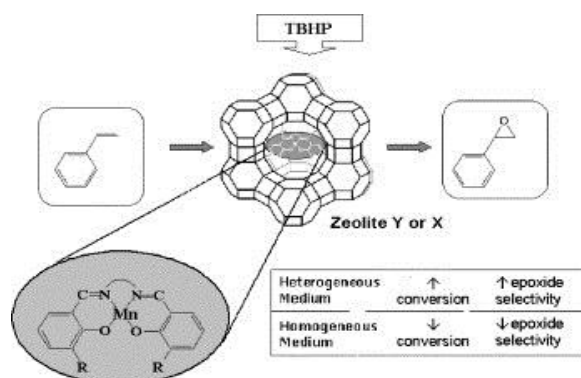
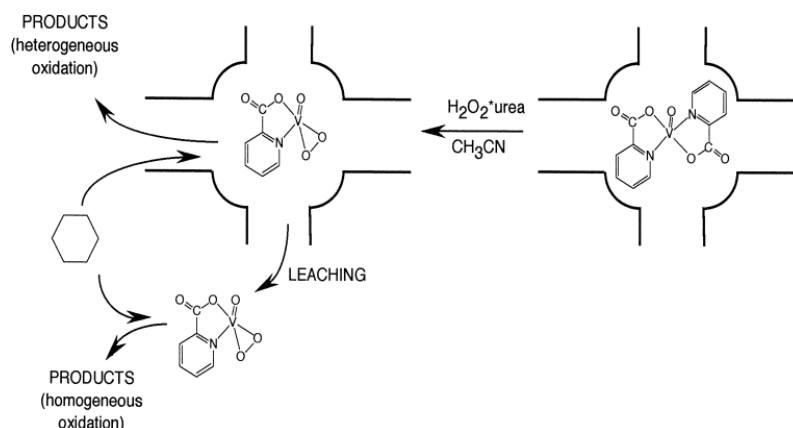


Figure 2.1 Manganese Schiff-base complex physically entrapped in zeolite Y [69].



Scheme 2.6 : The pathway of intrazeolitic complexes when the complex size is smaller than zeolite pores leading to the complex leaching out of the zeolite [70].

Two variables in the preparation of a redox molecular sieve having an encapsulated complex are the nature of the molecular sieve such as its pore size, hydrophobicity and acidity and the method of confinement. Molecular sieves are categorised into small pore ($< 4 \text{ \AA}$), medium pore ($4 - 6 \text{ \AA}$), large pore ($6 - 8 \text{ \AA}$), extra-large pore ($8 - 14 \text{ \AA}$) and mesoporous ($15-100 \text{ \AA}$) [71]. Encapsulation causes no change in the chemical properties of an entrapped catalyst except for the steric confinement of the porous supports whilst three dimensional supports may also provide site isolation of the catalyst [72]. Encapsulation within inorganic supports can be further subdivided into encapsulation within layered and porous supports, and within the latter, between microporous (free diameter 2 nm) and mesoporous ($2\text{nm} < \text{free diameter} < 50 \text{ nm}$) materials. Encapsulation of transition metal complexes relies either on intercalation, or synthesis of the complex into or within the pores or entrapment of the metal complex [73].

In most reactions studied, heterogenization of homogeneous catalysts through encapsulation, high selectivity in competitive reactions is observed that is correlated to molecular sieving effects and a better regioselectivity is obtained [74 - 76].

While these materials do allow for simple recycle of a truly homogeneous catalyst, these materials also present some disadvantages *viz.*, decreased activity due to slow diffusion of reactants and products into and out of the porous material and difficult characterization of the catalyst which might be due to the low catalyst loadings [55].

2.3.3.3.3 Entrapment in silicate layers

Encapsulation of metal complexes through intercalation occurs when the cationic catalyst is introduced as such between the silicate layers of swelling clays, such as smectites [77], layered double hydroxides [78] or pillard clays [79, 80] by an ion-exchanged procedure. An important factor of clays is their high surface area, with the consequence that ion-exchange sites on the surface of the clay are well dispersed. These considerations suggest that clays might be suitably employed as supports for those homogeneous metal complex catalysts which are prone to undergo deactivation in solution [81]. Examples of complexes entrapped in silicate layers are illustrated in Fig.2.2.

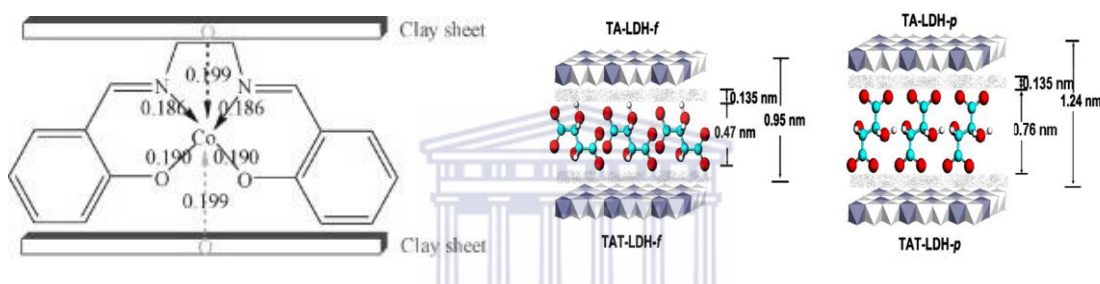


Figure 2.2 A model structure of intercalated catalysts (i) whereby the catalyst is located between sheets of clay [82] or between interlayer spaces of (ii) Mg/Al layered double hydroxide (LDH) [83]

The advantage of ion-exchange methods of catalyst immobilization on layered silicates is simple in comparison to the multistep procedures for covalent attachment of complexes to polymers or amorphous metal oxide supports. Moreover, the catalysts exhibit potentially controllable selectivity effects when exchanged into the structures of these ubiquitous minerals. However, under certain conditions, the layered silicate systems can exhibit undesirable properties. For instance, desorption of a catalytically active, presumably uncharged species, occurs during reactions when certain silicate-supported cationic complexes are employed as hydrogenation, or hydroformylation catalysts. In addition, the lack of numerous, well-studied, cationic homogeneous catalysts limits the range and type of complexes that might be supported [84]. In order to avoid the drawbacks of encapsulation of catalysts in sol-gels or in clays, regular and ordered materials were used for this research programme.

2.4 Types of support used in heterogenization of homogeneous catalysts

When immobilizing homogeneous catalysts on supports, these usually fall into two broad categories: organic and inorganic. The organic supports used for immobilization are generally soluble or insoluble polymers or dendrimers. Inorganic supports are the most widely used supports in the immobilization of homogeneous catalysts. Inorganic supports are porous materials with discrete surface areas, which are exemplified by alumina and silica. The advantages of using inorganic materials over organic supports are that they are mechanically rigid, chemically stable, not affected by temperature and solvent. Therefore they can withstand high temperatures which are usually used in industry and resisting the oxidative conditions. The relatively high surface area and appropriate pore sizes of inorganic supports also maintain their competitive advantages over other supports.

Polymer supports in contrast, suffer from various difficulties. Organic polymers are not rigid materials and their shape and structures are strongly influenced by the solvent, temperature and pressure. These supports are also vulnerable to some chemicals. Solvents cause polymers to swell, which results in greater accessibility to inner surfaces of the support increasing the mass transport. In general, inorganic supports do not tend to swell, as in the case for organic supports which make them ideal supports for use in continuous reactors [42, 85 - 88]. The most common reported organic supports used are insoluble polymeric materials, which are used with great success in solid phase organic synthesis. The difficulties of these materials are their restricted loading capacity, the often restricted accessibility of active sites, the wettability issues, their reactivity towards reactive reagents, such as organometallics and their polydispersity [89]. These drawbacks have prompted many research groups to explore the use of soluble polymers such as poly ethylene oxide polymers, linear polystyrene and dendrimers as supports [90, 91]. Therefore, in order to avoid the difficulties of organic supports only inorganic supports will be discussed in this section as this is the choice of support that will be studied in this investigation.

2.4.1 Inorganic Supports

Inorganic supports such as zeolites, glass and metal oxides (e.g. MCM - 41) have also been observed as highly promising supports in solid-phase assisted synthesis, mainly as catalysts [30]. Among inorganic supports, silica and alumina are easily and readily available and are used by various researchers for immobilization of different catalysts by direct reaction of

surface hydroxyl groups with reactive species [92 – 96]. Inorganic molecular sieves such as MCM-41, SBA-15 and FSM-16 have free hydroxyl groups on their surface and also have tiny channels and windows at the nanometer scale. Therefore these mesoporous materials can be employed for immobilization of macro cycles and metal complexes (Fig.2.3). Immobilized complexes of these materials show unique properties in adsorption and catalysis [97, 98]. Zeolites, with their crystalline framework and well-defined cavities are usually used in the encapsulation of homogeneous catalysts. Among inorganic supports, they tend to be the most promising and are widely used for immobilization of metal complexes. The distinct advantage of these materials over other supports is that the metal complex can be physically entrapped in the super cages without aggregation [99].

Other commonly used supports are negatively charged layered double hydroxides (LDH) that immobilize anionic metal complexes, crystalline microporous aluminophosphates and hydroxyapatites, alumina and titania. Mesoporous and microporous materials have become very important in recent years. Typically, micropores have an inner radius of < 1.5 nm, whilst mesopores range between 1.5 and 15 nm and macropores are larger than 15 nm. Another important group of supports are the sol-gels which are characterized by high porosity and a large specific surface [38].

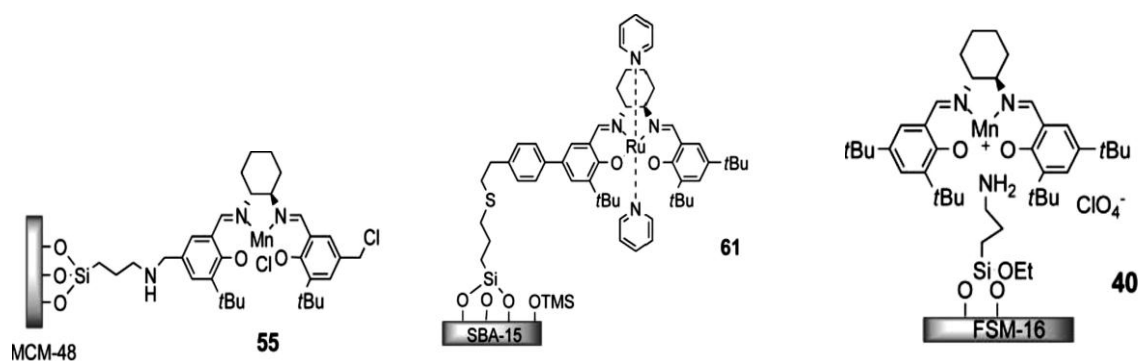


Figure 2.3 Illustrating immobilization of catalysts on various mesoporous silica supports, MCM-41, SBA-15 and FSM-16 [100].

2.5 Zeolites as supports for immobilization of homogeneous catalysts

2.5.1 Structure

Zeolites are crystalline aluminosilicates that have natural or synthetic origin and have shown promising potential as selective heterogeneous catalysts, adsorbents and ion exchange media in certain industrial and commercial areas, especially in petroleum refining. They are made up of TO_4 ($T = Si, Al$) tetrahedra that are linked through oxygen atoms leading to a three dimensional network through which long channels run. Water molecules and alkali metal ions are located in the interior of these channels, which can be exchanged with other cations. The interior of the pore system, having atomic scale dimensions, is the catalytically active surface of the zeolite [101, 102]. The geometry of the cavities and channels formed by the rigid framework of SiO_4 and AlO_4^- tetrahedra distinguishes zeolites from one another.

The aluminosilicate structure incorporating Si^{4+} , Al^{3+} and O^{2-} are ionic. When Si^{4+} ions are replaced in the SiO_4 tetrahedra in the framework with Al^{3+} ions, an excess negative charge is generated. These non-framework cations play a central role in determining the catalytic nature of zeolites [103].

Sodalite (SOD, a cubooctahedron), Faujasite (FAU) and Linde Type A (LTA) which are three types of zeolites are built from a SOD cage formed by connected single four and six rings. These different zeolites are distinguished by the connection of the SOD cages. The differences in their structures are presented in Fig.2.4 (a). The FAU zeolite structure (zeolite X, Y, and natural Faujasite) is characterized by double six ring (D6R, a hexagonal prism), SOD cavity and supercage. A unit cell consists of eight sodalite supercages (16D6Rs), 16 12-rings and single 6-rings (S6Rs) [104]. The SOD-cage is connected to four nearest neighbouring SOD-cages through double T6-rings (T6 = tetrahedral six membered ring), D6R. In LTA zeolite, each SOD-cage is connected to six nearest neighbouring SOD-cages through double T4-rings (T4 = tetrahedral four membered ring) [105].

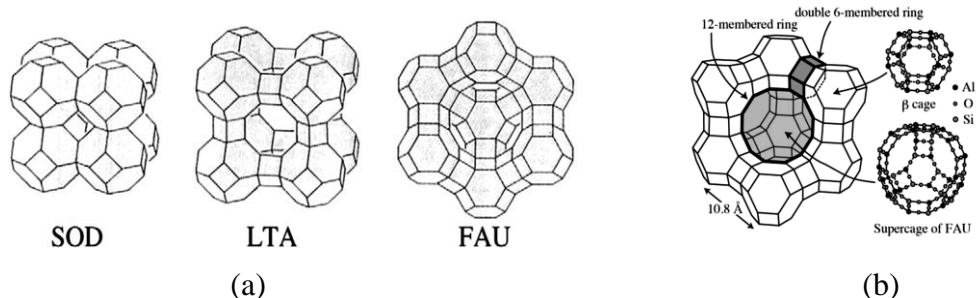


Figure 2. 4 (a) Different types of zeolites (b) various units Faujasite zeolite [106, 107].

2.5.2 Supported materials in catalysis

Zeolites tend to be excellent supports for catalysts due to their stability, regularity of their pore structure and their high surface area. It is thus important that as little active material ends up on the external surface of the zeolite when preparing the supported catalyst. An advantage of zeolites over other supports is their ability to isolate metal atoms in the pores and therefore prevent sintering of the metal atoms that would greatly reduce the surface area of the catalyst. The cationic sites in zeolites can be substituted with metal cations, and thus could potentially introduce potentially new catalytic species into the structure [108]. In this work, zeolites were chosen as suitable supports due to their high thermal and chemical stability as well as their good crystalline structures [74].

The possibility of employing zeolites as supports for transition metal complexes was first demonstrated by Lunsford's and Ben Taarit's groups in the 1970's [109 - 112]. Herron, Meyer and co-workers further developed this work by incorporating organometallic complex into the zeolite host [113, 114].

There are strong similarities between zeolites and the protein portion of natural enzymes. The zeolites and protein protect the active site from side reactions, sieves the substrate molecules and provide a stereochemically demanding void. As a result of these similarities, it induced research in the field of metal complexes encapsulated in zeolites which would mimic metalloenzymes for oxidation reactions [115, 116].

The advantage of using zeolites as supports for transition metal complexes, are the restrictive pore openings of the zeolite which could enable the catalysts to retain their high activity and selectivity in homogeneous catalysis. Zeolites also have a stabilizing effect on the metal complex as a result of the site isolation of the metal complex. The multimolecular deactivation pathways such as the formation of μ -oxo- or peroxy-bridge species that usually

occur in homogeneous complexes causing the catalyst to become inactive are also reduced [117 – 123].

The well-defined pore structure of zeolites means that when they are employed as supports for catalysts, they can impose selectivity on the reaction products.

Shape-selectivity by zeolites occurs by differentiating reactants, products, and/or reaction intermediates according to their shape and size in the sterically restricted environments of the zeolite structure. Because zeolite structures contain different pore window and channels sizes in the range 4 – 13 Å, they are able to recognize, discriminate and organize molecules with precisions that can be less than 1 Å [124]. Early work demonstrated that zeolites act as molecular sieves by excluding molecules too large to enter or preventing the production of molecules too large to exit (i.e. high-mass transfer limited products). Therefore, only molecules having dimensions less than the pore size of the zeolite can enter the channels and react at internal catalytic sites thereby limiting formation of products larger than the pore size of the zeolite [125, 126]. Therefore, only smaller molecules are able to diffuse out as observed products when the product mixture is formed in zeolite pores. These considerations are evident that exclusion of bulky molecules from the zeolite channels is a key factor for shape-selective catalysis by zeolites [127].

Both reactant and product shape selectivity have their origins in mass transfer limitations, in the hindered diffusion of product and reactant molecules in the zeolite pores [128, 129]. Most shape-selective catalysts used today are molecular sieve zeolites [130-132].

Smaller molecules will thus exhibit higher conversion when compared to bigger molecules in oxidation reactions. For a number of catalytic reactions, the site of the pores control the size of the products formed. The restricted spaces in the pores of zeolite.

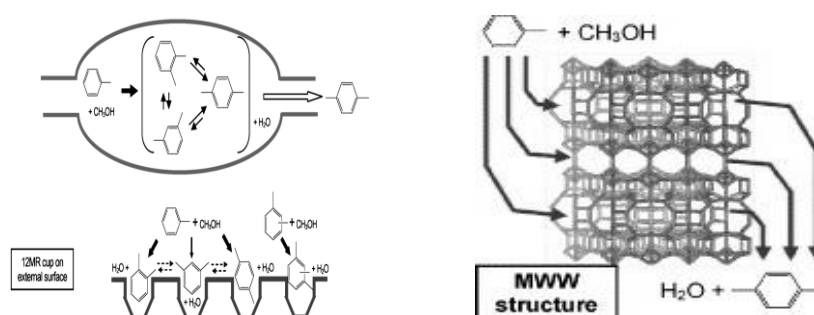
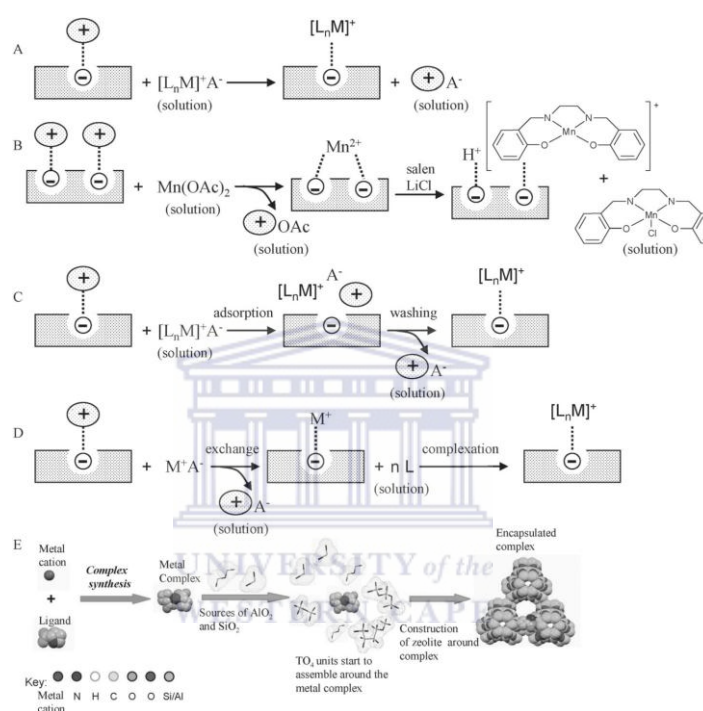


Figure 2.5 A schematic model for illustrating how the pores of zeolites controls shape selectivity [138].

2.6 Encapsulation strategies

In general, three routes are known for preparation of metal complexes inside zeolites, *viz.*, flexible ligand method, zeolite synthesis method and template synthesis method. In addition, the adsorption and ion-exchange method may also be considered. Scheme 2.7 illustrates the encapsulation methods of complexes in zeolites.

The preferred method and the one chosen for this investigation, is the flexible ligands method.



Scheme 2.7: Methods for encapsulating metal complexes within zeolites: Ion exchange (A), flexible ligand (B), ligand adsorption (C), ‘ship in a bottle’ (D) and zeolite synthesis methods (E) [139].

2.6.1 Flexible Ligand method

This method is based on the principle that the free ligand guests can easily enter into the zeolite pores because of their flexibility to pass through the restricted zeolite voids. Once the ligand enters the zeolite cage, it has the advantage to chelate with a previously exchanged metal ion to form a complex. The formed complex becomes too large and rigid and unable to escape from the zeolite cage due its larger size than the zeolite pore diameter. The flexible ligand method is one of the more extensively studied methods as it involves a straightforward and simple strategy [140 – 142]. This method is commonly employed for encapsulation of metal salen complexes (Salen = *N,N'*-bis (salicylaldehyde)ethylene

diimine), since the Salen ligand provide the desired flexibility. A large variety of cobalt [143], manganese [144], iron [145], rhodium [142] and palladium [118] Salen complexes was prepared according to this approach within the zeolite Y supercages.

2.6.2 Zeolite synthesis method

This method is based on the building of the bottle around the around the ship by crystallization of the zeolite around the metal complex which serves as a template for zeolite synthesis [146 -148]. Therefore, the metal complex is trapped in the cage of the zeolite, while it is being built up [149]. The advantage is that the nature of the intrazeolitic complex is well-defined and removal of excess ligand can be ignored. On the other hand it possess the disadvantage that there is a heterogeneous distribution of metal complex in the precursor gel and these complexes are not evenly distributed within the crystals, thereby effecting the % metal content of the intrazeolitic species [150].

2.6.3 Template (Ship-in-the-bottle) synthesis method

The template synthesis method involves the diffusion of ligand precursors into zeolite pores where they assemble around an intrazeolite metal ion that acts as a template and forms a complex [151 - 153]. The main problem results from the fact that uncomplexed metal species or free ligand may block diffusion pathways. Therefore, characterization of the intrazeolitic complex may also be poorly defined even with the use of various spectroscopic techniques and physical methods used in combination [70].

2.6.4 Adsorption method

The adsorption method could be illustrated by the reaction of metal exchange zeolite-Y with CO/H₂O or CO/H₂ to form metal carbonyls in the cavity of zeolite-Y. Several metal carbonyls, such as Ni(CO)₄, Rh₄(CO)₁₂, Rh₆(CO)₁₆, Ir₄(CO)₁₂, [Fe₂Rh₄(CO)₁₆] have been encapsulated in the cavities of zeolite-Y employing this methodology [154 – 157].

2.6.5 Ion-exchange strategy

The ion-exchange strategy involves, example, the exposure of a sodium-ion charge balanced Faujasite zeolite to a solution containing other cations, facilitating an exchange of the sodium ions. This method has been used for encapsulating metal–amino acid complexes

inside a zeolite structure and an example of this is encapsulated Cu–histidine complex [158]. The Na^+ ion present in the zeolite cavity could also be exchanged with a complex, e.g. $[\text{Cu}(\text{en})_2]^{2+}$, allowing the complex to pass through the pore opening of zeolites [159]. Several other types of zeolite encapsulated complexes have been synthesized and characterized in the voids of zeolites under this method [160].

2.7 Schiff-bases and their complexes

2.7.1 General Overview

Schiff-base ligands have been in the chemistry catalogue for over 150 years [161]. H. Schiff was the first to report the synthesis of Schiff-base metal complexes as early as in the 1860's [162]. It was not until the 1950's that intensive studies and rapid advances in this field became evident.

In recent studies, Schiff-base ligands have shown to play a huge role in the chemistry of transition metal complexes. The literature clearly shows that the study of this diverse ligand system is linked with many key advances made in inorganic chemistry [163 - 170]. They are usually formed by condensation between amines and aldehydes. The resulting imine ($\text{R}_1\text{HC}=\text{N}-\text{R}_2$) can participate in binding to metal ions through the nitrogen atom with its lone pair electrons. Ketones can also form Schiff-base ligands ($\text{R}_1\text{R}_2\text{C}=\text{N}-\text{R}_3$) but aldehydes are more reactive than ketones [171].

This ligand system has not only played a seminal role in the development of modern coordination chemistry, but can be found at key points in the development of inorganic, biochemistry, catalysis medical imaging, optical materials and thin films [172]. Advantages of these ligands in catalysis show that they enhance the solubility and stability of either homogeneous or heterogeneous catalytic complexes. Catalysts in homogeneous medium with Schiff-base containing transition metals such as Cu(II), Ni(II) and Co(II) were also employed for the hydroxylation of phenol to specific products [173-175]. An advantage of Schiff-base transition metal complexes is they are attractive oxidation catalysts for different kinds of organic substrates as these ligands are cheap and convenient to synthesize, and are thermally and chemically stable. There are also several reports on different catalysts for the transformation of various simple organic substrates to functionalized derivatives which are of commercial interest [176 - 179]. Figure 2.6 represents some examples of Schiff-base ligand structures.

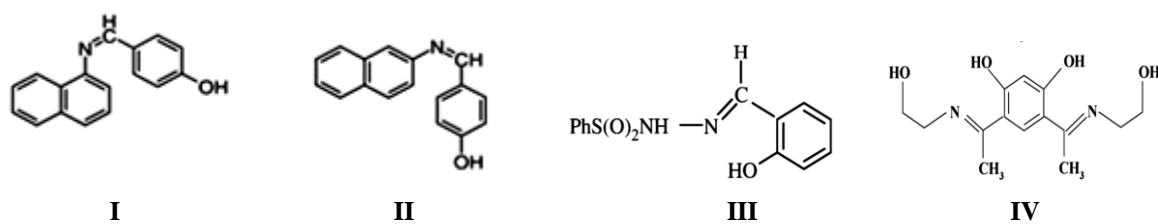


Figure 2.6 Examples of different types of Schiff-base ligands with its characteristic C=N group [180 - 182].

Schiff-base transition metal complexes are now also employed as catalysts for Suzuki-Miyaura cross coupling reactions as they were found to display high catalytic activity under mild reaction conditions [183]. Schiff-base metal complexes are important systems in asymmetric catalysis and they often mimic biological sites [184]. A wide range of different ligands can be prepared and complexed to transition metals to form transition metal complexes which find wide application in catalysis. Metal complexes of these ligands are widely reported in the literature and find application as catalysts for numerous chemical transformations [168, 185-191]. These complexes could also be immobilized on polymeric organic materials such as resins, or polystyrene [192], supported on inert porous solid such as alumina [193] and silica or encapsulated in the pores of zeolite-Y [194]. Schiff-base complexes encapsulated inside zeolite Y form chelate complexes which could be considered as the most extensively studied as this type of complex has a flexible conformation consisting of various geometries namely planar, umbrella-type and stepped configurations. As a result, they could generate active-site environments for different oxidation reactions [191, 195].

Numerous studies on the hydroxylation of phenol have been published using different Schiff base transition metal complexes such as encapsulated complexes in zeolite-Y, alumina-supported [196-198].

It is clear from the review of the literature that zeolite encapsulated metal complexes have provided opportunities to explore effective catalysts for various industrial processes. For the oxidation reactions, specifically, contributions of these types of catalysts are widely documented. The present study is aimed to describe the syntheses of zeolite-Y encapsulated

metal complexes of Cu(II) and OV(IV) with the following ligands: 7-amino-5-aza-4-methylhept-3-en-one and bis(acetylaceton)ethylenediamine, for the first time. Previous studies on oxovanadium and copper complexes indicate their uses as potential catalysts to influence the yield and selectivity in chemical transformations [199, 200]. As we go through various oxidation reactions *viz.* benzene, phenol, cyclohexene and styrene oxidation, we observe that, in spite of considerable research, catalytic activity studies of these reactions using the above mentioned encapsulated synthesized complexes have not been investigated. It was, therefore, reasonable to undertake systematic study of the synthesis and characterization of these catalysts and test their catalytic potential under optimized reaction conditions towards the oxidation of these substrates.



References

- [1] Holm R.H., Berg J.M., Toward functional models of metalloenzyme active sites: analog reaction systems of the molybdenum oxo transferases, *Acc Chem Res*, 19 (1986) 363-370.
- [2] Gheller S.F., Schultz B.E., Scott M.J., Holm R.H., A broad-substrate analog reaction system of the molybdenum oxotransferases, *J Am Chem Soc*, 114 (1992) 6934 -6935
- [3] Dinda R., Sengupta P., Ghosh S., Sheldrick W.S., Synthesis, structure, and reactivity of a new mononuclear molybdenum(VI) complex resembling the active center of molybdenum oxotransferases, *Eur J Inorg Chem*, (2003) 363 - 369.
- [4] Gupta K.C., Sutar A. K., Lin C., Polymer-supported Schiff base complexes in oxidation reactions, *Coord Chem Rev* 253 (2009) 1927.
- [5] Parshall G.W, Ittel S. D., *Homogeneous catalysis: the applications and chemistry of catalysis by transition metal complexes* Wiley (1992).
- [6] Van de Coevering R., Klein Gebbink R. J.M., van Koten G., Soluble organic supports for the non-covalent immobilization of homogeneous catalysts; modular approaches towards sustainable catalysts, *Prog Polym Sci* 30 (2005) 475.
- [7] He Y., Cai C., Polymer-supported macrocyclic Schiff base palladium complex: An efficient and reusable catalyst for Suzuki cross-coupling reaction under ambient condition, *Catal Commun*, 12 (2011) 678.
- [8] Kamer P.C.J, van Leeuwen P.W.N.M., *Phosphorus(III) Ligands in Homogeneous Catalysis: Design and Synthesis*, Wiley (2012) 464.
- [9] Fahlman B.D., *Materials Chemistry*, Springer (2007) 237.
- [10] Cornils B., Herrmann W.A., *Aqueous-Phase Organometallic Catalysis*, Wiley-VCH (2006) 3.
- [11] Wang C.-C. , Li W.-S., Cheng S.-K., Chen C.-Y., Chen C.-Y., Kuob J.-F., Peroxidation of benzaldehyde by polymer-immobilized cobalt-EDTA complex, *React Funct Polym*, 51 (2002) 69.
- [12] Li Y., Fu X., Gong B., Zou X., Tu X., J. Chen, Synthesis of novel immobilized tridentate Schiff base dioxomolybdenum(VI) complexes as efficient and reusable catalysts for epoxidation of unfunctionalized olefins, *J Mol Catal A: Chem*, 322 (2010) 55.

- [13] Wang X.L., Wu G.D., Li J.P., Zhao N., Wei W., Sun Y.H., Selective oxidation of benzyl alcohol catalyzed by Cr(salen) complexes immobilized on MCM-41, *J Mol Catal A: Chem* 276 (2007) 86-94.
- [14] Clark J.H., Green chemistry: challenges and opportunities, *Green Chem* 1 (1999) 1.
- [15] Bhaduri S., Mukesh D., *Homogeneous Catalysis: Mechanisms and Industrial Applications*, Wiley-Interscience (2000) 7.
- [16] Varma G.R., Graydon W.F., Heterogeneous catalytic oxidation of cumene (isopropyl benzene) in liquid phase, *J Catal* 28 (1973) 236.
- [17] Neuburg H.J., Basset J.M., Graydon W.F., Heterogeneous liquid-base oxidation of cyclohexene with manganese dioxide as catalyst, *J Catal* 25 (1972) 425.
- [18] Hrones M., Hrabe Z., *Ind Eng Chem Prod Res* 25 (1986) 257.
- [19] Chou T.C., Lee C.C., Heterogenizing homogeneous catalyst. 1. Oxidation of acetaldehyde, *Ind Eng Chem Fundam* 24 (1985) 32.
- [20] Prasad K.M., Athappan R., Srivastava R.D., Kinetics of oxidation of tetralin over supported NiO catalyst *J Catal* 59 (1979) 460.
- [21] Sadana A., Katzer J.R., Catalytic Oxidation of Phenol in Aqueous Solution over Copper Oxide, *Ind Eng Chem Fundam* 13 (1974) 127
- [22] Yokoyama T., Nishizawa M., Kimura T., Suzuki T.M., Catalytic Epoxidant of olefins with t-butyl hydroperoxide in the presence of polymer-supported vanadium (5) and (6) complexes, *Bull., Chem Soc Jpn* 58 (1985) 3271.
- [23] Gates B.C., Knoezinger H., Jentoft F.C., *Advances in Catalysis*, Elsevier, V54 (2011) 111.
- [24] Iwasawa Y., *Catalysis by complexes: Tailored Metal Catalysis*, D. Reidel Publishing Company (1986) 4
- [25] Kozlov A., Asakura K., Iwasawa Y., Synthesis and characterization of vanadium (IV) complexes in NaY zeolite supercages, *Micropor Mesopor Mater* 21 (1998) 579.
- [26] Ichikawa M., "Ship-in-Bottle" Catalyst Technology: Novel templating fabrication of platinum group metals nanoparticles and wires micro/mesopores, *Platinum Met Rev* 44 (2000) 3.
- [27] Kowalak S., Weiss R.C., Balkus Jr. K.J., Zeolite encapsulated Pd(salen), a selective hydrogenation catalyst, *J Chem Soc, Chem Commun* (1991) 57.
- [28] Freemantle M., *An Introduction to Ionic Liquids*, RSC publishing (2009) 48

- [29] Buchmeiser M.R., *Polymeric Materials in Organic Synthesis and Catalysis*, Wiley-VCH, (2003) 207, 278.
- [30] Kohlpaintner C. W., Fischer R. W., Cornils B., *Aqueous biphasic catalysis: Ruhrchemie/Rhône-Poulenc oxo process*, *Appl Catal A: Gen* 221 (2001) 219.
- [31] Dyson P. J., Geldbach T. J., *Metal Catalysed Reactions in Ionic Liquids*, Springer (2005) 2.
- [32] Arhancet J.P, Davis M.E, Merola J. S, Hanson B. E, *Hydroformylation by supported aqueous-phase catalysis: a new class of heterogeneous catalysts*, *Nature* 339 (1989) 454-455.
- [33] Beckmann A., Keil F. J., *Increasing yield and operating time of SLP-catalyst processes by flow reversal and instationary operation*, *Chem Eng Sci* 58 (2003) 841.
- [34] Kirschning A., *Immobilized Catalysts: Solid Phases, Immobilization and Applications* 242 Springer (2004) 243.
- [35] Wicke E., Bartsch A., *Percolation and blocking in supported liquid-phase catalysts: styrene catalyst as a particular case*, *Ind. Eng. Chem. Res.* 29 (1990) 994.
- [36] Lucke, Kockritz A., Vorlop K.D., Bischoff S., Kant M., *Heterogenization of Homogeneous Catalysts by Encapsulation - Stiff Cage Versus Flexible Skin*, *Top Catal* 29 (2004) 111- 118
- [37] Behr A., Neubert P., *Applied Homogeneous Catalysis*, Wiley (2012) 213.
- [38] Voit A., Adler H.J, Bohme F., *Synthesis of defined Polymer Architectures*, Wiley-VCH (2002) 164.
- [39] Chaudhari R.V, Bhattacharya A., Bhanage B.M, *Catalysis with soluble complexes in gas-liquid-liquid systems*, *Catal Today* 24 (1995) 123-133.
- [40] Figueiredo, J.L., Pereira M.M., Faria J., *Catalysis from Theory to Application: An Integrated Course*, University Coimbra Press (2008) 214 - 216.
- [41] Serp P., Figueiredo J. L., *Carbon Materials for Catalysis*, John Wiley & Sons (2009) 268-269.
- [42] Barbaro P., Liguori F., *Heterogenized Homogeneous Catalysts for Fine Chemicals Production: Materials and Processes*, Springer Vol 33 (2010) 125, 369.
- [43] Saluzzo C., ter Halle R., Touchard F., Fache F., Schulz E., Lemaire M., *Recent progress in asymmetric heterogeneous catalysis: use of polymer-supported catalysts*, *J Organomet Chem* 603 (2000) 30.

- [44] Brunel D., Functionalized micelle-templated silicas (MTS) and their use as catalysts for fine chemicals, *Micropor Mesopor Mater* 27 (1999) 329.
- [45] Heckel A., Seebach D., Immobilization of TADDOL on porous silica gel with high loading and first applications in enantioselective catalysis, *Angew Chem Int Ed* 112 (2000) 165.
- [46] Sayah R., Le Floch M., Framery E., Dufaud V., Immobilization of chiral cationic diphosphine rhodium complexes in nanopores of mesoporous silica and application in asymmetric hydrogenation, *J Mol Catal A: Chem* 315 (2010) 54.
- [47] Blum J., Avnir D., Schumann H., *Chemtech* 29 (1999) 32.
- [48] Abu-Reziq R., Avnir D., Miloslavski I., Schumann H., Blum J., Entrapment of metallic palladium and a rhodium(I) complex in a silica sol-gel matrix: Formation of a highly active recyclable arene hydrogenation catalyst *J Mol Catal A: Chem*, 185 (2002) 179-185.
- [49] Graham B., Spiccia L., Hearn M. T.W., Comparison of the binding behavior of several histidine-containing proteins with immobilized copper(II) complexes of 1,4,7-triazacyclononane and 1,4-bis(1,4,7-triazacyclononan-1-yl)butane, *J Chrom B* 879 (2011) 844.
- [50] Derouane E.G., Roberts S.M., *Catalysts for Fine Chemical Synthesis, Microporous and Mesoporous Solid*, Wiley Vol 4 (2006) 208-209.
- [51] Selke R., Capka M., Carbohydrate phosphinites as chiral ligands for asymmetric syntheses catalyzed by complexes: Part VIII1: Immobilization of cationic rhodium(I) chelates of phenyl 4,6-O-(R)-benzylidene-2,3-bis(O-diphenylphosphino)- β -D-glucopyranoside on silica, *J Mol Catal A: Chem.* 63 (1990) 319.
- [52] Tas D., Jeanmart D., Parton R.F., Jacobs P.A., The immobilization of sulfonated Ru-BINAP chloride by anion exchange on layered double hydroxides *Stud Surf Sci Catal.* 108 (1997) 493.
- [53] McDonagh C., O'Conghaile P., Klein Gebbink R. J. M., O'Leary P., Electrostatic immobilisation of copper(I) and copper(II) bis(oxazoliny)pyridine catalysts on silica: application to the synthesis of propargylamines via direct addition of terminal alkynes to imines, *Tetrahedron Lett* 48 (2007) 4388.
- [54] Zhang L., Luo S., Cheng J., Non-covalent immobilization of asymmetric organocatalysts, *Catal Sci Technol* 1 (2011) 512.

- [55] Gill C.S., Novel hybrid organic/inorganic, single sited catalysts and supports for fine chemical and pharmaceutical intermediates synthesis, Georgia Institute of Technology, (2009) 4-6.
- [56] Gelman F., Avnir D., Schumann H., J. Blum, Sol-gel entrapped chiral rhodium and ruthenium complexes as recyclable catalysts for the hydrogenation of itaconic acid, *J Mol Catal A* 146 (1999) 123.
- [57] Bansal N.P., Boccaccini A. R., *Ceramics and Composites Processing Methods*, Wiley -American Ceramic Society (2012) 183-184.
- [58] Niederberger M., Nonaqueous Sol-Gel Routes to Metal Oxide Nanoparticles, *Acc Chem Res* 40 (2007) 794.
- [59] Niederberger M., Pinna N., *Metal Oxide Nanoparticles in Organic Solvents: Synthesis, Formation, Assembly and Application*, Springer (2009) 12-13.
- [60] Bilecka I., Niederberger M., New developments in the nonaqueous and/or non-hydrolytic sol-gel synthesis of inorganic nanoparticles, *Electrochim Acta* 55 (2010) 7720.
- [61] Blum J., Avnir D., Schumann H., Sol-gel encapsulated transition-metal catalysts *Chemtech* 29 (1999) 32.
- [62] Riedel R., Chen I.W., *Ceramics Science and Technology, Structures*, Wiley-VCH (2008) 302.
- [63] Balkus Jr. K.J., Gabrielov A.G, Zeolite encapsulated metal complexes, *J Inclusion Phenom Mol Recognit Chem* 21 (1995) 159.
- [64] De Vos D.E., Thibault-Starzyk F., Knops-Gerrits P.P., Parton R.F., Jacobs P.A., A critical overview of the catalytic potential of zeolite supported metal complexes, *Macromol Symp* 80 (1994) 157.
- [65] De Vos D.E., Knops-Gerrits P.P., Parton R.F., Weckhuysen B.M., Jacobs P.A., Schoonheydt R.A., *Coordination Chemistry in Zeolites*, *J Inclusion Phenom Mol Recognit Chem* 21 (1995) 185
- [66] Romanovsky B., Transition metal complexes in inorganic polymers as enzyme mimics *Macromol Symp* 80 (1994) 185.
- [67] Díaz J. F, Balkus K. J, Enzyme immobilization in MCM-41 molecular sieve, *J Mol Catal B: Enzym* 2 (1996) 115-126.

- [68] Balkus Jr. K.J., Khanmamedova A.K., Dixon K.M., Bedioui F., Oxidations catalyzed by zeolite ship-in-a-bottle complexes, *Appl Catal A: Gen* 143 (1996) 159-160.
- [69] Silva M., Freire C., de Castro B., Figueiredo J.L., Styrene oxidation by manganese Schiff base complexes in zeolite structures, *J Mol Cat A: Chem* 258 (2006) 328.
- [70] Kozlov A., Kozlova A., Asakura K., Iwasawa Y., Zeolite-encapsulated vanadium picolinate peroxo complexes active for catalytic hydrocarbon oxidations, *J Mol Cat* 137 (1999) 235.
- [71] Derouane E.G., Haber J., Lemos F., F. Ramôa Ribeiro, Guisnet M., *Catalytic Activation and Functionalisation of Light Alkanes: Advances and Challenges*, Kluwer Academic Publishers (1998).
- [72] Salavati-Niasara M., Ganjali R.M, Norouzi, Host (nanopores of zeolite Y)- guest (oxovanadium(IV) tetradentate schiff-base complexes) nanocomposite materials: synthesis, characterization and liquid phase hydroxylation of phenol with hydrogen peroxide, *J Porous Mater* 14 (2007) 423-424.
- [73] Basset J., Psaro R., Roberto D., Ugo R., *Modern Surface Organometallic Chemistry*, Wiley-VCH (2009) 210.
- [74] Jacob C.R., Varkey S.P., Ratnasamy P., Selective oxidation over copper and manganese salens encapsulated in zeolites, *Micropor Mesopor Mater* 22 (1998) 465.
- [75] Jacob C.R., Varkey S.P., Ratnasamy P., Oxidation of para-xylene over zeolite-encapsulated copper and manganese complexes, *Appl Catal A* 182 (1999) 91.
- [76] Jacob C.R., Varkey S.P., Ratnasamy P., Zeolite-encapsulated copper (X2-salen) complexes, *Appl Catal A* 168 (1998) 353.
- [77] Pinnavaia T.J., Raythatha R., John Guo-Shuh Lee, L. J. Halloran, James F. Hoffman, Intercalation of catalytically active metal complexes in mica-type silicates. Rhodium hydrogenation catalysts, *J Am Chem Soc*, 101 (1979) 6891.
- [78] Miyata S., The Syntheses of Hydrotalcite-Like Compounds and Their Structures and Physico-Chemical Properties I: The Systems $Mg^{2+}-Al^{3+}-NO_3^-$, $Mg^{2+}-Al^{3+}-Cl^-$, $Mg^{2+}-Al^{3+}-ClO_4^-$, $Ni^{2+}-Al^{3+}-Cl^-$ and $Zn^{2+}-Al^{3+}-Cl^-$, *Clays Clay Minor* 23 (1975) 369.
- [79] Pinnavaia T.J., Intercalated clay catalysts, *Science* 220 (1983) 365.
- [80] Butruille J.M., Pinnavaia T.J., in I.E. Wachs, *Characterization of Catalytic Materials*, Butterworth - Heinemann, Boston, (1992) 149.

- [81] Crocker M., Herold R.H.M., Stabilisation of cationic iridium hydrogenation catalysts via intercalation in montmorillonite clay, *Cat Lett* 18 (1993) 243.
- [82] Kshirsagar V.S, Garade A.C., Mane R.B, Patil K.R, Yamaguchi A., Shirai M., Rode C.V, Characterization of clay intercalated cobalt-salen catalysts for the oxidation of p-cresol, *Appl Catal A: Gen* 370 (2009) 20.
- [83] Shi H., He J., Orientated intercalation of tartrate as chiral ligand to impact asymmetric catalysis *J Catal* 279 (2011) 157.
- [84] W.H Quayle, T. J Pinnavaia, Utilization of a cationic ligand for the intercalation of catalytically active rhodium complexes in swelling, layer-lattice silicates, *Inorg Chem* 18 (1979) 2841.
- [85] Somanathan R., Cortez N.A., Parra-Hake M., Chávez D., Aguirre G., Immobilized Chiral Metal Catalysts for Enantioselective Hydrogenation of Ketones, *Mini-Rev Org Chem*, 5 (2008) 313.
- [86] Walsh P.J., M. C. Kozlowski, *Fundamentals of Asymmetric Catalysis*, University Science Books (2009) 497 - 498.
- [87] Yang Y., Zhang Y., Hao S., J. Guan, H.Ding, F. Shang, P. Qiu, Q. Kan, Heterogenization of functionalized Cu(II) and VO(IV) Schiff base complexes by direct immobilization onto amino-modified SBA-15: Styrene oxidation catalysts with enhanced reactivity, *Appl Catal A: Gen* 381 (2010) 275.
- [88] Benaglia M., *Recoverable and Recyclable Catalysts*, Wiley (2009) 17.
- [89] P. R. Dvornic, Owen M. J., *Silicon-Containing Dendritic Polymers*, Springer (2009)197.
- [90] (a) Dickerson T.J, Reed N.N, K.D Janda., Soluble Polymers as Scaffolds for Recoverable Catalysts and Reagents, *Chem Rev* 102 (2002) 3325 – 3344.
(b) Bergbreiter D.E., Using Soluble Polymers To Recover Catalysts and Ligands, *Chem Rev* 102 (2002) 3345-3384.
- [91] Hamidi A., Rashidi M. R., Asgari D., Aghanejad A., Davaran S., Covalent Immobilization of Trypsin on a Novel Aldehyde-Terminated PAMAM Dendrimer, *Bull Korean Chem Soc* 33 (2012) 2181.
- [92] Kishore M.J.L., Kumar A., Heteronuclear macrocyclic iron-copper complex catalyst covalently bonded to modified alumina catalyst for oxidation of cyclohexane, *Ind Eng Chem Res* 46 (2007) 4787- 4798.

- [93] Lal S., Anisia K.S, Kumar A., Depolymerization of HDPE to wax in the presence of a catalyst formed by homonuclear macrocyclic zirconium complex chemically bonded to alumina support, *Appl. Catal. A: Gen.* 303 (2006) 9-17.
- [94] Kishore M.J.L, Mishra G.S, Kumar A., Synthesis of hetero binuclear macrocyclic Co^{V} complex bonded to chemically modified alumina support for oxidation of cyclohexane using oxygen, *J Mol Catal A: Chem* 230 (2005) 35-42.
- [95] Rao Y.V.S, Devos D.E, Wouters B., Grobet P.J, Jacobs P.A, Immobilization of triazacyclononane-type metal complexes on inorganic supports via covalent linking: spectroscopy and catalytic activity in olefin oxidation, *Stud Surf Sci Catal* 110 (1997) 973-980.
- [96] Pillinger M., Goncalves I.S, Lopes A.D, Madureira J., Ferreira P., Valente A.A, Santos T.M, Rocha J., Menenez J.F.S, Carlos L.D., Synthesis and characterisation of a $\text{RuII}([14]\text{aneS4})$ complex immobilised in MCM-41-type mesoporous silica, *J Chem Soc Dalton Trans*, 10 (2001) 1628 - 1633.
- [97] Sojandi, Han S.C, Han D.S, Park, S.E, Microwave assisted-direct synthesis of highly ordered large pore functionalized mesoporous SBA, *Stud Surf Sci Catal* 172 (2007) 353-356.
- [98] Herron N., Ismaeeli M., Farzaneh F., Ghandi M., Nickel(macrocycle) Complexes Immobilized within Montmorillonite and MCM-41 as Catalysts for Epoxidation of Olefins, *J Incl Phenom Macro*, 54 (2006) 23-28.
- [99] Fukuoka A., Higashimoto N., Sakamoto Y., Sasaki M., Sugimoto N., Inagaki S., Fukushima Y., Ichikawa M., Ship-in-bottle synthesis and catalytic performances of platinum carbonyl clusters, nanowires, and nanoparticles in micro- and mesoporous materials, *Catal Today*, 66 (2001) 23.
- [100] Zulauf A., Mellah M., Hong X., Schulz E., Recoverable chiral salen complexes for asymmetric catalysis: recent progress, *Dalton Trans* 39 (2010) 6924, 6928
- [101] Roth W.J., Dorset D.L., Expanded view of zeolite structures and their variability based on layered nature of 3-D frameworks, *Micropor Mesopor Mater* 142 (2011) 32-36.
- [102] Dyer A., *An introduction to zeolite molecular sieves*, NY: John-Wiley & Sons (1988).
- [103] Gates B.C, *Catalytic chemistry*, NY: John-Wiley & Sons, (1992).

- [104] Lim W.T, Seo S.M, Wang L., Lu G.Q., Heo N.H., Seff K., Single-crystal structures of highly NH_4^- -exchanged, fully deaminated, and fully Ti^+ -exchanged zeolite Y (FAU, $\text{Si}/\text{Al} = 1.56$), all fully dehydrated, *Micropor Mesopor Mat* 129 (2010) 15
- [105] Baerlocher A., Meier W.M., Olson D.H, *Atlas of Zeolite Framework Types*, Elsevier, (2001).
- [106] Buchwald A., Zellmann H.D., Kaps C., Condensation of aluminosilicate gels-model system for geopolymer binders, *J Non-Cryst Sol*, 357 (2011) 1378.
- [107] Rios R., C.A.; Oviedo V., J.A.; Henao M., J.A.; Macias L., M.A., NaY zeolite synthesized from Colombian industrial coal by-products: Potential catalytic applications, *Catal Tod* 190 (2012) 62.
- [108] Mortensen A., *Concise Encyclopedia of Composite Materials*, Elsevier (2007) 837.
- [109] Naccache A., Ben Taarit Y., ESR study of copper(II) ions in Y zeolite: Effect of water, ammonia and pyridine adsorption, *Chem Phys Lett* 11 (1971) 11-15
- [110] Vansant E.F., Lunsford J.H., Electron paramagnetic resonance study of copper(II)-ammonia complexes in Y-type zeolites, *J Phys Chem* 76 (1972) 2860-2865.
- [111] Lunsford J.H., E.F. Vansant, Formation and structure of penta- and hexa-coordinate cobalt (II)-methyl isocyanide complexes in Y-type zeolites, *J Chem Soc Faraday Trans 2*, 69 (1973)1028-1035.
- [112] Flentge D.R., Lunsford J.H., Jacobs P.A., Uytterhoeven J.B., Spectroscopic evidence for the tetraamminecopper(II) complex in a Y-type zeolite, *J Phys Chem* 79 (1975) 354-360.
- [113] Meyer G., Wöhrle D., Mohl M., Schulz-Ekloff G., Synthesis of faujasite supported phthalocyanines of cobalt, nickel and copper, *Zeolites* 4 (1984) 30-34.
- [114] Herron N., Stucky G.D., Tolman C.A., Shape selectivity in hydrocarbon oxidations using zeolite encapsulated iron phthalocyanine catalysts, *J Chem Soc Chem Commun* (1986) 1521-152
- [115] Sheldon R.A., Kochi J.K., *Metal Catalyzed Oxidations of Organic Compounds*, Academic Press, New York (1981).
- [116] Traylor T.G., Mikszta A.R., Alkene epoxidations catalyzed by iron(III), manganese(III), and chromium(III) porphyrins. Effects of metal and porphyrin substituents on selectivity and regiochemistry of epoxidation, *J Am Chem Soc* 111 (1989) 7443.

- [117] Medina J.C., Gabriunas N., Pa´ez-Mozo E., Cyclohexene oxidation with an iron cyclam-type complex encapsulated in Y-zeolite, *J Mol Catal A*, 115 (1997) 233-239.
- [118] Kowalak S., Weiss R.C., Balkus Jr. K.J., Zeolite encapsulated Pd(salen), a selective hydrogenation catalyst, *J Chem Soc Chem Commun*, (1991) 57-58.
- [119] Herron N., Tolman C.A., A highly selective zeolite catalyst for hydrocarbon oxidation. A completely inorganic mimic of the alkane .omega.-hydroxylases, *J Am Chem Soc* 109 (1987) 2837-2839.
- [120] Maurya M.R., Titinchi S.J.J., Chand S., Mishra I.M., Zeolite-encapsulated Cr(III), Fe(III), Ni(II), Zn(II) and Bi(III) salpn complexes as catalysts for the decomposition of H₂O₂ and oxidation of phenol, *J Mol Catal A* 180 (2002) 201-209.
- [121] Pires E.L., Magalhaes J.C., Schuchardt U., Effects of oxidant and solvent on the liquid-phase cyclohexane oxidation catalyzed by Ce-exchanged zeolite Y, *Appl Catal A: Gen* 203 (2000) 231-237.
- [122] Varkey S.P., Ratnasamy C., Ratnasamy P., Zeolite-encapsulated manganese(III)salen complexes, *J Mol Catal A* 135 (1998) 295-306.
- [123] Kimura T., Fukuoka A., Ichikawa M., Characterization of zeolite-encapsulated iron phthalocyanines and butadiene hydrogenation catalyzed by their electron donor-acceptor complexes with sodium, *Catal Lett* 4 (1990) 279-285.
- [124] Bedioui F., Zeolite-encapsulated and clay-intercalated metal porphyrin, phthalocyanine and Schiff-base complexes as models for biomimetic oxidation catalysts: an overview, *Coord Chem Rev* 144 (1995) 43.
- [125] V. J. Frilette, P.B. Weisz, R. L. Golden, Catalysis by crystalline aluminosilicates I. Cracking of hydrocarbon types over sodium and calcium "X" zeolites, *J Catal* 1 (1962) 301-306.
- [126] Weisz P.B., Frilette V. J., Maatman, Mower E.B., Catalysis by crystalline aluminosilicates II. Molecular-shape selective reactions, *J Catal*, 1 (1962) 307.
- [127] Sugi Y., Maekawa H., Hasegawa Y., Ito A., Asai R., Yamamoto D., Komura K., Kubota Y., Kim J., Seo G., The alkylation of biphenyl over three-dimensional large pore zeolites: The influence of zeolite structure and alkylating agent on the selectivity for 4,4'-dialkylbiphenyl, *Catal Today* 131 (2008) 413-422.
- [128] Weisz P.B., Molecular Shape Selective Catalysis, *Pure Appl Chem* 52 (1980) 2091.

- [129] Karge H.G., Weitkamp J., *Molecular Sieves: Science and Technology Characterization II*, Springer-Verlag Berlin Heidelberg, Vol 5 (2007) 126.
- [130] Csicsery S.M, *Catalysis by shape selective zeolites-science and technology*, Pure App Chem 58 (1986) 841-856.
- [131] Weitkamp J., Puppe L., *Catalysis and Zeolites: Fundamentals and Applications*, Springer (1999) 382.
- [132] Niwa M., Katada N., Okumura K., *Characterization and design of zeolite catalysts* Springer (2010).
- [133] Huheey J.E., *Inorganic Chemistry*, Harper Collins Publishers, NewYork, (1992)
- [134] Inui T., Namba S., Tatum T., *Chemistry of Microporous Crystals*, Stud Surf Sci Catal, Elsevier, 60 (1991) 225.
- [135] Chen N.Y., Garwood W.E., Dwyer F.G., *Shape Selective Catalysis in Industrial Applications*, Marcel Dekker, NewYork (1989).
- [136] Corbin D.R., Herron N., *Designing zeolite catalysts for size and shape selective reactions*, J Mol Catal 86 (1994) 343.
- [137] Herron N., *The Selective Partial Oxidation of Alkanes using Zeolite Based Catalysts. Phthalocyanine (PC) "Ship-in-Bottle" Species*, J Coord Chem 19 (1988) 25.
- [138] Inagaki S., Kamino K., Kikuchi E., Matsukata M., *Shape selectivity of MWW-type aluminosilicate zeolites in the alkylation of toluene with methanol* Appl Cat A:Gen, 318 (2007) 26.
- [139] Xuereb A. J., Raja R., *Design strategies for engineering selectivity in bio-inspired heterogeneous catalysts*, Catal Sci Technol 1 (2011) 521.
- [140] Ozin G. A, Gil C., *Intrazeolite organometallics and coordination complexes: internal versus external confinement of metal guests*, Chem Rev 89 (1989) 1749
- [141] Herron N., *A cobalt oxygen carrier in zeolite Y. A molecular "ship in a bottle"*, Inorg Chem 25 (1986) 4714.
- [142] Balkus Jr. K.J, Welch A.A, Gnade B.E, *The preparation and characterization of Rh(III) SALEN complexes encapsulated in zeolites X and Y*, Zeolites 10 (1990) 722.
- [143] G. Schulz-Ekloff, S. Ernst, G. Ertl, et al. (Eds.), *Handbook of Heterogeneous Catalysis* Wiley-VCH (1997) 374.
- [144] Bowers A., Dutta, *Olefin oxidation by zeolite-encapsulated Mn(salen)⁺ complexes under ambient conditions*, J Catal 122 (1990) 271.

- [145] Gaillon L., Sajot N., Bedioui F., Devynck J., Balkus Jr. K.J, Electrochemistry of zeolite-encapsulated complexes : Part 3. Characterization of iron and manganese SALEN entrapped in Y faujasite type zeolite, *J Electroanal Chem* 345 (1993) 157.
- [146] Gabrielov A., Balkus Jr. K.J, Bell S.L, Bedioui F., Devynck J., Faujasite-type zeolites modified with iron perfluorophthalocyanines: Synthesis and characterization, *Micropor Mater* 2 (1994) 119.
- [147] Balkus Jr. K.J, Gabrielov A., Bell S.L, Bedioui F., Roue L., Devynck J., "Zeolite Encapsulated Co(II) and Cu(II) Perfluorophthalocyanines: Synthesis and Characterization, *Inorg Chem* 33 (1994) 67.
- [148] Parton R.F., Bezoukhanova, Grobet J., Grobet P.J, Jacobs P.A, Synthesis, Characterization and Catalytic Performance of Nitro-substituted Fe-phthalocyanines on Zeolite Y, *Stud Surf Sci Catal* 83 (1994) 371.
- [149] Zsigmond A., Notheisz F., Frater Z., Backvair J.E., Selective oxidation of benzyl alcohol on a zeolite ship-in-a-bottle complex, *Stud Surf Sci Catal* 108 (1997) 453.
- [150] Yaun X., Li F., Wang L., Luo H.A, Synthesis, characterization of CoSalen/NaY and the catalytic performance for aerobic oxidation of cyclohexane, *Lat Am Appl Res* 37 (2007) 151.
- [151] Chan Y.W, Wislon R.B, Partial oxidation of methane using supported porphyrin and phthalocyanine complexes, *Preprint Papers – ACS, Div Fuel Chem* 33 (1988) 453.
- [152] Oyama S.T., Gaffney A.M., Lyons J.E., Grasselli R.K., *Studies in surface science and catalysis : Third World Congress on Oxidation Catalysis*, Elsevier (1997) 160.
- [153] V. Yu. Zakharov, O. M. Zakharova, B. V. Romanovsky, R. E. Mardaleishvili, *React Kinet Catal Lett* 6 (1977) 133.
- [154] Rao L.F, Fukuoka A., Ichikawa M., Selective formation of lower alkenes and alcohols in CO + H₂ reaction catalysed on NaY zeolite-encapsulated Rh₆ and RhFe bimetallic cluster-derived catalysts, *J Phys Chem Soc Chem Commun* 7 (1988) 458-460.
- [155] Takahashi N., Mijin A., Suematsu H., Shinohara S., Matsuoka H., An infrared study of the Rh-Y zeolite related to activity for ethylene hydroformylation, *J Catal*, 117 (1989) 348- 354.

- [156] Rao L.F., Fukuoka A., Kosugi N., Kuroda H., M. Ichikawa, Characterization of NaY-entrapped hexadecacarbonylhexarhodium cluster by FTIR and EXAFS spectroscopies and the catalytic behavior in carbon-13 monoxide isotopic exchange reaction, *J Phys Chem* 94 (1990) 5317-5327.
- [157] Henson B.E., Davis M.E., Taylor D., Rode E., Intrazeolite rhodium carbonyl and rhodium carbonyl phosphine complexes, *Inorg Chem* 23 (1984) 52-56.
- [158] Weckhuysen B.M., Verberckmoes A.A., Fu L., Schoonheydt R.A, *J. Phys Chem*, 100 (1996) 9456–9461.
- [159] Velghe F., Schoonheydt R.A, Uytterhoeven J.B., Peigneur P., Lunsford J.H., *J. Phy. Chem.* 81 (1997) 1187 – 1194.
- [160] Vadrine J.C., Deroune F.G., Taarit Y.B. *J. Phys. Chem.* 8 (1974) 531 – 535.
- [161] Yamada S., Advancement in stereochemical aspects of Schiff base metal complexes, *Coord Chem Rev* 192 (1999) 537.
- [162] Valent A., Melni'k M., Hudecova' D., Dudova' B., Kiveka's R., Sundberg M.R., Copper(II) salicylidene-glycinate complexes as potential antimicrobial Agents, *Inorg Chim Acta* 340 (2002) 16.
- [163] Holm R.H., Studies on Ni(II) Complexes. I. Spectra of Tricyclic Schiff Base Complexes of Ni(II) and Cu(II), *J Am Chem Soc*, 82 (1960) 5632.
- [164] Niederhoffer E.C., Timmons J.H., Martell A.E., Thermodynamics of oxygen binding in natural and synthetic dioxygen complexes, *Chem Rev* 84 (1984) 137.
- [165] Srinivasan K., Michaud P., Kochi J.K., Epoxidation of olefins with cationic (salen) manganese (III) complexes. The modulation of catalytic activity by substituents, *J Am Chem Soc* 108 (1986) 2309.
- [166] Zhang W., Loebach J.L., Wilson S.R., Jacobsen E.N., Enantioselective epoxidation of unfunctionalized olefins catalyzed by salen manganese complexes, *J Am Chem Soc* 112 (1990) 2801.
- [167] Tisato F, Refosco F., Bandoli F., Structural survey of technetium complexes, *Coord Chem Rev* 135 (1994) 325.
- [168] Lacroix P.G., Second-Order Optical Nonlinearities in Coordination Chemistry: The Case of Bis(salicylaldiminato)metal Schiff Base Complexes, *Eur J Inorg Chem*, 2 (2001) 339.

- [169] Nagel J., Oertel U., Friedel P., Komber H., Mobius D., Langmuir-Blodgett Layers from Schiff Base Copper(II) Complexes, *Langmuir* 13 (1997) 4698.
- [170] Sundari S.S., Dhathathreyan A., Kanthimathi M., Balachandran U.N., Langmuir-Blodgett Films of Schiff Base Complexes of Copper(II), *Langmuir* 13 (1997) 4923.
- [171] Gupta K.C, Sutar A.K, Catalytic activities of Schiff base transition metal complexes, *Coord Chem Rev* 252 (2008) 1421.
- [172] Reglinski J., Morris S., Stevenson D. E., Supporting conformational change at metal centres. Part 1: octahedral systems, *Polyhedron* 21 (2002) 2167.
- [173] Chakraborty J., Patel R.N, Copper-, cobalt- and zinc(II) complexes with monofunctional bidentate Schiff base and monodentate neutral ligands, *J Ind Chem Soc* 73 (1996) 191.
- [174] Hugo J.N, Mapolie S. F, Van Wyk J.L, Cu(II) and Ni(II) complexes based on monofunctional and dendrimeric pyrrole-imine ligands: Applications in catalytic liquid phase hydroxylation of phenol, *Inorg Chim Acta* 363 (2010) 2643-2651.
- [175] Ray S., Mapolie S.F, Darkwa J., Catalytic hydroxylation of phenol using immobilized late transition metal salicylaldehyde complexes, *J Mol Cat A: Chem* 267 (2007) 143.
- [176] Yamada M., Araki K., Shiraishi S., Oxygenation of 2,6-di-*t*-butylphenol catalysed by a new cobalt(II) complex [Co(babp)]: a salen analogue having higher catalytic activity, selectivity, and durability, *J Chem Soc, Perkin Trans 1* (1990) 2687.
- [177] Sheldon R.A., Fine Chemicals by Catalytic Oxidation, *Chemtech* 21 (1991) 566.
- [178] Sheldon R.A., Arends I.W.C.E., Lempers H.E.B., Liquid phase oxidation at metal ions and complexes in constrained environments, *Catal Tod* 41 (1998) 387.
- [179] Grasselli R.K., Advances and future trends in selective oxidation and ammoxidation catalysis, *Catal Tod* 49 (1999) 141.
- [180] Abbo H.S, Titinchi S.J.J, Prasad R., Chand S., Synthesis, characterization and study of polymeric iron(III) complexes with bidentate *p*-hydroxy Schiff bases as heterogeneous catalysts, *J Mol Cat A: Chem* 225 (2005) 226.
- [181] Ahmed A.H, Mostafa A.G., Synthesis and identification of zeolite-encapsulated iron (II), iron (III)-hydrazone complexes, *Mater Sci Eng C* 29 (2009) 878.
- [182] Shebl M., Synthesis, spectral and magnetic studies of mono- and bi-nuclear metal complexes of a new bis(tridentate NO₂) Schiff base ligand derived from 4,6-diacetylresorcinol and ethanolamine, *Spec Acta Part A* 73 (2009) 314.

- [183] Liu J., Li Y., W Zheng, Synthesis of immobilized nanopalladium on polymer-supported, Schiff base, and study of its catalytic activity in the Suzuki–Miyaura reaction, *Monatsh Chem* 140 (2009) 1425-1429.
- [184] Morris G.A., Zhou H., Stern C.L., Nguyen S.T., A General High-Yield Route to Bis(salicylaldehyde) Zinc(II) Complexes: Application to the Synthesis of Pyridine-Modified Salen-Type Zinc(II) Complexes, *Inorg Chem* 40 (2001) 3222.
- [185] Jacobsen E.N., Pfaltz A., Yamamoto H., *Comprehensive Asymmetric Catalysis Vol 2* Springer (1999) 649.
- [186] Katsuki T., Catalytic asymmetric oxidations using optically active (salen) manganese(III) complexes as catalysts, *Coord Chem Rev* 140 (1995) 189-214.
- [187] Canali L., Sherrington D.C., Utilisation of homogeneous and supported chiral metal(salen) complexes in asymmetric catalysis, *Chem Soc Rev* 28 (1999) 85-93.
- [188] Kim G.J., Shin J.-H., Application of new unsymmetrical chiral Mn(III), Co(II,III) and Ti(IV) salen complexes in enantioselective catalytic reactions, *Catal Lett* 63 (1999) 83.
- [189] O'Connor K.J., Wey S.J., Burrows C.J., Alkene aziridination and epoxidation catalyzed by chiral metal salen complexes, *Tetrahedron Lett* 33 (1992) 1001-1004.
- [190] Palucki M., McCormick G.J., Jacobsen, E.N., Low temperature asymmetric epoxidation of unfunctionalized olefins catalyzed by (salen)Mn(III) complexes, *Tetrahedron Lett* 36 (1995) 5457
- [191] Kureshy K.I., Khan N.H., Abdi S.H.R., Iyer P., Bhatt A.K., Enantioselective catalytic epoxidation of nonfunctionalized prochiral olefins by dissymmetric chiral Schiff base complexes of Mn(III) and Ru(III) metal ions II, *J Mol Catal A: Chem* 120 (1997) 101.
- [192] Krishan R., Vancheesan S., Synthesis, characterization and catalytic activity of polynuclear manganese complexes of 2,5-dihydroxyterephthalaldehyde for epoxidation of olefins with H₂O₂, *J Mol Catal A: Chem* 157 (2000) 15.
- [193] Bousquet C., Gilheany D.G., Chromium catalysed asymmetric alkene epoxidation. greater selectivity for an E-alkene versus its Z-isomer, *Tetrahedron Lett* 36 (1995) 7739

- [194] Imanishi H., Katsuki T., Unusual solvent-effect in stereochemistry of asymmetric epoxidation using a (salen) chromium(III) complex as a catalyst, *Tetrahedron Lett* 38 (1997) 251
- [195] Kureshy R.I., Khan N.H., Abdi S.H.R., Patel S.T., Iyer P., Chiral Ru(II) Schiff base complex-catalysed enantioselective epoxidation of styrene derivatives using iodosyl benzene as oxidant. II, *J Mol Catal A: Chem* 150 (1999) 175.
- [196] Maurya M.R., Kumar A., Oxovanadium(IV) based coordination polymers and their catalytic potentials for the oxidation of styrene, cyclohexene and trans-stilbene, *J Mol Catal A: Chem* 250 (2006) 190-198.
- [197] Salavati-Niasari M., Amiri A., Synthesis and characterization of alumina-supported Mn(II), Co(II), Ni(II) and Cu(II) complexes of bis(salicylaldiminato)hydrazone as catalysts for oxidation of cyclohexene with tert-butylhydroperoxide, *Appl Catal A: Gen* 290 (2005) 46-53.
- [198] Salavati-Niasari M., Salimi Z., Bazarganipour M., Davar F., Synthesis, characterization and catalytic oxidation of cyclohexane using a novel host (zeolite-Y)/guest (binuclear transition metal complexes) nanocomposite materials, *Inorg Chim Acta* 362 (2009) 3716.
- [199] Rayati S., Ghaemi A., Sadeghzadeh N, Electronic effects of substituents on the oxidation potentials of vanadyl complexes with tetradentate Schiff base ligands derived from 1,2-propylenediamine, *Catal Commun* 11 (2010) 792.
- [200] Heshmatpour F., Rayati S., Hajiabbas M.A, Abdolalian P., Neumüller B., Copper(II) Schiff base complexes derived from 2,20-dimethyl-propandiamine: Synthesis, characterization and catalytic performance in the oxidation of styrene and cyclooctene, *Polyhedron* 31 (2012) 443 – 450.

CHAPTER 3

3. EXPERIMENTAL

3.1 Materials

The chemicals were used as received without any further purification. Absolute ethanol (99%) purchased from Saarchem, copper(II) chloride and glacial acetic acid were bought from Merck. Hydrochloric acid (32%): C&L. H-Y zeolite was purchased from Zeolyst. Carbon tetrachloride purchased from Riedel- de Haen. Dichloromethane, phenol (99%), hydrogen peroxide (29-32%), cyclohexene, ethylenediamine, vanadyl acetylacetonate, ethyl acetate, acetonitrile, acetylacetone were purchased from Sigma Aldrich.

3.2 Synthesis of Schiff-base ligands (L1 – L2)

The structures of ligands and complexes were shown in Scheme 3.1.

3.2.1 7-Amino-5-aza-4-methyl-hept-3-en-one, L1

7-amino-5-aza-4-methyl-hept-3-en-one was synthesized according to a method described by Styring *et.al* with slight modifications [1]. A cooled solution of ethylenediamine (0.3g, 0.005mol) in (25 ml) DCM was added dropwise to a cooled solution of acetylacetone (0.5 g, 0.005mol) in (25 ml) DCM at 0 °C under stirring conditions at ambient temperature. The solution was stirred for 5 min and refluxed for an additional 5 minutes at 40 °C. Afterwards, the solvent was removed *in vacuo* to give viscous oil. Yield = 0.97 g (68 %).

3.2.2 Bis(acetylacetone-ethylene) diamine, L2

Bis(acetylacetone)ethylenediamine was synthesized according to literature procedure [2]. A solution of acetylacetone (2 g, 0.02mol) in 25 ml DCM was added dropwise to a solution of ethylenediamine (0.6g, 0.01mol) in 25 ml DCM under stirring conditions. After addition, the pH of the solution was adjusted to 6 with a few drops glacial acetic acid. The yellow solution was refluxed for 3-4h at 40 °C. Afterwards, the solvent was removed *in vacuo* and gave a yellow solid. The solid product was recrystallized by dissolving it in a 1:1 mixture of ethylacetate and DCM by heating. After recrystallization two times from the same solvent and two times from CCl₄ the product was filtered and air dried to give straw like crystals. Yield = 2.07 g (55.6 %); m.p. = 111-113 °C. (Lit. 111-111.5° C [2])

3.3 Synthesis of Cu(II) and OV(IV) complexes

3.3.1 Preparation of Cu(II) complexes (1 – 2)

3.3.1.1 Cu(L1)Cl, (1)

Cu(L1)Cl were prepared according to a method described by Kwiatkowski *et.al* [3]. To a metal solution of CuCl₂.2H₂O (0.85g, 0.005 mol) in 10 ml ethanol was added a solution of L1 (0.714g, 0.005 mol) in 10 ml ethanol under stirring conditions. The reaction mixture was stirred at room temperature for 1h. The needle-like complex immediately separated out of the violet filtrate from which it was filtered and recrystallized from EtOH: MeCN (1:3) twice and dried in air to give violet solid.

Yield = 0.35g (34.3 %); m.p = 162-165 °C

3.3.1.2 Cu(L2), (2)

The general methodology of McCathy *et.al* was used to prepare Cu(L2) [2]. The ligand L2 (0.142g, 0.001mol) were dissolved in 10ml absolute ethanol. To this yellow mixture, a solution of CuCl₂.2H₂O (0.17 g, 0.001mol) in 10 ml absolute ethanol was added dropwise under stirring conditions. The reaction mixture was refluxed for 4 h at 78.5 °C. The dark purple filtrate was kept overnight and purple needle-like crystals slowly separated out which was filtered, washed with cold ethanol. The product was recrystallized from EtOH: MeCN (1:3) twice and dried in air to give analytically pure products then dried at 100 °C for 1 h. Yield = 0.162g (56.8 %); m.p = 137-139 °C (Lit. 137 °C [2])

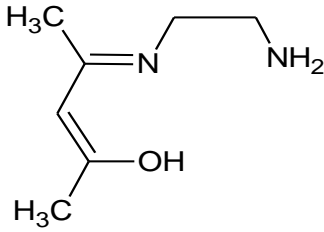
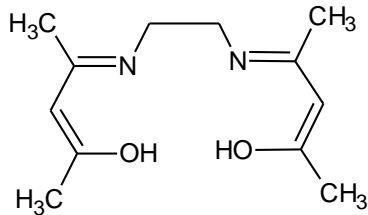
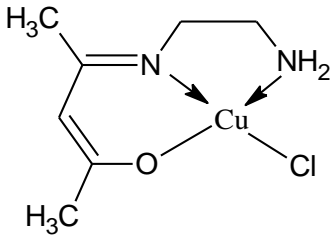
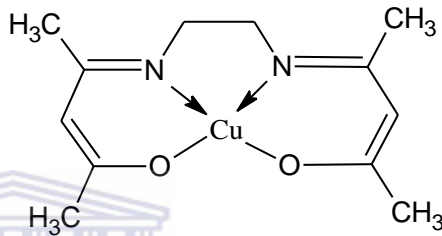
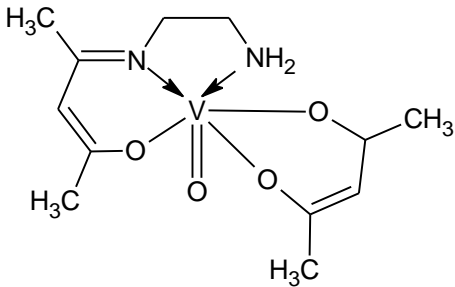
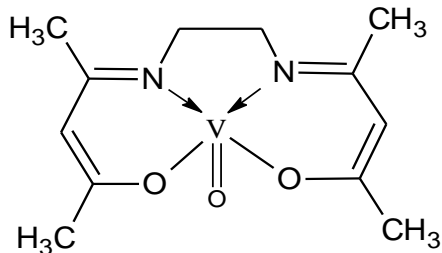
3.3.2 Preparation of oxovanadium(IV) complexes (5 - 6)

Both oxavanadium(IV) complexes were synthesized using a general methodology described by Alsalim *et.al* with slight modifications [4]. An hot solution of VO(acac)₂ (0.265g, 0.001 mol) in ethanol (10ml) was added dropwise to ethanolic solution (10 ml) of L1 or L2 (0.001 mol). The reaction mixture was heated and stirred under reflux for 5 h. After keeping the green filtrate in the flask at ambient temperature for a week, the complex slowly separated out, which was filtered, washed with hot water then ethanol and dried at 100 °C. Recrystallization from MeCN gave analytically pure products.

VO(L1)(acac), (5): light green solid, yield = 0.20g (65.5 %); m.p > 300 °C and

VO(L2), (6): green powder, yield = 0.18g; (61.7 %); m.p = 235-238 °C (Lit. 236 °C [5])

Scheme 3.1 Structures of Ligands and Cu(II) and OV(IV) complexes.

 <p><i>7-amino-5-aza-4-methyl-hept-3-en-one,</i> (L1)</p>	 <p><i>Bis(acetylaceton)ethylenediamine, (L2)</i></p>
 <p><i>Cu(L1)Cl, (1)</i></p>	 <p><i>Bis(acetylaceton)ethylenediiminocopper(II);</i> <i>Cu(L2), (2)</i></p>
 <p><i>VO(L1)(acac), (5)</i></p>	 <p><i>Ethylenebis(acetylacetonylideiminato)oxovana-</i> <i>dium(IV) VO(L2), (6)</i></p>

3.4 Preparation of zeolite encapsulated Cu(II) and OV(IV) complexes

The synthetic route of encapsulated complexes is presented in Scheme 3.2.

The synthesis was carried out in two steps employing the general flexible ligand method:

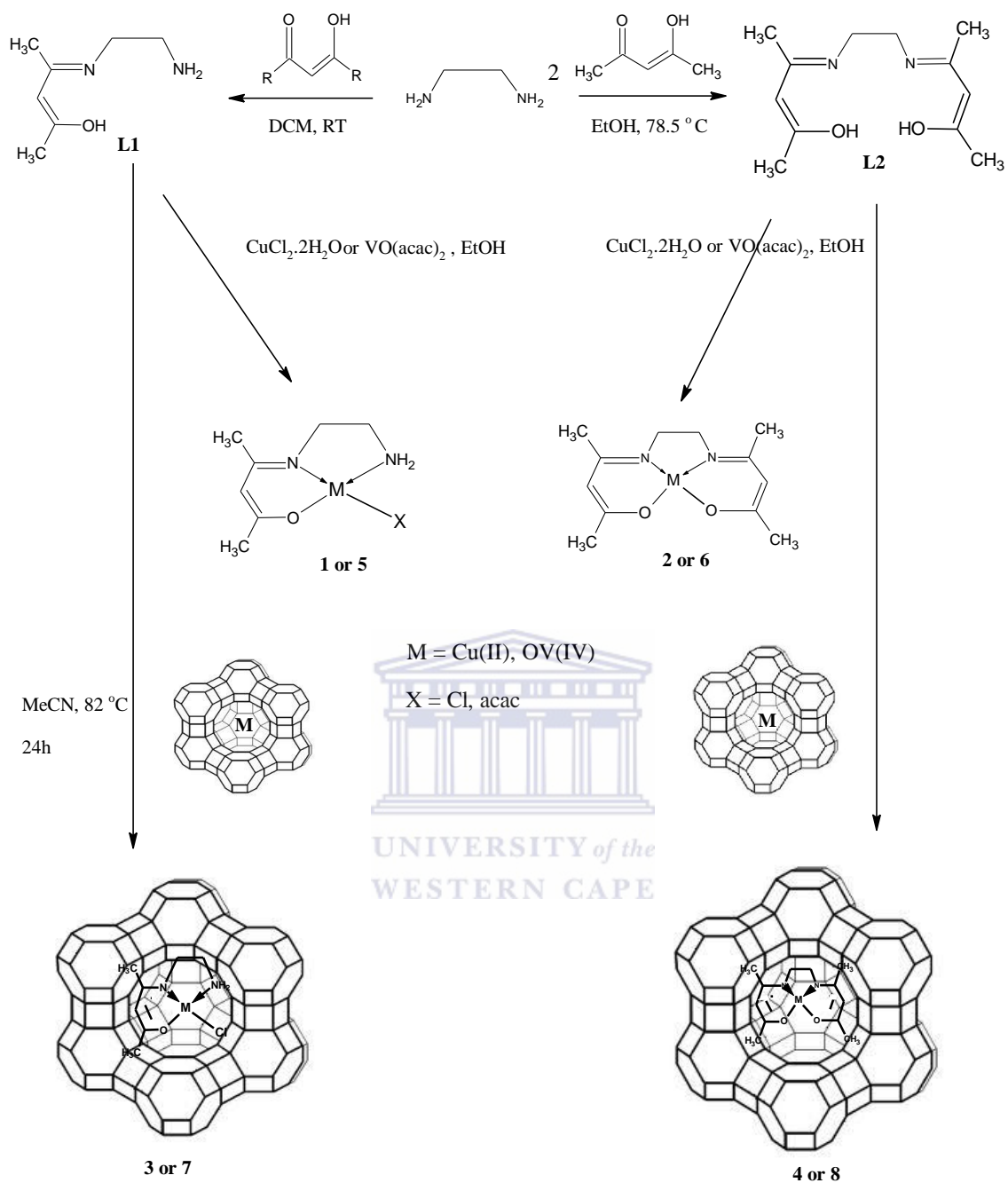
1. Preparation of metal exchanged zeolite, M-Y (M = Cu(II) and OV(IV))
2. Synthesis of zeolite-Y encapsulated metal complexes (3 - 4 and 7 - 8)

3.4.1 Preparation of metal exchanged zeolite, M-Y (M = Cu(II) or OV(IV))

Cu(II) and V(IV)-exchanged-H-Y zeolites were synthesized according to the method described by Titinchi *et.al* [6]. To 1.0 g H-Y suspended in 50 ml deionized water was added $\text{CuCl}_2 \cdot 2\text{H}_2\text{O}$ (0.34 g, 2 mmol) or $\text{VO}(\text{acac})_2$ (0.53 g, 2 mmol,) in order to exchanged H-ions of H-Y with Cu(II) or OV(IV) ions. The reaction mixture was stirred gently at 90 °C for 24 h, filtered, precipitate washed with copious amount of hot deionised water followed by Soxhlet extraction with acetonitrile for 1 h till the filtrate contained no copper or vanadium ions. The resulting precipitate was dried at 150 °C in air for 24 h.

3.4.2 Synthesis of zeolite-Y encapsulated metal complexes

General procedure for encapsulation: All encapsulated complexes were prepared using the flexible ligand method (Scheme 3.2). An amount of 0.3 g of Cu-H-Y or OV(IV)-H-Y and 0.70 g of ligand were mixed 30 ml MeCN in a round bottom flask. The reaction mixture was refluxed and stirred in an oil bath for overnight. After cooling, the resulting material was subjected to Soxhlet extraction in acetonitrile for 48 h to remove excess uncomplexed ligand that remained in the cavities of the zeolite as well as any free metal complex located on the surface of the zeolite. The solid products obtained were dried at 150 °C for several hours to constant weight.



Scheme 3.2 A schematic description for the synthesis of neat and encapsulated copper(II) and oxovanadium(IV) complexes.

3.5 Analytical techniques and instruments used

Various kinds of analytical and spectroscopic techniques were used to determine the composition of the ligands and complexes and the catalytic activity and selectivity of the reaction products. The physical and analytical methods applied here are given below.

3.5.1 Nuclear Magnetic Resonance (NMR) spectroscopy

Proton nuclear magnetic resonance (^1H NMR) and carbon nuclear magnetic resonance (^{13}C NMR) spectroscopy were used for structural determination of all ligands. ^1H and ^{13}C NMR spectra were recorded in CDCl_3 using a Varian Gemini 2000 spectrometer and chemical shifts are indicated in ppm. Sample signals are relative to the resonance of residual protons on carbons in the solvent. Samples were prepared weighing out between 30 – 60 mg of sample and dissolved in deuterated chloroform (CDCl_3).

3.5.2 Fourier - Transform Infrared (FT-IR) spectroscopy

FT-IR measurements were used to determine the presence of functional groups in the spectrum of Schiff base ligands and complexes. The ATR-IR measurements were carried out on a Perkin-Elmer Spectrum 100 FTIR spectrometer. This technique is also used to confirm complex formation in the zeolite cavities by comparing their spectral patterns with their parent zeolites. The presence of new peaks in the encapsulated complexes correspond to the complex confirming the encapsulation of Schiff-base metal complexes in zeolite Y.

3.5.3 Inductively Coupled Plasma – Optical Emission Spectrometry (ICP – OES)

Inductively Coupled Plasma – Optical Emission Spectrometry (ICP – OES) Varian 710-ES, was employed to determine the % metal content of Cu(II) and OV(IV) in the encapsulated complexes. The sample was prepared by dissolving 10 mg complex in a conc mixture of 3 ml HNO_3 and 1 ml HCl. The mixture was evaporated until complete dryness on a hot plate. The solid obtained was dissolved in deionized water and filtered. The filtrate was made up to a 50 ml solution of 2 % HNO_3 .

3.5.4 Scanning Electron Microscopy (SEM)

Scanning Electron Micrographs (SEM) is an effective technique and was used to study the shape, particle size and surface structure of the catalysts were recorded on Hitachi X-650 EM. The samples were dusted on alumina and coated with a thin film of gold to prevent surface changing and to protect the surface material from thermal damage by the electron beam. In all analyses, a uniform thickness of about 0.1 mm was maintained. This technique was used to obtain images of zeolite encapsulated metal complex ZEMC's and to determine their particle size and morphology.

3.5.5 Ultraviolet-Visible spectroscopy (UV-Vis)

This technique was used to determine the transitions in the ligands, neat and encapsulated complexes. The electronic spectra of ligands and complexes were studied at a concentration of 10^{-4} M in methanol in the UV region and at a concentration 10^{-3} M in methanol in the visible region. In case of encapsulated complexes, Nujol was used to prepare the paste by layering in the mull of the sample to the inside of one of the cuvette while keeping another one layered with nujol as reference. This technique was also employed to determine the reaction mechanism of these catalysts and the intermediate species formed during the oxidation of the substrates. Methanolic solution of neat complex was treated with a methanolic solution of 30 % H_2O_2 and the progress of the reaction was monitored employing UV-Vis spectrophotometer. The Electronic spectra of the encapsulated complexes were recorded on a GBC UV/VIS 920 UV-Visible spectrophotometer.

3.5.6 Gas Chromatography (GC)

Chromatography is a technique used for separating and analyzing compounds that can be vaporized without decomposition. The organic compounds are separated due to differences in their partitioning behaviour between a flowing the mobile gas phase and the stationary phase in the column to separate the components in a mixture (the relative amounts of such components can also be determined). The retention time of all peaks was compared with authentic samples.

Agilent 7890 gas chromatograph fitted with flame ionization detector fitted with HP-5 (phenylmethylsilicon) capillary column (30 m x 330 μ m x 0.25 μ m film thickness, Agilent

technologies) was used to monitor the reaction process and determine conversion and chemoselectivity.

3.5.7 X-Ray Powder Diffraction (XRPD)

This technique was used to study the structure of the zeolite, identify the crystallinity of these catalysts and test the stability of the zeolite framework after metal ion exchange and encapsulation of complexes. This technique indicates the insertion of transition metal complexes and ion-exchanged metals, M-Y in the cavities of the zeolite Y. New diffraction lines could be located in the XRD pattern of the encapsulated zeolites corresponds to the metal complex and ion-exchanged metals. These observations clearly suggest the presence of metal complexes in zeolite matrix. The samples was recorded by Bruker AXS D8 Advance, High – Resolution diffractometer with Cu K Radiation ($\lambda = 1, 5406 \text{ \AA}$) fitted to a PSD Vantec gas detector at Ithemba labs, Cape Town, South Africa.

X-ray spectrometry is suitable for all elements in periodic table. The intensity of the radiation of each wavelength is proportional to the corresponding element and the amount of each element present can be determined by quantitative analysis.

3.5.8 Brunauer-Emmett-Teller (BET) Surface Area Analysis

BET theory aims to explain the physical adsorption of gas molecules on a solid surface. This technique serves as the basis for an important analysis for the measurement of the specific surface area of a material. BET analysis provides specific external surface area and pore volume evaluation of materials yielding important information in studying the effects of surface porosity and particle size in many applications. This technique characterises the pore size distribution independent of external area due to particle size of the material. However, in the field of solid catalysis, the surface area of catalysts is an important factor in catalytic activity. Porous inorganic materials such as mesoporous silica and layered materials exhibit high surface areas, indicating the possibility of application for efficient catalytic materials. This type of analysis is used to determine the change in surface area, pore volume and pore size after the encapsulation process to confirm the presence of complexes in zeolite-Y.

References

- [1] Styring P., Grindson C., Fischer C. M, A Polymer-Supported Nickel(II) Catalyst for Room Temperature Tamao-Kumada-Corriu Coupling Reactions, *Catal Lett* 77 (2001) 219-225.
- [2] McCarthy P.J, Hovey R J., Ueno E., Martell A. E., Inner complex chelates. I. Analogs of bisacetylacetonethylenediimine and its metal chelates, *J Am Chem Soc* 77 (1955) 5821–5823.
- [3] Kwiatkowski M., Kwiatkowski E., Olechnowicz A., Bandoli G., Molecular structure and magnetic properties of bis(μ -chloro)bis[7-amino-4-methyl-5-azahept-3-en-2-onato(1-)]dicopper(II), *Inorg Chim Acta* 182 (1991) 117–118.
- [4] Alsalim T.A., Hadi J.S, Al-Nasir E.A, Abbo H.S, Titinchi S.J.J, Hydroxylation of Phenol Catalyzed by Oxovanadium(IV) of Salen-Type Schiff Base Complexes with Hydrogen Peroxide, *Catal Lett* 136 (2010) 228–233.
- [5] Boucher L.J, Tynan E.C, Yen T.F, Spectral Properties of Oxovanadium(IV) Complexes. I. p-Ketimines, *J Am Chem Soc* 90 (1968) 733.
- [6] Titinchi S.J.J, Abbo H.S, Metallo Salicylidenetriazol Complexes Encapsulated in Zeolite-Y: Synthesis, Physicochemical Properties and Catalytic Studies *Top Catal* 53 (2010) 1401–1410.

CHAPTER 4

4. CHARACTERIZATION

Synthesis of metal complexes encapsulated in zeolite was carried out by a stepwise method adopted by Ratnasamy, Bowers and Balkus *et al.* [1] who described this process as a “flexible ligand method”. The metal exchanged M-Y zeolite [M = Cu(II), and V(IV)] was prepared by exchanging H⁺ of an H-Y molecule with a 0.001M solution of copper nitrate or vanadium acetylacetonate, respectively, in aqueous solution. Heating of the M-Y zeolite in excess of ligand at 90 °C for about 20 h effected insertion of the ligand in the cavity followed by complex formation with metal ions. The crude mass was finally purified by Soxhlet extraction in acetonitrile.

An attempt was made to characterize these complexes by comparing their physico-chemical properties with that of the simple complexes prepared by the reaction of L1 or L2 with the respective metal salts. The formulation of the encapsulated complexes is, thus, based on the respective simple complex.

4.1 Characterization of ligands

4.1.1 ¹H and ¹³C NMR spectroscopic studies of Schiff-base ligands

The ¹H NMR spectrum of Schiff base ligand L1 shows a sharp singlet at 1.48 ppm assigned to the two methyl groups and corresponds to six protons. Two methylene groups are observed and centred at 2.46 and 3.42 ppm, respectively, and both appear as multiplets corresponding to two protons each. The peak at 3.42 ppm is assigned to methylene protons at position 6. This peak is more downfield than the methylene group at position 7 due to deshielding by the azomethine group as shown in Table 4.1 and Fig 4.1. The ¹H NMR spectrum for L1 is similar to that reported [2].

The ¹³C NMR spectrum of L1 exhibited seven peaks as shown in Fig.4.2 and Table 4.2. The signal observed at 162.89 ppm is due to the azomethine carbon.

The proton NMR spectrum for L2 (Fig 4.3 and Table 4.3) shows two methyl groups as singlets at 1.95 and 1.88 ppm corresponding to three protons each. The methyl groups at position 5,5' are more deshielded than the methyl groups at position 1 since they are attached to the azomethine moiety. The methyl signal at 1.88 ppm is assigned to protons at position 3,3'. The methylene protons are located in the region 3.35 – 3.42 ppm

Chapter 4: Characterization

corresponding to four protons. No peaks were observed for NH₂ protons indicating condensation with the carbonyl of acetylacetone had occurred.

¹³C NMR (Fig 4.4 and Table 4.4) spectrum illustrates the presence of six carbon signals which further supports the structure of the ligand.

The ¹H and ¹³C-NMR data are fully consistent with the values previously reported [3].



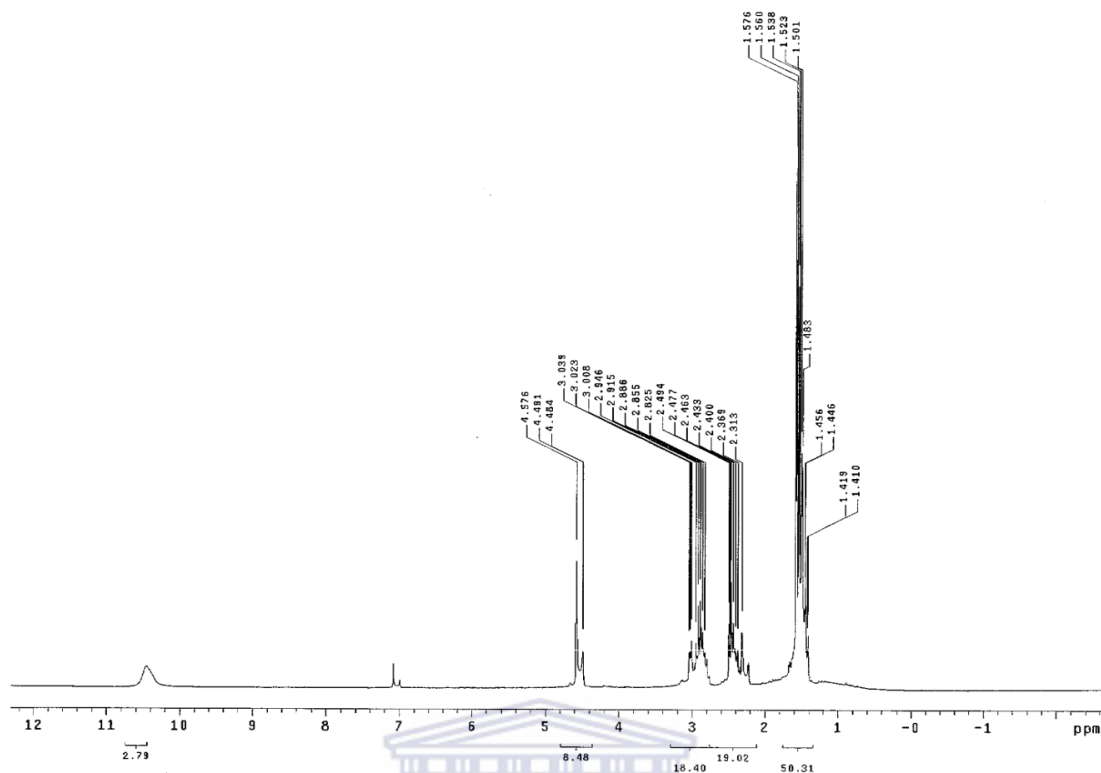


Figure 4.1 ^1H NMR of 7-amino-5-aza-4-methyl-hept-3-en-one, L1

Table 4.1 ^1H NMR data of 7-amino-5-aza-4-methyl-hept-3-en-one, L1

Ligand structure	Proton position	Chemical Shift (ppm)	No. of protons	Multiplicity	Assignment
	2	10.45	1	s	<u>OH</u>
	3	4.58	1	s	=C- <u>H</u>
	6	3.42	2	m	C=N- <u>CH</u> ₂
	7	2.46	2	m	H ₂ N- <u>CH</u> ₂
	1 and 5	1.48	6	s	2 <u>CH</u> ₃
		1.56	2	m	<u>NH</u> ₂

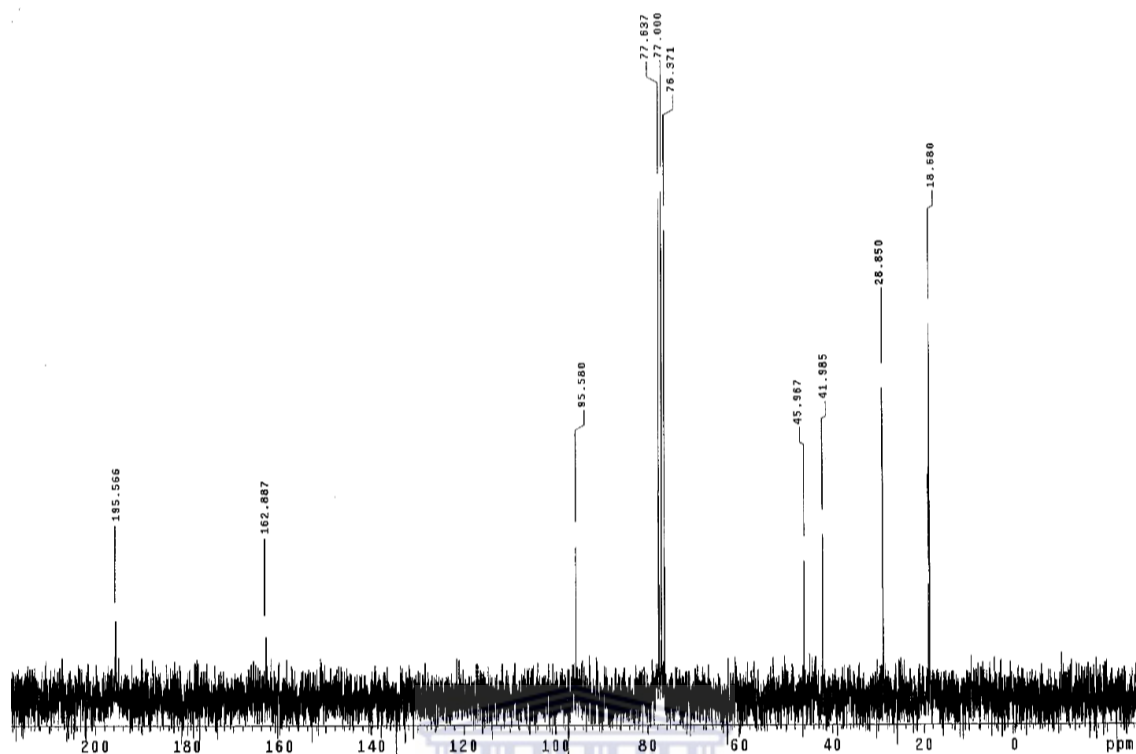


Figure 4.2 ^{13}C NMR spectra of 7-amino-5-aza-4-methyl-hept-3-en-one, L1

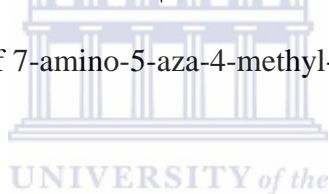


Table 4.2 ^{13}C NMR data of 7-amino-5-aza-4-methyl-hept-3-en-one, L1

Ligand structure	Carbon position	Chemical Shift (ppm)	Assignment
<p>L1</p>	C 5	28.85	$\text{N}=\text{C}-\underline{\text{C}}\text{H}_3$
	C 4	162.89	$\text{N}=\underline{\text{C}}-\text{CH}_3$
	C 3	95.58	$\underline{\text{C}}=\text{C}-\text{OH}$
	C 2	195.57	$\text{C}=\underline{\text{C}}-\text{OH}$
	C 1	18.85	$\text{C}=\text{C}-\underline{\text{C}}\text{H}_3$
	C 6	45.97	$\text{N}=\text{C}-\underline{\text{C}}\text{H}_2$
	C 7	41.96	$\text{C}=\text{C}-\underline{\text{C}}\text{H}_3$

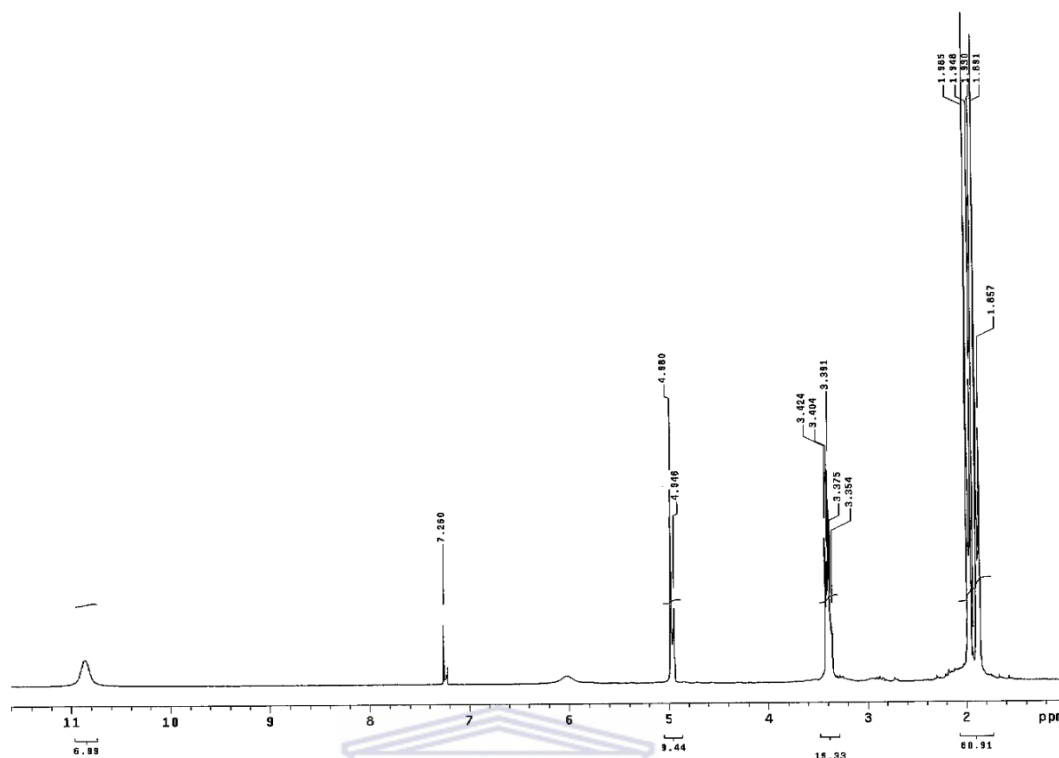


Figure 4.3 ^1H NMR of bis(acetylacetonate ethylene diamine), L2

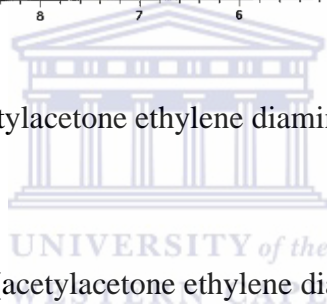


Table 4.3 ^1H NMR data of bis(acetylacetonate ethylene diamine), L2

Ligand structure	Protons position	Chemical Shift (ppm)	No. of protons	Multiplicity	Assignment
<p>L2</p>	2,2'	10.86	2	s	O- <u>H</u>
	3,3'	4.97	2	s	C=C- <u>H</u>
	6,6'	3.43	4	t	2 <u>CH</u> ₂
	5,5'	1.95	6	s	N=C- <u>CH</u> ₃
	1,1'	1.88	6	s	C=C- <u>CH</u> ₃

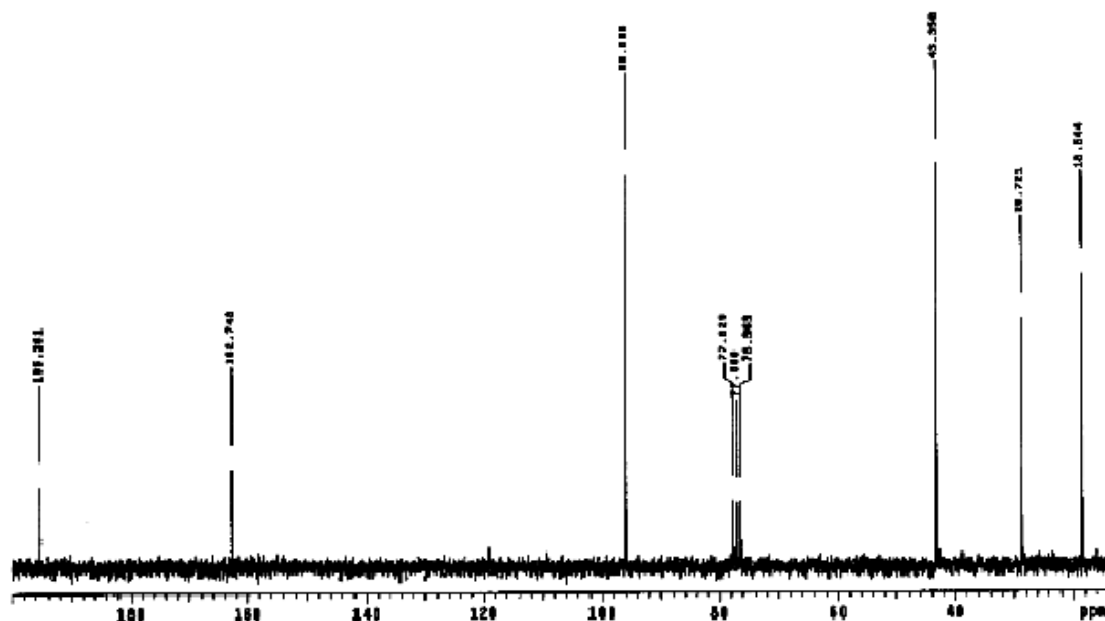


Figure 4.4 ^{13}C NMR spectra of bis(acetylacetonate ethylene diamine), L2



Table 4.4 ^{13}C NMR data of bis(acetylacetonate ethylene diamine), L2

Ligand structure	Carbon position	Chemical Shift (ppm)	Assignment
	C 4,4'	195.52	$\text{N}=\underline{\text{C}}-$
	C 2,2'	162.83	$\text{HO}-\underline{\text{C}}=$
	C 3,3'	96.14	$-\underline{\text{C}}=\underline{\text{C}}-$
	C 6,6'	43.48	$\text{H}_2\underline{\text{C}}-\underline{\text{C}}\text{H}_2$
	C 5,5'	28.84	$\text{N}=\text{C}-\underline{\text{C}}\text{H}_3$
	C 1,1'	18.66	$\text{C}=\text{C}-\underline{\text{C}}\text{H}_3$

4.1.2 FT-IR spectroscopic studies of Schiff-base ligands

Three bands at 1602, 1559 and 1515 cm^{-1} for L1 are assigned to $\nu(\text{C}=\text{O})$, $\nu(\text{C}=\text{N})$ and $\nu(\text{C}=\text{C})$, respectively. A weak broad band observed at 3358 cm^{-1} is due to $\nu(\text{OH})$ stretching vibrations. L1 further shows two sharp weak bands at 2920 and 2862 cm^{-1} , which is attributed to the free NH_2 group [4].

The IR spectrum of L2 exhibits two bands at 1599 and 1518 cm^{-1} , which are assigned to $\nu(\text{C}=\text{O})$ and $\nu(\text{C}=\text{C})$, respectively. The disappearance of the NH_2 band and the carbonyl group bands of the starting materials and the appearance of new peak at 1570 cm^{-1} corresponds to $\nu(\text{C}=\text{N})$ band confirms formation of Schiff base ligand L2.

These data support the NMR assignment for the formation of the respective Schiff-base ligands, L1 and L2 as reported previously [3,5].

4.1.3 UV/Vis spectroscopic of Schiff-base ligands

Fig.4.5 illustrates the spectra of the ligands *viz.* L1 and L2. Both ligands exhibit a band at ca 320 nm and a shoulder at ~300 nm. These bands are assigned to $n \rightarrow \pi^*$ transitions due to the azomethine chromophore in these ligands. The shoulder band at higher energies is associated with benzene $\pi \rightarrow \pi^*$ transitions. These results confirm previously reported data [9].

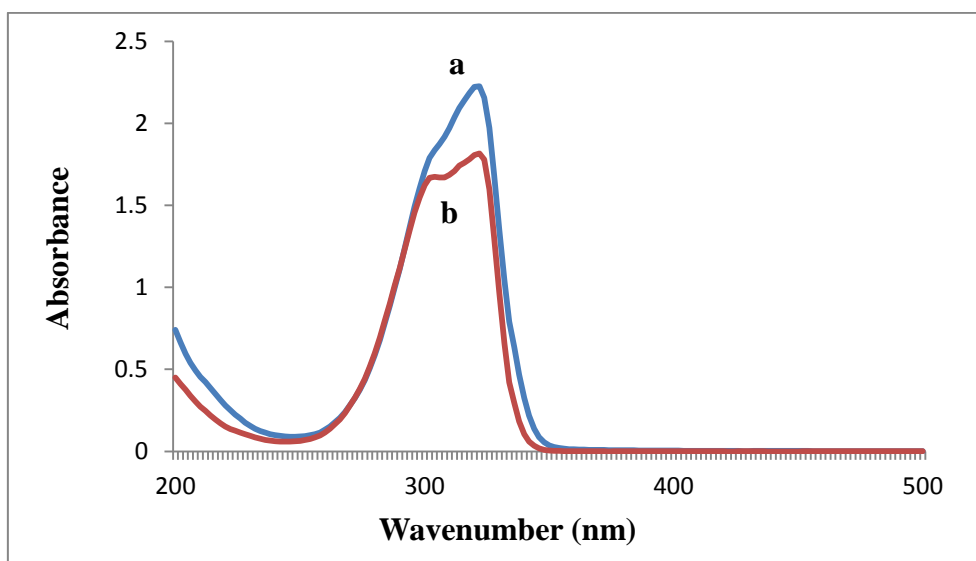


Figure 4.5 Electronic spectra in methanol of (a) L1 and (b) L2

4.2 Characterization of Cu(II) complexes

4.2.1 FT-IR spectroscopy

IR spectral data of the neat and encapsulated complexes are presented in Fig. 4.6 and Table 4.5. The intensity of the peaks of the encapsulated complexes are essentially similar to that of the free metal complexes. However, a significant change in some important bands compared to the free ligand is identified.

The IR spectra of Cu(L1)Cl and Cu(L2) show that the $\nu(\text{C}=\text{N})$ band has shifted downwards to 1504 cm^{-1} and 1560 cm^{-1} , respectively due to the coordination of the metal ion to the nitrogen atom which reduces the electron density of the azomethine group and therefore lowers the $\nu(\text{C}=\text{N})$ frequency [7-8]. The metal complexes exhibit a new weak-medium peaks in the far IR region ($400 - 600\text{ cm}^{-1}$) which are assigned to $\nu(\text{M}-\text{O})$ and $\nu(\text{M}-\text{N})$ modes indicating coordination of metal to nitrogen and oxygen atom of the respective ligands [9]. The coordination of the NH_2 group in L1 to the metal centre results in a shift in N-H stretching and bending bands to 2916 cm^{-1} [10,11] upon complexation. In Cu(L1)Cl where an NH_2 group is still present coordination occurs through the NH_2 to the metal centre and normally results in a upward or downward shift in N-H stretching and bending bands [10,11]. This N-H band shifted to 2916 cm^{-1} in Cu(L1)Cl. The broad band assigned to $\nu(\text{OH})$ stretching vibration in the L1 and L2 disappeared in the spectra of the complexes indicating coordination of the metal ion to the ligand after deprotonation (Fig.4.6). In addition, Cu(L1)Cl exhibits a new peak at 310 cm^{-1} due to $\nu(\text{M}-\text{Cl})$ bond (Fig 4.7) [12].

Table 4.5 FT-IR vibrations of the ligands and Cu(II) complexes

Compound	$\nu\text{ (cm}^{-1}\text{)}$		
	$\nu(\text{C}=\text{N})$	$\nu(\text{M}-\text{O})/(\text{M}-\text{N})$	$\nu(\text{M}-\text{Cl})$
L1	1559(s)	-	-
L2	1570(s)	-	-
Cu(L1)Cl	1504(s)	385(w),455(s), 521(str),607(m)	310
Cu(L2)	1560(s)	418(w), 568 (w), 456 (s)	-

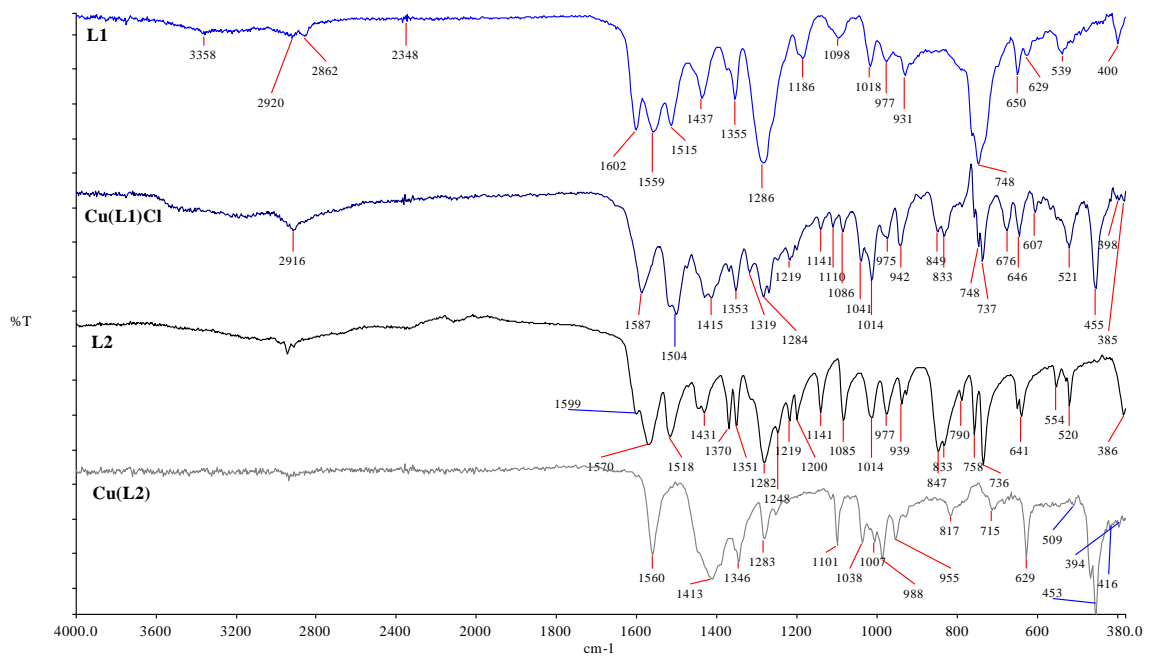


Figure 4.6 FT-IR spectra of L1, Cu(L1)Cl, L2 and Cu(L2).

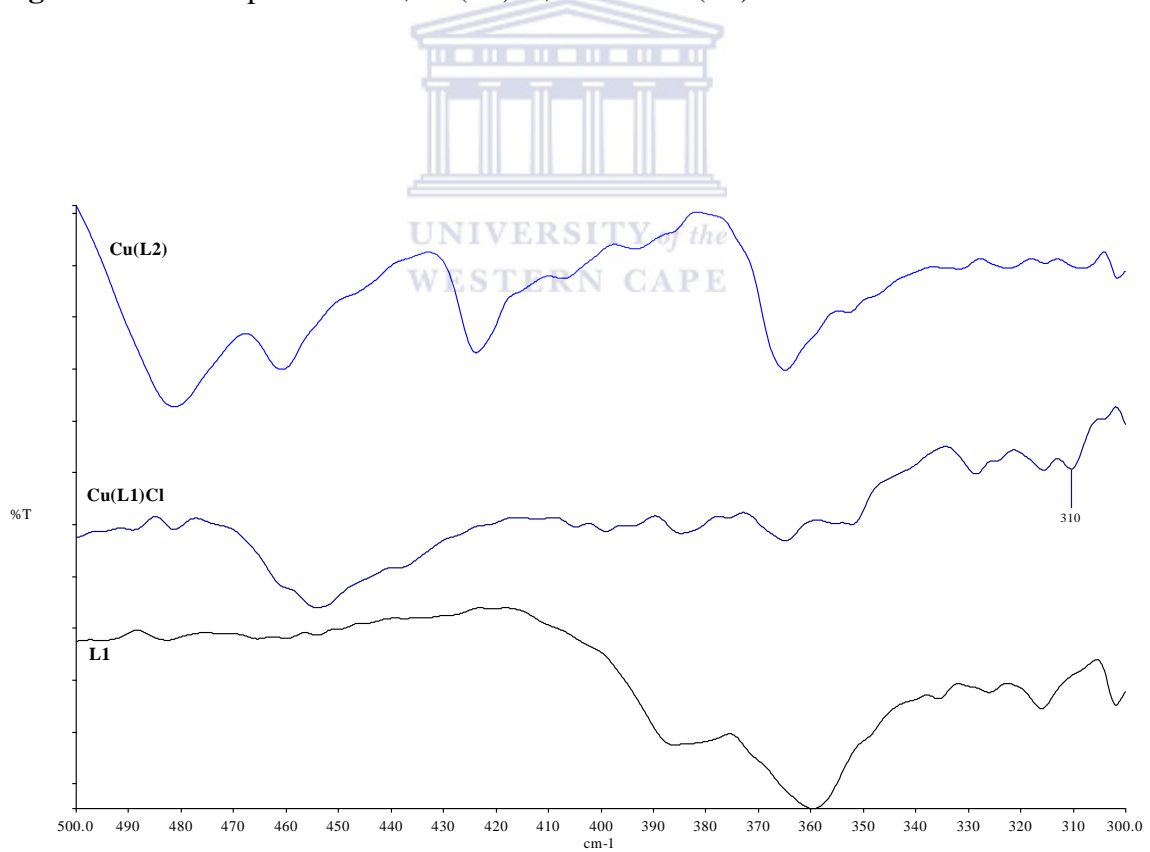


Figure 4.7 FT-IR spectra of L1, Cu(L1)Cl and Cu(L2).

From the IR spectra (Fig.4.8), it is evident that the framework vibrational band of zeolite Y dominates the spectra of all samples. These characteristic bands corresponding to the zeolite framework in all samples are found at 1040, 450, 780 and 394 cm^{-1} [13,14]. No shift or broadening in the structure sensitive band around 1050 cm^{-1} (due to asymmetric T-O stretch) occurred which indicates that little changes in the zeolite framework upon encapsulation or ion exchange took place. This indicates that there is no significant expansion of zeolite cavity or dealumination and proving that the metal complex fits in the cavity of the zeolite and the zeolite matrix remain unchanged [15].

The presence of several bands of medium intensity in 2700-2900 cm^{-1} region correspond ethylene groups of the ligand. Thus, IR data indicates the encapsulation of the complexes in the zeolite cavity.

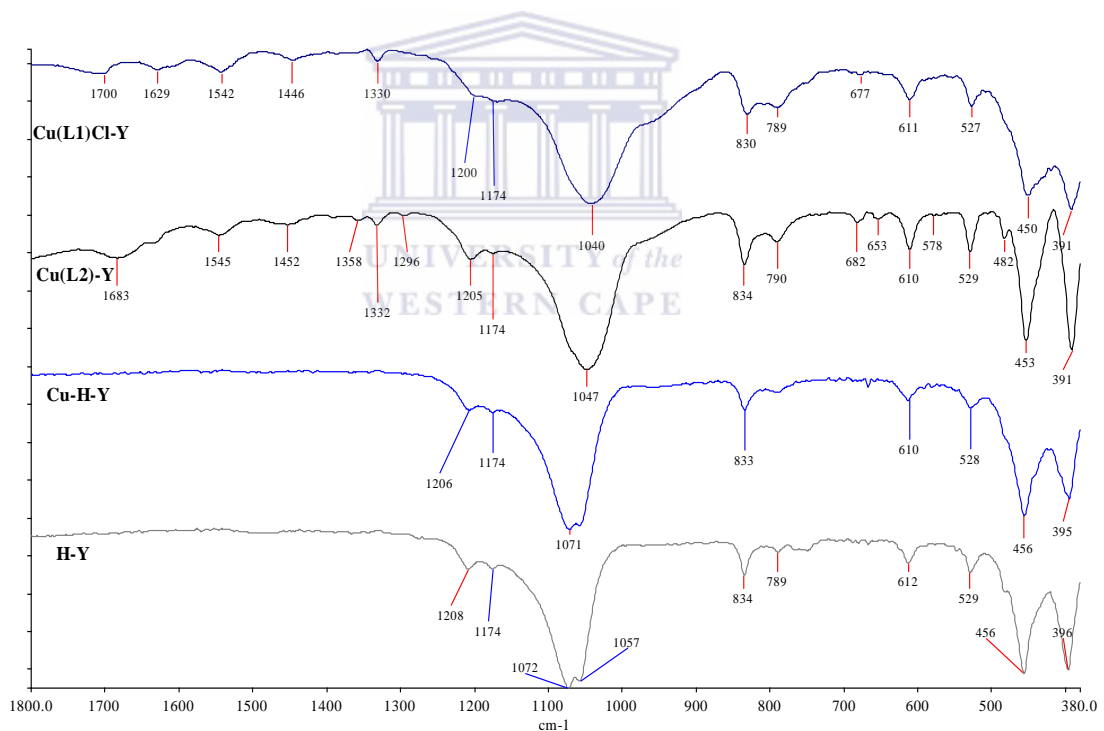


Figure 4.8 FT-IR spectra of H-Y, Cu-exchanged zeolite and their zeolite encapsulated metal complexes

4.2.2 UV/Vis spectroscopy

The electronic spectral data of the complexes viz. Cu(L1)Cl and Cu(L2) were recorded in methanol over the range 200-900 nm (Fig.4.9).

Three distinctly different bands are observed in Cu(L1)Cl at 204, 305 and 324 nm. The first two bands are assigned to $\sigma \rightarrow \sigma^*$ and $\pi \rightarrow \pi^*$ transitions, respectively. The shoulder band present at 324 nm is as a result of a ligand to metal charge transfer (LMCT) band assigned as an $n \rightarrow \pi^*$ transition[16]. In Fig.4.9, Cu(L2) five adsorption bands are observed at 204, 226, 276, 322 and 342 nm in the UV region. The first bands can be assigned to $\sigma \rightarrow \sigma^*$ and $\pi \rightarrow \pi^*$ transitions. The broad band at 342 nm is probably due to a symmetry forbidden ligand to metal charge transfer (LMCT) transition [17].

The UV-visible spectrum of Cu-Y does not show any absorption band above 300 nm, while the spectra for both complexes display one broad band around 300 nm, which is probably due to a symmetry forbidden ligand \rightarrow metal charge transfer transition. A very weak but broad absorption 610-650 nm is also observed in both encapsulated complexes when highly concentrated sample in nujol mull was used to record the spectrum and this is due to d-d transition in the complex (Fig.4.10). These data compare closely with that of pure complexes and is indicative of a square planer structure present in the cavity of the zeolite [17,18].

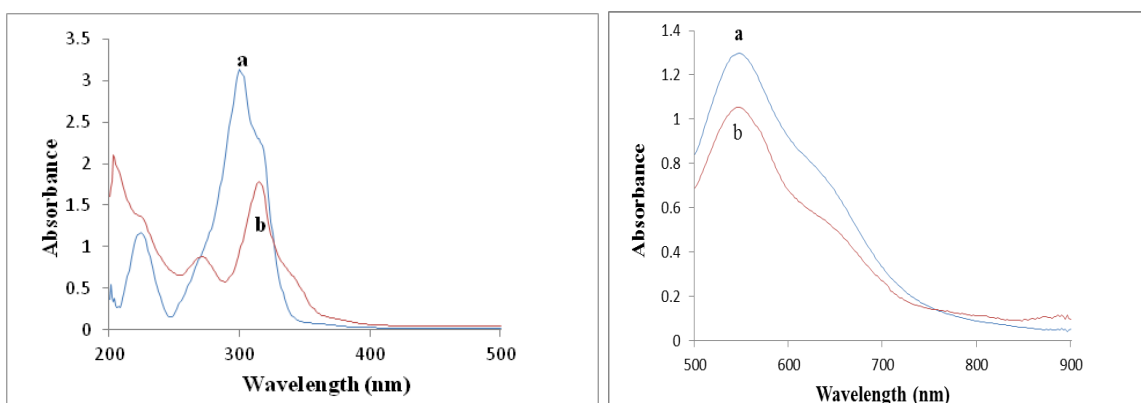


Figure 4.9 Electronic spectra of (a) Cu(L1)Cl and (b) Cu(L2)

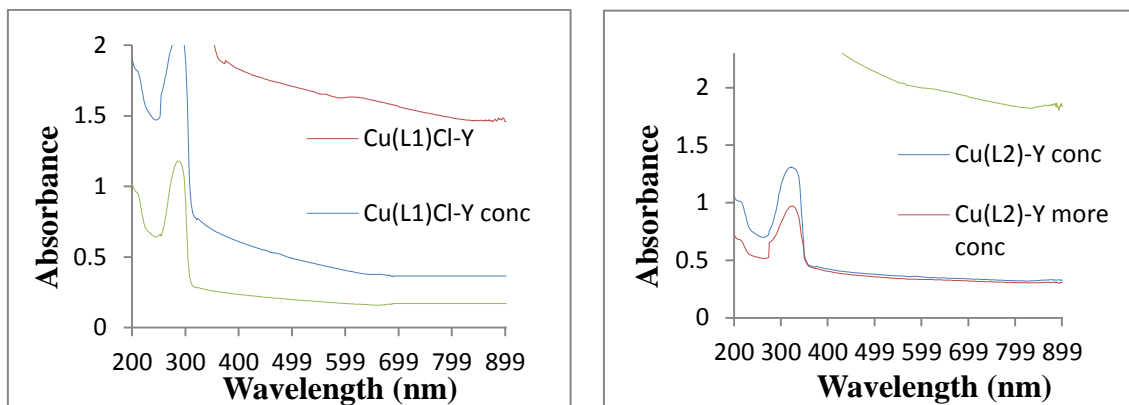


Figure 4.10 Electronic spectra of (a) Cu(L1)Cl-Y and (b) Cu(L2)-Y

Table 4.6 Electronic spectral data of the ligands (L1-L2) and Cu(II) complexes.

Complex	λ_m/nm ($\epsilon/\text{M}^{-1} \text{cm}^{-1}$)
L1	320
L2	322, 304 (sh)
Cu(L1)Cl	224, 305, 324 (sh), 540
Cu(L1)Cl-Y	200, 280, 602, 589
Cu(L2)	204, 226 (sh), 278, 322, 342(sh), 546
Cu(L2)-Y	200, 274(sh), 309, 616

4.3 Characterization of VO(IV) complexes

4.3.1. FT-IR spectroscopy

The major spectral data of ligands, neat complexes and encapsulated complexes are presented in Table 4.7.

The FT-IR spectra of VO(L1)(acac) and VO(L2) complexes show a shift in $\nu(\text{C}=\text{N})$ to lower frequency from 1559 and 1570 to 1517 and 1560 cm^{-1} , respectively. The disappearance of the weak broad band, $\nu(\text{OH})$, in both vanadium complexes indicates the coordination of metal ion to the enolic oxygen atom after deprotonation.

The appearance of new weak to sharp bands in the far IR region $600 - 400 \text{ cm}^{-1}$ is assigned to $\nu(\text{M-O})$ and $\nu(\text{M-N})$ modes which further indicates the coordination of metal ion to nitrogen and oxygen atoms of the respective ligands [9].

Complexes, VO(L1)(acac) and VO(L2) exhibit a medium sharp band at 978 and 970 cm^{-1} respectively, due to $\nu(\text{V=O})$ stretch. This is evidence of the presence of oxovanadium complexes [19, 20].

In the spectra of the encapsulated vanadyl complexes the band due to $\nu(\text{V=O})$ stretching vibration was not observed due to the presence of a strong and broad band of the zeolite framework in the $\sim 1000 \text{ cm}^{-1}$ region.

From Fig. 4.11, it is evident that the framework vibrational bands of zeolite Y dominate the spectra of all samples. These characteristic bands corresponding to the zeolite framework in all samples are found around at $1050, 450, 780$ and 394 cm^{-1} [13,14]. No shift or broadening in the structure sensitive band at 1050 cm^{-1} (due to an asymmetric T-O stretch) occurred which indicates that little change in the zeolite framework upon encapsulation or ion exchange took place. This indicates that there is no significant expansion of the zeolite cavity or dealumination and proving that the metal complex fits in the cavity of the zeolite and the zeolite matrix remains unchanged [15]. In the case for VO(L1)(acac)-Y and VO(L2)-Y the bands in this region were rather weak. The FT-IR spectra of encapsulated complexes in comparison with their neat complexes are rather weak and this is as a result of the low loading of complexes present in the zeolite matrix.

Thus, IR and UV-vis data indicate the encapsulation of complexes in the super cages of zeolite-Y.

Table 4.7 FT-IR vibrations of the ligands and VO(IV) complexes

Compound	$\nu(\text{cm}^{-1})$		
	(C=N)	$\nu(\text{M-O})/(\text{M-N})$	$\nu(\text{V=O})$
L1	1559(s)	-	-
L2	1570(s)	-	-
VO(L1)(acac)	1517(s)	485, 408(w), 386(m), 418(w), 453(s)	978(m)
VO(L2)	1560(s)	482(w), 554(w), 520	970(m)

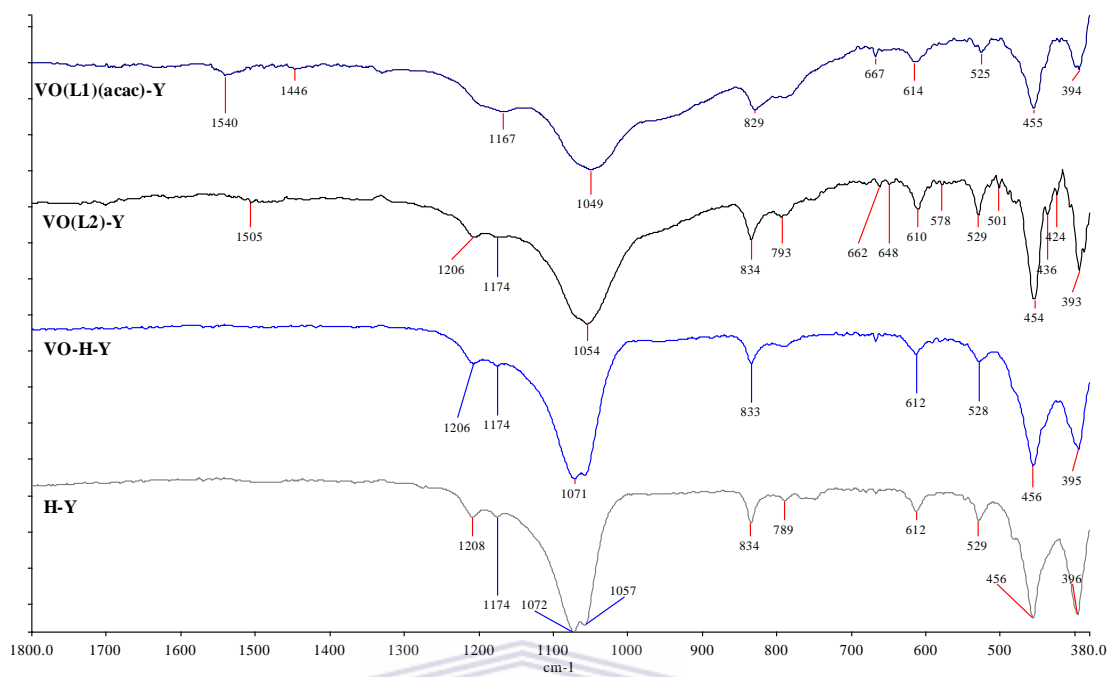
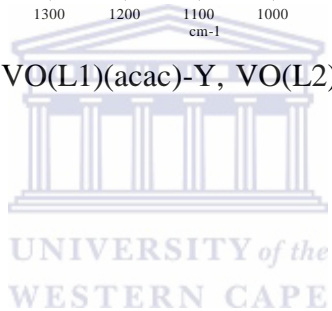
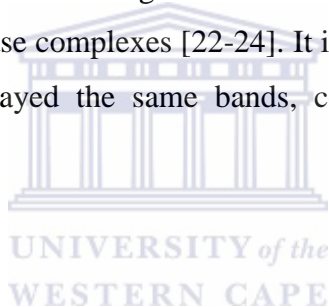


Figure 4.11 FT-IR spectra of VO(L1)(acac)-Y, VO(L2)-Y and their parent compound in the range 380 - 1800 cm^{-1} .



4.3.2. UV/Vis spectroscopy

In Fig. 4.12, there are four distinctly different adsorption bands observed in VO(L1)(acac) in the UV region at 200, 241 (sh), 318 and a weak shoulder at 342 nm. The first two bands are assigned to $\varphi \rightarrow \varphi^*$ whilst the band at 318 nm is due to $\pi \rightarrow \pi^*$ transitions. The azomethine chromophore's $n \rightarrow \pi^*$ transition shifted to higher energy and is located at 342 nm in VO(L1)(acac). VO(L2) exhibits three absorption bands at 200, 295 and a weak shoulder at 312 nm as presented in Table 4.8 and Fig.4.13. These bands are assigned to $\varphi \rightarrow \varphi^*$, $\pi \rightarrow \pi^*$ and $n \rightarrow \pi^*$ transitions. In VO(L2), the azomethine chromophore transition $n \rightarrow \pi^*$ shifted to lower wavelength. This shift in azomethine chromophore indicates coordination of the metal ion to the nitrogen atom of the azomethine group. It is known that oxovanadium complexes normally display three d-d transitions in the 330 - 470, 690-520 and 625-900 nm regions [21]. These neat complexes show only two d-d bands located at 562-573 and 750-773 nm. This is in agreement with a previously reported analysis on similar oxovanadium Schiff-base complexes [22-24]. It is noted that the UV patterns of the encapsulated complexes displayed the same bands, confirming the presence of metal complex inside zeolite cage.



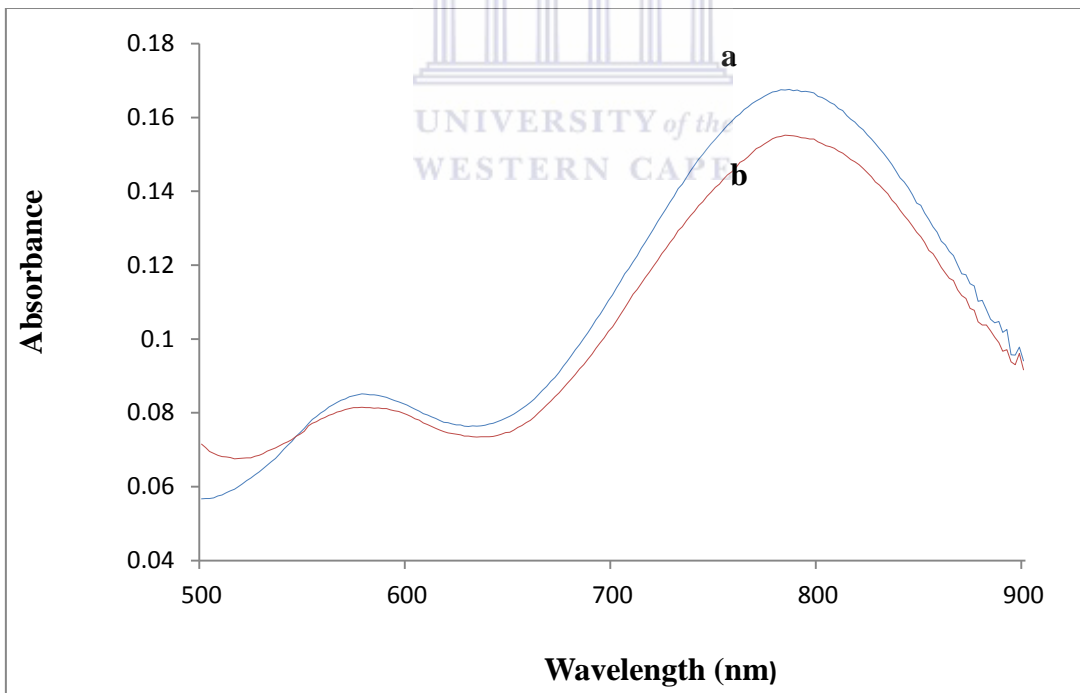
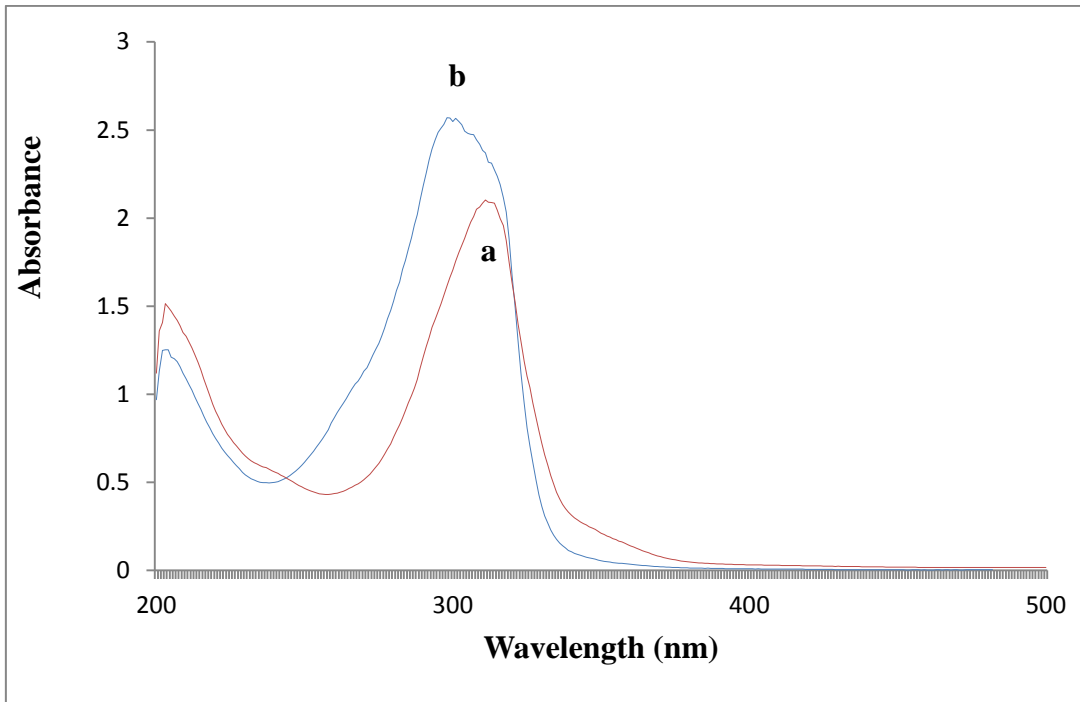


Figure 4.12 Electronic spectra: UV (top) and vis. region (bottom) of (a) VO(L1)(acac) and (b) VO(L2).

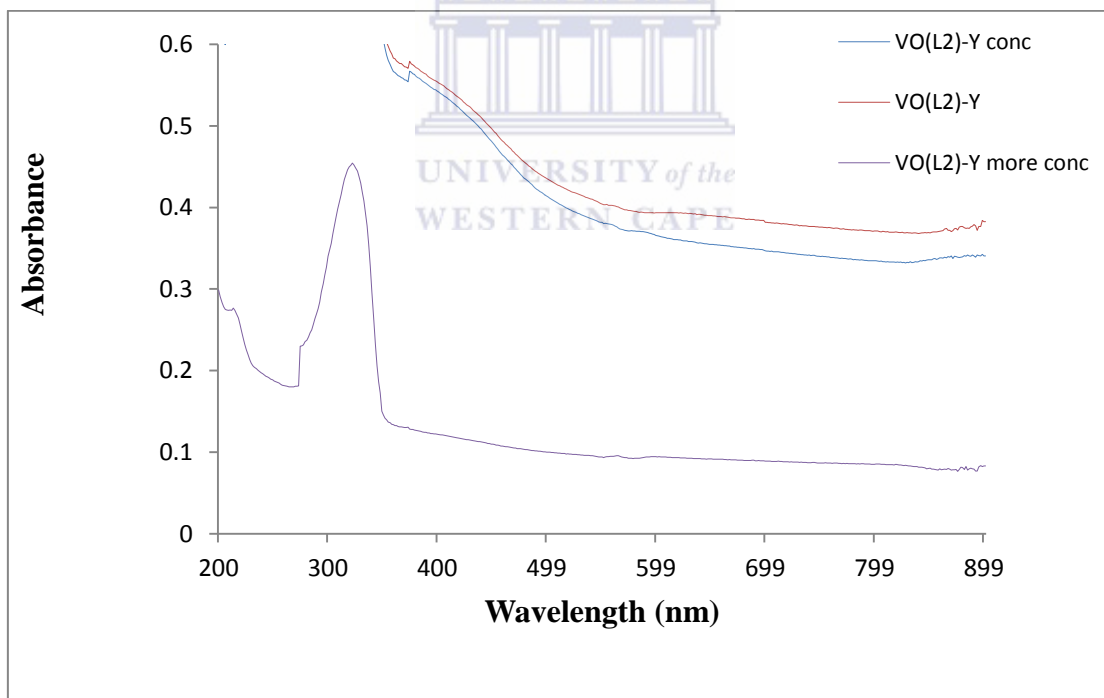
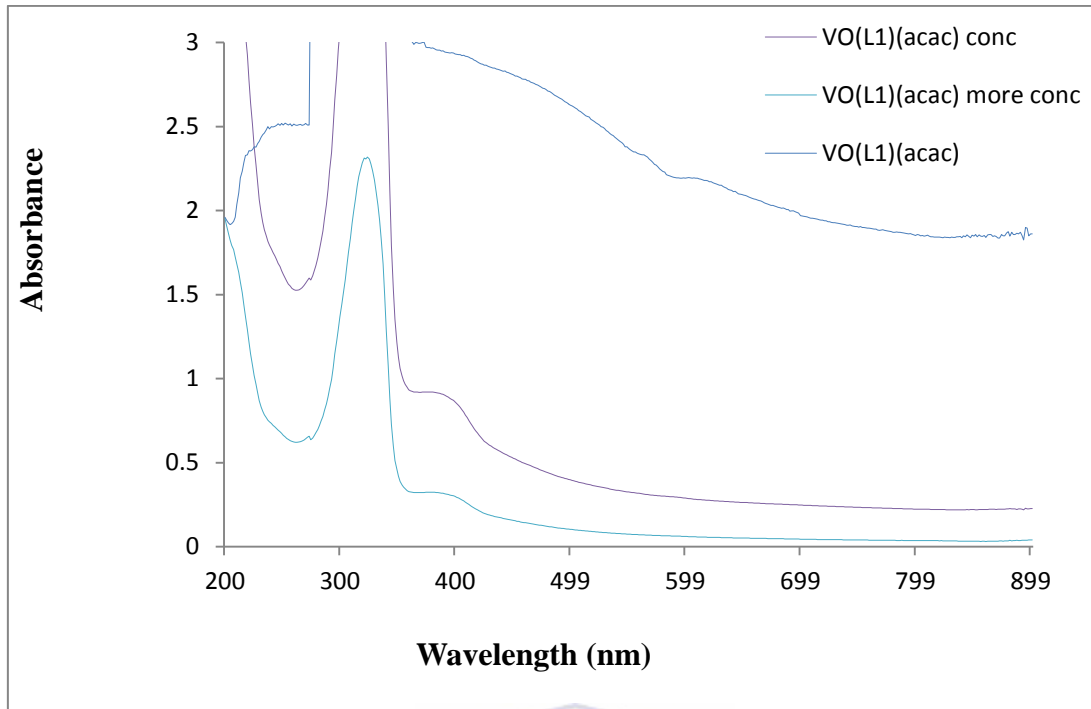


Fig.4.13 Electronic spectra: UV (top) and vis. region (bottom) of VO(L1)(acac)-Y and VO(L2)-Y

The zeolite encapsulated oxovanadium complexes viz. VO(L1)(acac)-Y and VO(L2)-Y exhibit a broad asymmetric band in the region 600–650 nm ascribed to a d–d transition that was slightly blue shifted from the corresponding free metal complex suggesting square pyramidal geometry around the metal ion of VO(IV) ions (Fig.4.15).

This confirms the formation of vanadium complexes in the cavity of the zeolite matrix.

Table 4.8 Electronic spectral data of ligands and VO(VI) complexes

Complex	λ_m /nm ($\epsilon/M^{-1} \text{ cm}^{-1}$)
L1	320
L2	322, 304 (sh)
VO(L1)(acac)	200, 241(sh),318, 347(sh), 573, 773
VO(L1)(acac)-Y	203, 231(sh),315, 373(sh), 633
VO(L2)	200, 295, 312 (sh), 562, 750
VO(L2)-Y	201, 315, 598

4.4. X- Ray Powder diffraction of Cu (II) and VO(IV) encapsulated complexes

The powder X-ray diffractograms of the respective encapsulated copper complexes, Cu-H-Y and the parent H-Y are presented in Fig.4.14.

The comparison of encapsulated oxovanadium complexes are illustrated in Fig.4.15.

It can be seen that the XRD patterns observed in H-Y, M-H-Y and encapsulated complexes are similar, although a slight change in intensity of these typical lines in the encapsulated complexes was noticed. This indicates that the zeolite framework was not affected when introducing Cu(II),VO(IV)-ions or intrazeolitic complex formation inside the zeolite framework.

Therefore, the crystallinity of zeolite Y was preserved and remained intact and can accommodate these complexes [25,26]. This finding is also in agreement with the FT-IR results. The diffraction pattern for the metal or the metal complexes could not be detected in the diffractograms of the encapsulated complexes [27]. This could possibly be due to low loading of metal complexes present in the zeolite.

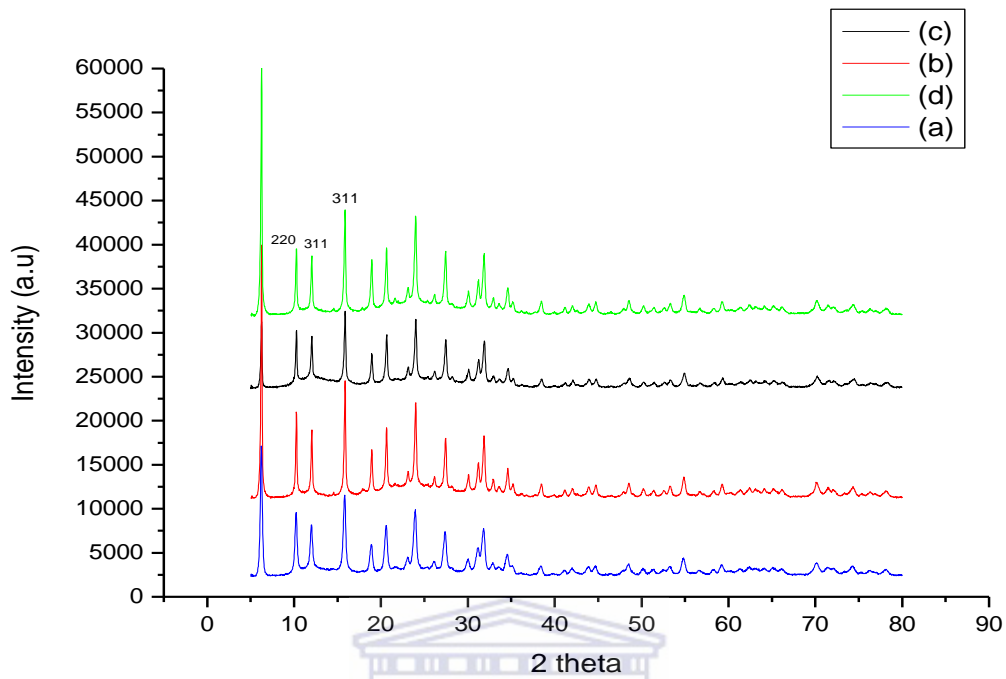


Figure 4.14 XRD patterns of (a) H-Y, (b) Cu-H-Y, (c) Cu(L2)-Y and (d) Cu(L1)(Cl)-Y

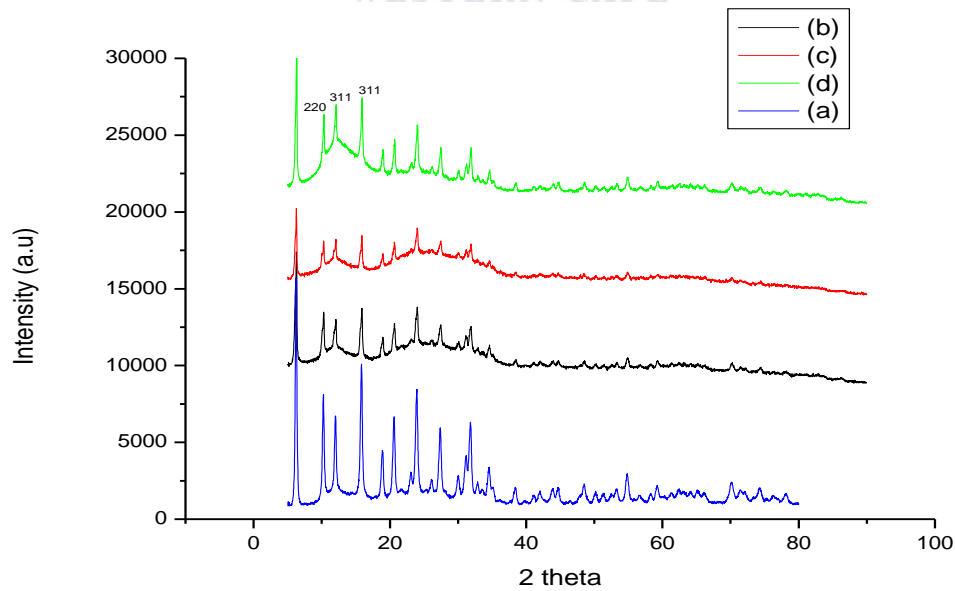


Figure 4.15 XRD of (a) H-Y, (b) VO-H-Y, (c) VO(L2)-Y and (d) VO(L1)(acac)-Y

4.5. Scanning electron microscopy of Cu(II) and OV(VI) encapsulated complexes

The Scanning Electron Micrograph (SEM) of the metal-exchanged zeolite and their respective encapsulated complexes indicate the presence of well-defined zeolite crystals without any shadow of metal ions or complexes present on their external surface. This confirms that the zeolite preserves its morphology and structure upon encapsulation of complexes [28]. This indicates that Soxhlet extraction was an excellent way of removal of uncomplexed ligand and complexes. The representative photographs of Cu-Y and Cu(L1)Cl-Y are reproduced in Figure 4.16.

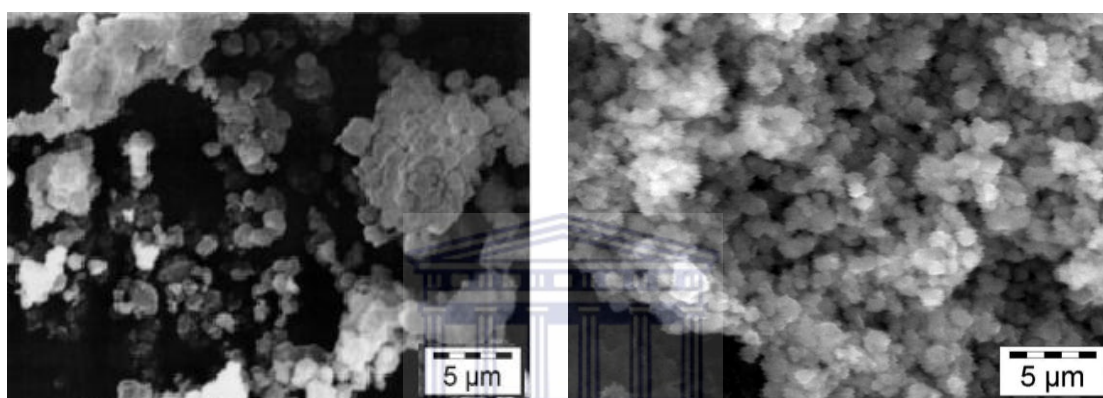


Figure 4.16 Scanning electron micrograph of Cu-Y (left) and Cu(L2)-Y (right)

4.6. Surface textural studies of Cu(II) and OV(VI) encapsulated complexes

The surface textural properties for the zeolite encapsulated complexes are presented in Table 4.9. A considerable reduction in the surface area and pore volume was observed for the zeolite encapsulated complexes when compared to their parent compounds, H-Y, Cu-H-Y and VO-H-Y.

Figures 4.17 - 4.19 shows the surface textural parameters (surface area, pore volume and pore sizes) of Cu-H-Y and VO-H-Y and their respective encapsulated catalysts, which are typical type I according to the IUPAC classification and are characteristics of the microporous nature of the materials. The surface area, pore volume and pore size of the encapsulated metal complex, along with that of the parent H-Y zeolite, are presented in Table 4.9. The surface area and pore volume were decreased due to the presence of the complex in the zeolite-Y cavities [29, 30] and not as a result of the presence of complexes on the external surface due to the removal of the ions and complexes attached the zeolite's

surface by soxhlet extraction. This supports the observation that the complexes are present within the zeolite cages and not on the external surface since the zeolite crystallinity was retained. However, the decreasing values in the surface area, pore volume and adsorption capacity depends on the amount of incorporated complexes as well as their molecular size and geometrical conformation inside the zeolitic host [31].

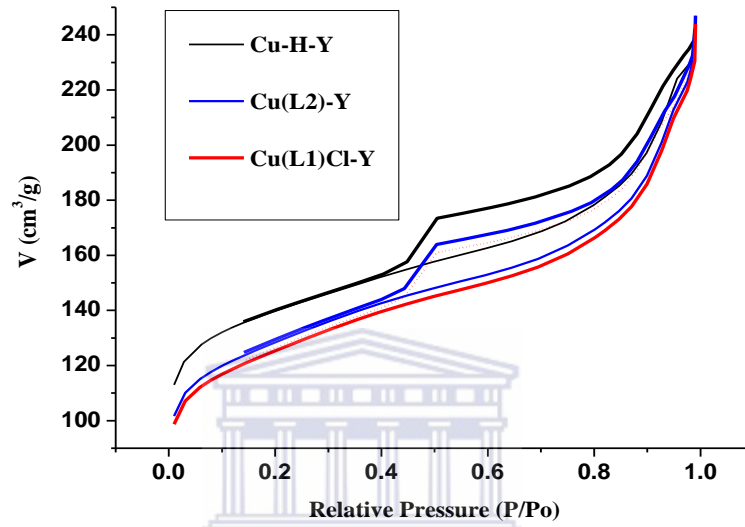


Figure 4.17 N₂ adsorption/desorption isotherms of Cu-H-Y, Cu(L1)Cl-Y and Cu(L2)-Y.

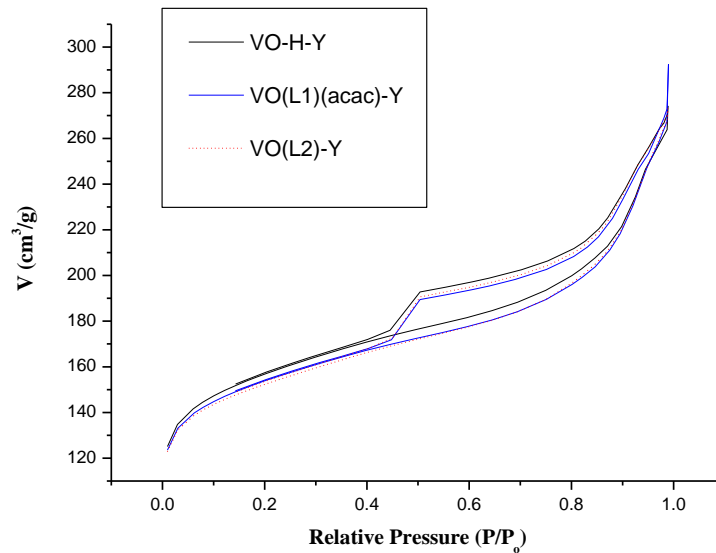


Figure 4.18 N₂ adsorption/desorption isotherms VO-H-Y, VO(L1)(acac)-Y and VO(L2)-Y

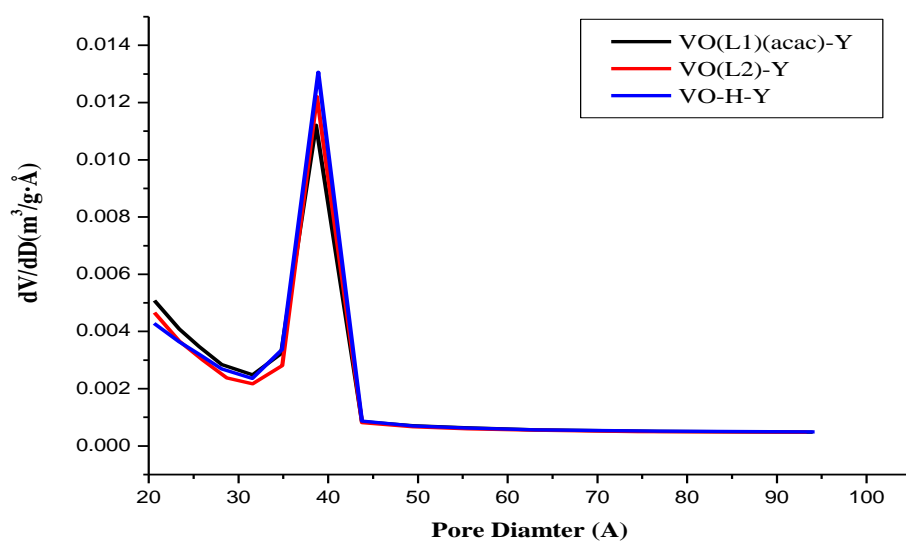


Figure 4.19 Pore size distribution of VO-H-Y, VO(L1)(acac)-Y and VO(L2)-Y.

Table 4.9 Physical, analytical data and surface area and pore volume data for the catalysts

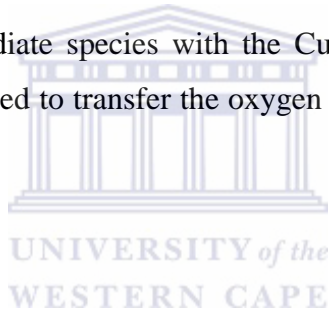
Catalyst	Colour	Metal Content (% wt)	Langmuir Surface area (m ² /g)	Pore Volume (mL/g)	Average Pore size (Å)
H-Y	White	-	780	0.48	42.5
Cu-H-Y	Light blue	0.17	476	0.36	31.33
OV-H-Y	Light green	0.28	535	0.41	31.01
[Cu(L1)Cl]-Y	Pale brown	0.13	452	0.33	30.43
[VO(L1)(acac)]-Y	Pale green	0.11	518	0.40	30.47
[Cu(L2)]-Y	Pale blue	0.18	439	0.34	30.06
[VO(L2)]-Y	Pale green	0.12	524	0.40	30.46

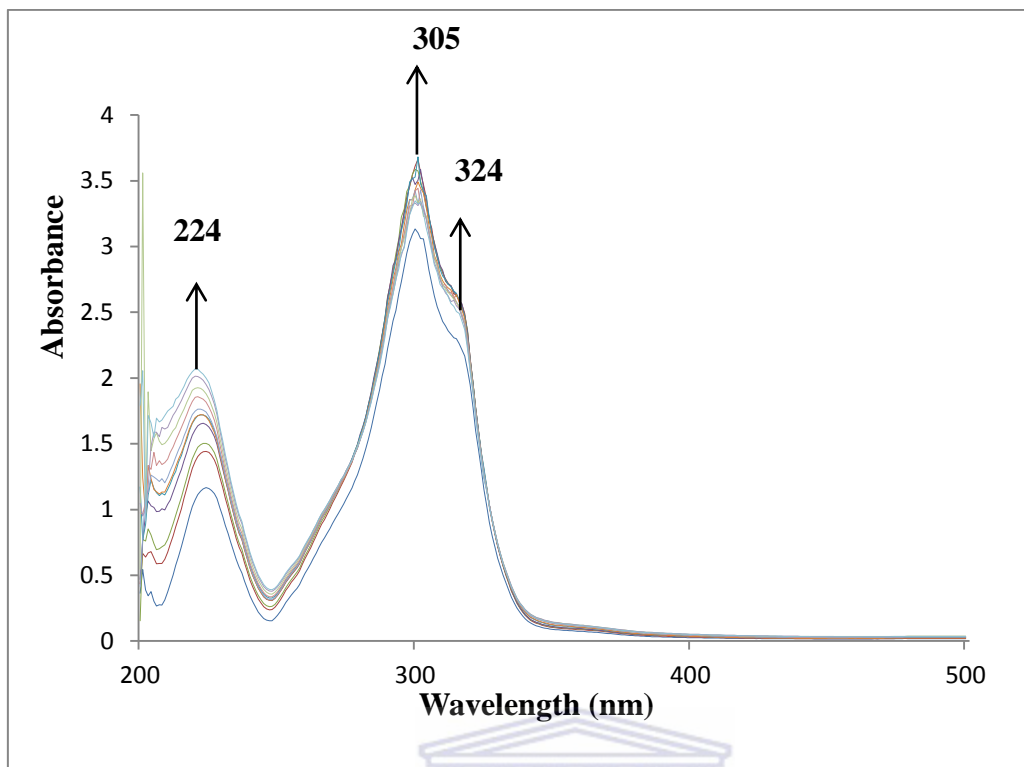
4.7. Possible reaction pathway of catalysts

4.7.1. Cu(II) system

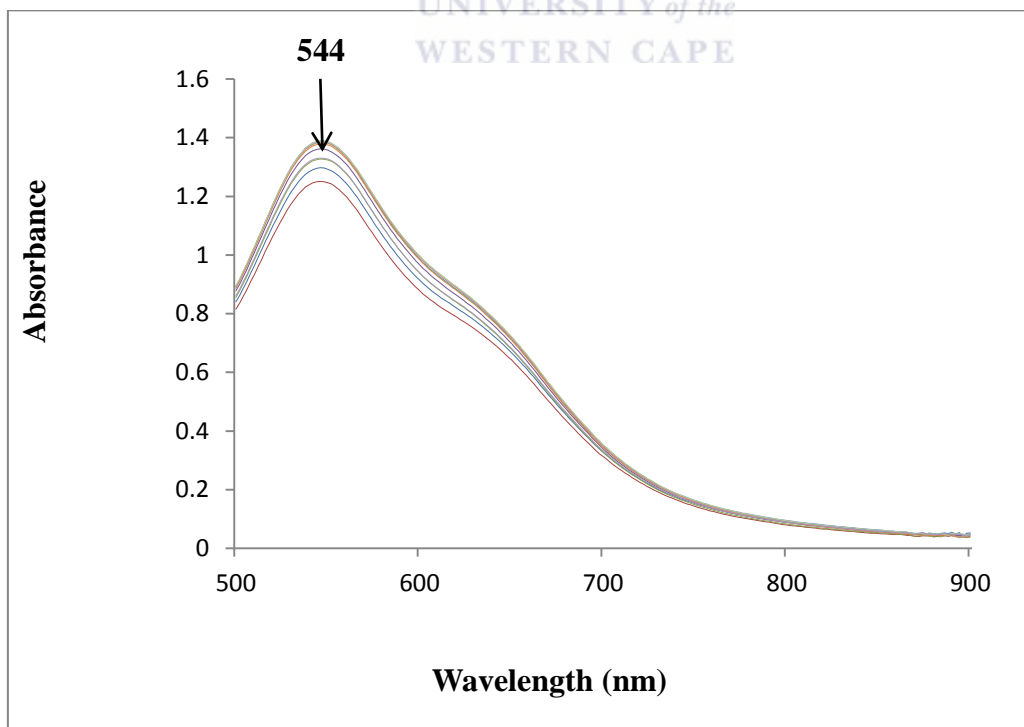
To understand reaction pathway and intermediate species formed during oxidation of the substrates, a methanolic solution of neat copper(II) complexes were treated with a methanolic solution of H₂O₂ (dropwise) and the progress of the reaction was monitored by electronic absorption spectroscopy.

As shown in Figs. 4.20 and 4.21, addition of one drop of 30 % H₂O₂ in methanol to a solution of Cu(L1)Cl or Cu(L2) (10⁻⁴ M solution) dissolved in methanol resulted in a considerable increase in the intensity of the band appearing at ~220 nm. Simultaneously, the other bands between 278-340 nm experienced a slight increase in their intensities. On the other hand, the intensities of the d-d bands in the region between 550-880 nm were decreased. Further addition of H₂O₂ did not reduce the peak's intensity. The spectral changes in the UV-Vis region indicate formation of an intermediate peroxo species and the interaction of peroxo intermediate species with the Cu(II) metal centre in the complex. These intermediates are expected to transfer the oxygen atoms to the substrates to give the products [23, 32].



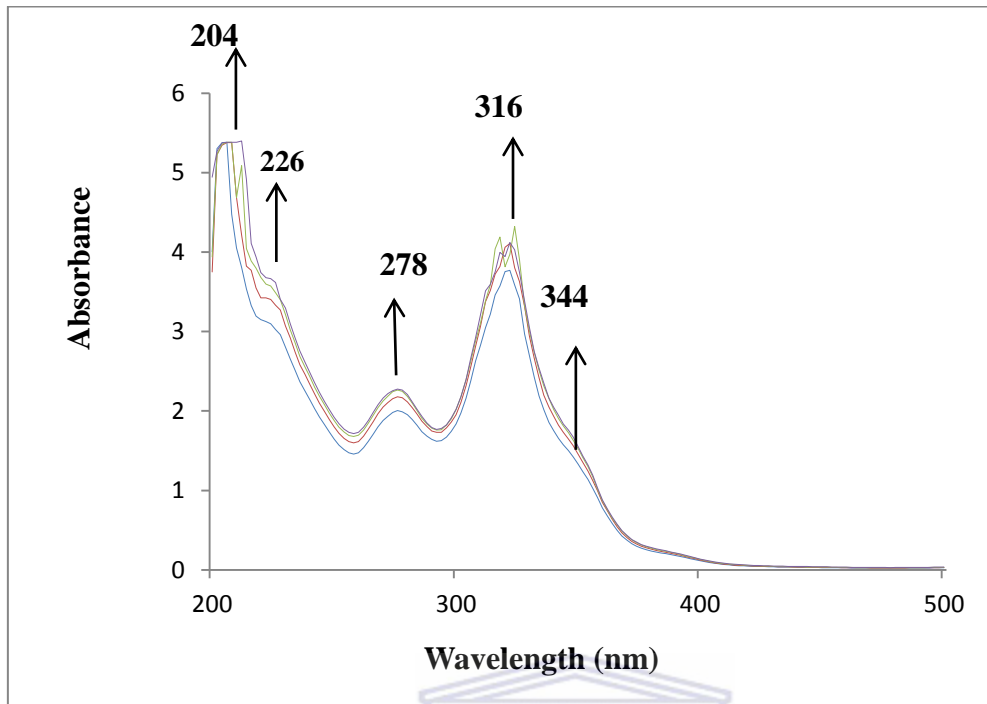


(a)

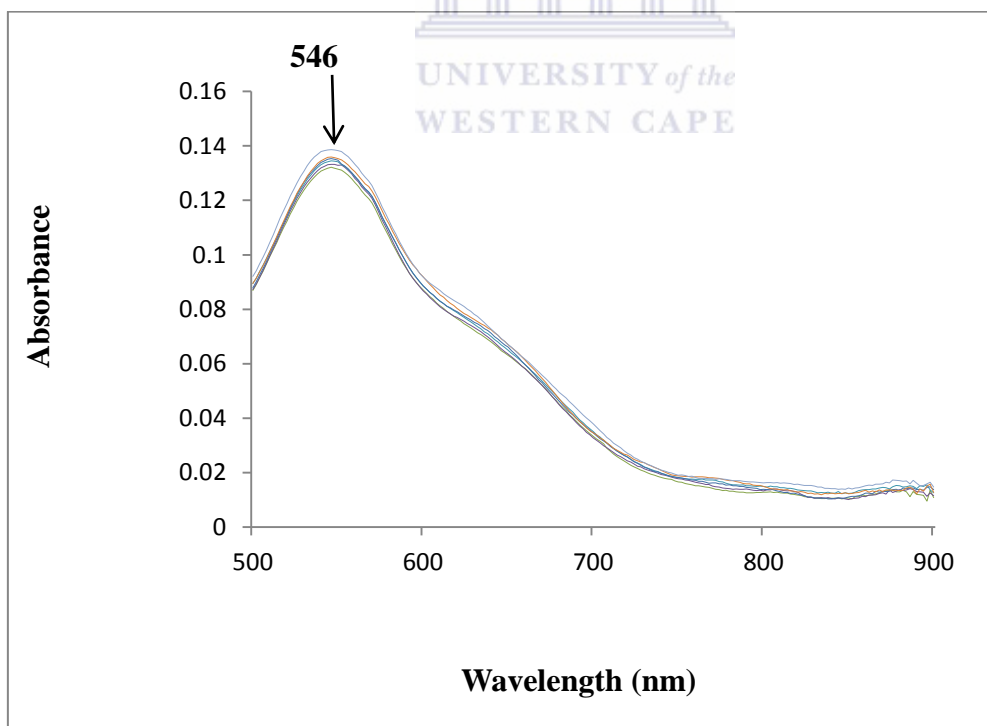


(b)

Figure 4.20 Kinetic studies of Cu(L1)Cl in (a) UV and (b) visible region.



(a)



(b)

Figure 4.21 : Kinetic studies of Cu(L2) in (a) UV and (b) visible region.

4.7.2. VO(IV) systems

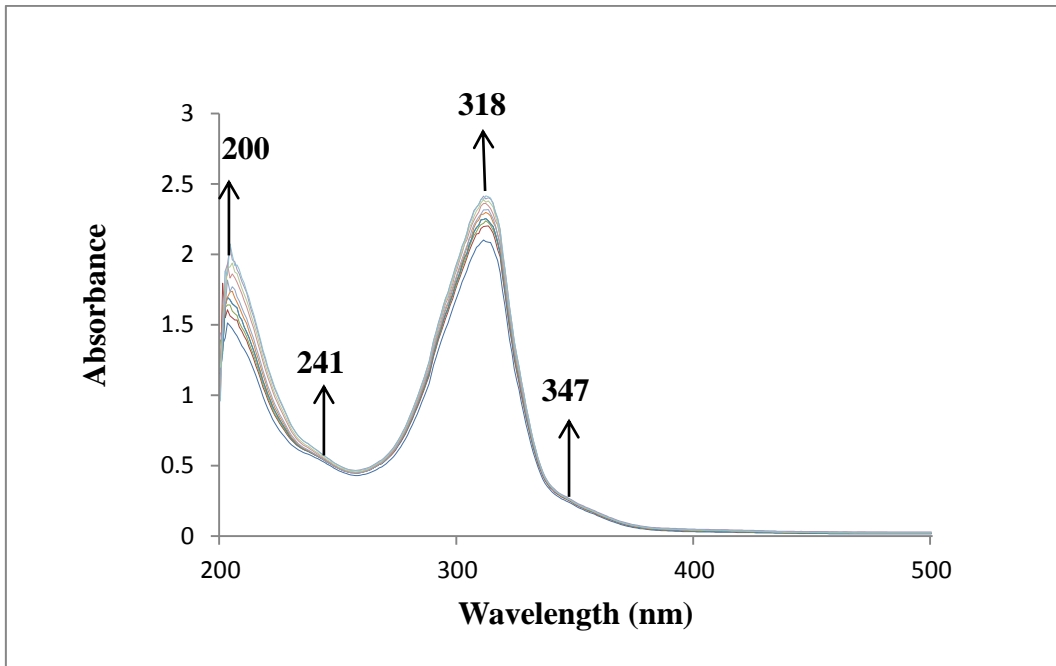
Similarly, the stepwise addition of aqueous H₂O₂ to a 10⁻⁴ M methanolic solution of oxovanadium complexes resulted in increase in the intensities of the bands at UV region without changing their position.

Addition of 30 % H₂O₂ dropwise to a 10⁻⁴ M methanolic solution of VO(L1)(acac) resulted in slight increase of the intensities for the bands at 202, 241, 318 and 347 nm without changing their position (Fig 4.22).

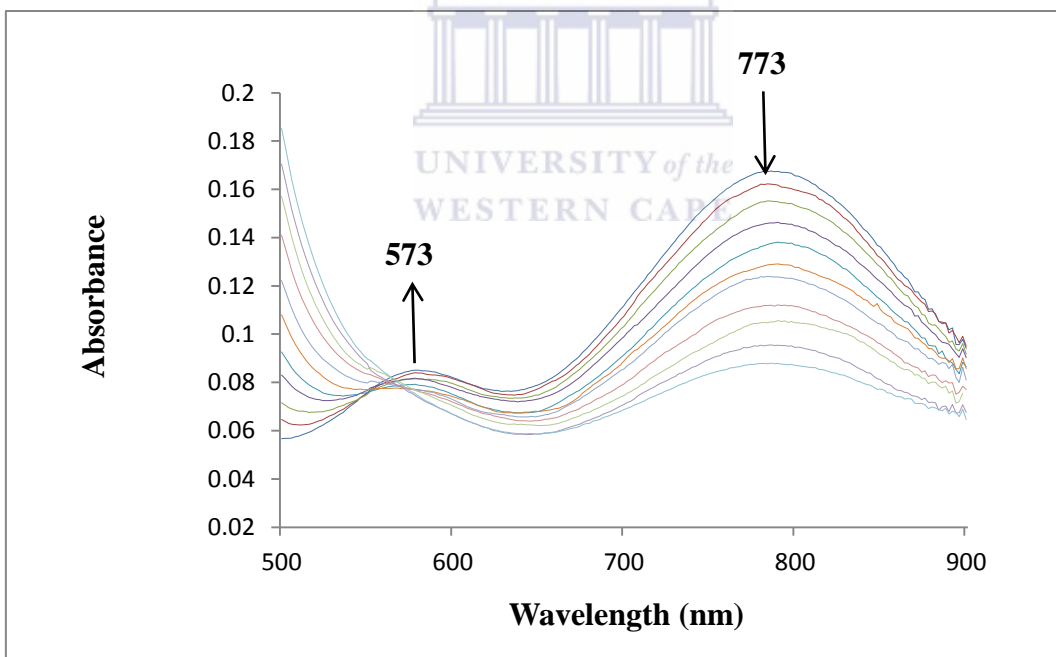
Addition of H₂O₂ solution to a methanolic solution of VO(L2) resulted in an immediate shifting of the strong band at 295 nm to 283 nm. This shifted band slowly increased in intensity upon addition of H₂O₂. The shoulder at 312nm becomes more distinguishable from the other band after the addition of further H₂O₂. Gradual addition of dilute H₂O₂ results in a slight increase in the intensity of this band (Fig.4.23).

The intensity of the d-d transition band at 562 nm is slowly broadens and finally disappeared whereas the other d-d transition band at 750 nm decreased with increasing the addition of H₂O₂ without changing its position. Further addition of H₂O₂ did not reduce intensity of this band.

These spectral changes observed, indicate the oxidation of V(IV) yielding oxoperoxovanadium(V) species [33]. Oxoperoxovanadium (V) complexes are very active intermediate species and participate in oxidation reaction by transferring one of its oxygens to the substrate [34, 35]. This is supported by the spectral changes with disappearance of d-d bands present in VO(L1)(acac) at 573 and 773 nm. The same pattern in the visible region was also observed with VO(L2). These spectral changes and the presence of isosbestic point at ~550 nm which indicates the presence of equilibrium between two substances and they have the identical absorbance. This suggests the oxidation of oxovanadium(IV) complex to give oxoperoxovanadium(V) species.

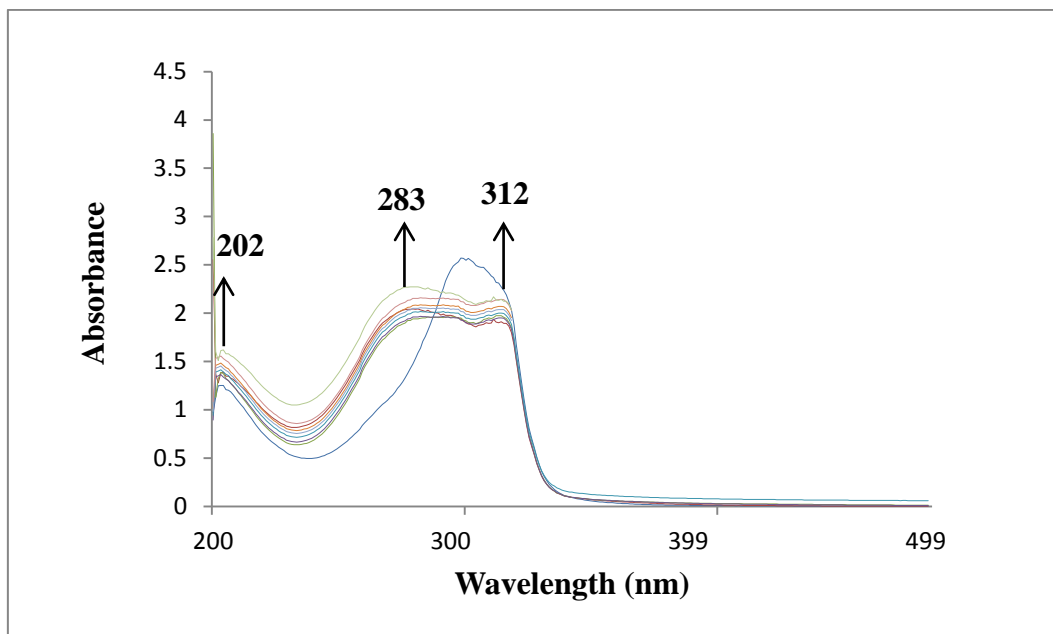


(a)

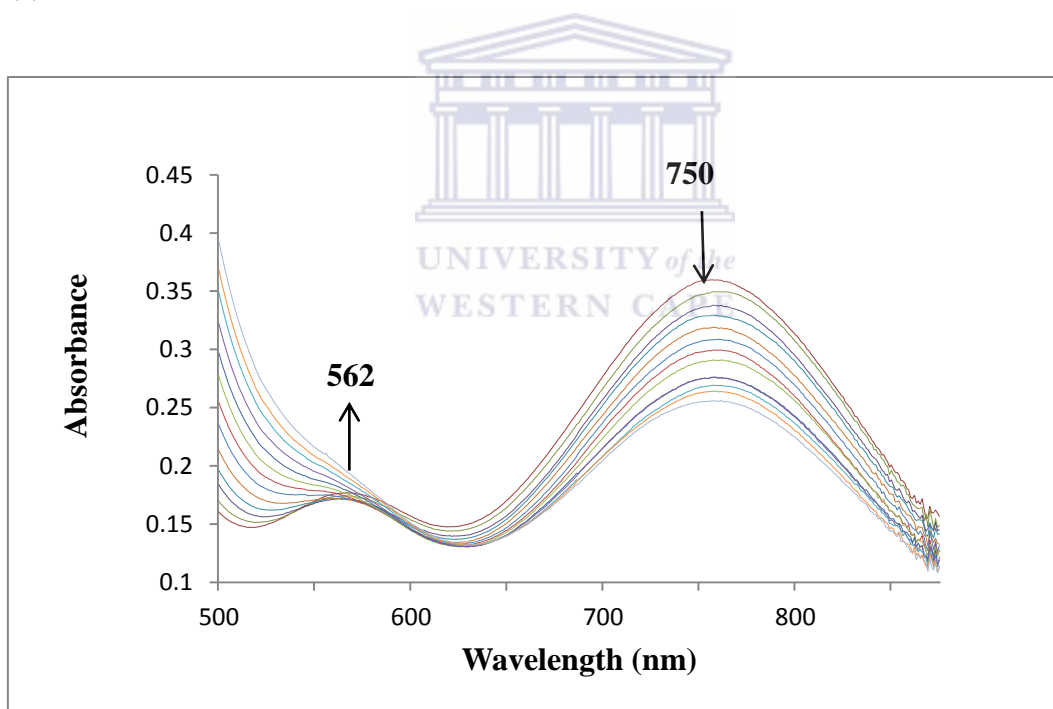


(b)

Figure 4.22 Kinetic studies of VO(L1)(acac) in (a) UV and (b) visible region



(a)



(b)

Figure 4.23 Kinetic studies of VO(L2) in (a) UV and (b) visible region.

References

- [1] (a) Jacob C.R., Varkey S.P., Ratnasamy P., "Selective oxidation over copper and manganese salens encapsulated in zeolites", *Microporous Mesoporous Mater*, 22 (1998) 465; (b) Bowers C., Dutta P.K., "Olefin oxidation by zeolite-encapsulated manganese (salen)⁺ complexes under ambient conditions", *J Catal*, 122 (1990) 271; (c) Balkus Jr. K.J., Gabrielov, A.G. "Zeolite encapsulated metal complexes", *J Incl Phenom Mol Recog Chem* 21 (1995) 159.
- [2] Ranganathan S., Tamilarasu N., *Chemical approaches to protein engineering 20: The transformation of coded amino acid tyrosine to pro-templates having metal uptake potential in peptidprotein segmentst*, *Indian J Chem* 40B (2001) 1084.
- [3] Ozkar S., Ulku D., L.T Yildirim, N. Biricik, Gumgum B., *Crystal and molecular structure of bis(acetylaceton)ethylenediimine: intramolecular ionic hydrogen bonding in solid state*, *J Mol Struct* 688 (2004) 208.
- [4] Kianfar A.H., Keramat L., Dostani M., Shamsipur M., Roushani M., Nikpour F., *Synthesis, spectroscopy, electrochemistry and thermal study of Ni(II) and Cu(II) unsymmetrical N₂O₂ Schiff base complexes*, *Spectrochim Acta A* 77 (2010) 425.
- [5] Costes J.P, Dahan F., Laurent J.P, *Experimental existence of the half unit 7-amino-4-methyl-5-aza-3-heptene-2-one (AEH).Crystal structure of a novel dibromo-bridge dicopper(II) complex (CuAEBr)₂*, *J Coord Chem* 13 (1984) 361.
- [6] Ueno K., Martell A.E, *Ultraviolet and Visible Absorption Spectra of Metal Chelates of Bisacetylacetonethylenediimine and Related Compounds*, *J Am Chem Soc* 61 (1957) 258.
- [7] Ghosh K., Kumar P., Goyal I., *Synthesis and characterization of chromium(III) complexes derived from tridentate ligands: Generation of phenoxy radical and catalytic oxidation of olefins*, *Inorg Chem Commun* 24 (2012) 82.
- [8] Maurya M.R., Saini P., Haldar C., Avecilla F., *Synthesis, characterisation and catalytic activities of manganese(III) complexes of pyridoxal-based ONNO donor tetradenatate ligands*, *Polyhedron* 31 (2012) 714.
- [9] Dolaz M., Tu'mer M., Dıg'rak M., *Synthesis, characterization and stability constants of polynuclear metal complexes*, *Transition Met Chem* 29 (2004) 531.

- [10] Mohamed G.G., El-Wahab Z.H.A, Mixed ligand complexes of bis(phenylimine) Schiff base ligands incorporating pyridinium moiety: Synthesis, characterization and antibacterial activity, *Spectrochim Acta A* 61 (2005) 1063.
- [11] Jeewoth T., Bhowon M.G., Wah H.L.K, Synthesis, characterization and antibacterial properties of Schiff bases and Schiff base metal complexes derived from 2,3-diaminopyridine, *Transition Met Chem* 24 (1999) 447.
- [12] Kulkarni A.D., Patil S.A., Badam P.S., Electrochemical Properties of some Transition Metal Complexes: Synthesis, Characterization and In-vitro antimicrobial studies of Co(II), Ni(II), Cu(II), Mn(II) and Fe(III) Complexes, *Int J Electrochem Sci*, 4 (2009) 721 – 722.
- [13] Abbo H.S., Titinchi S.J.J., Di-, tri- and tetra-valent ion-exchanged NaY zeolite: Active heterogeneous catalysts for hydroxylation of benzene and phenol, *Appl Catal A: Gen* 356 (2009) 168.
- [14] Salama T.M., Ahmed A.H., El-Bahy Z.M., Y-type zeolite-encapsulated copper(II) salicylidene-p-aminobenzoic Schiff base complex: Synthesis, characterization and carbon monoxide adsorption, *Micropor Mesopor Mater* 89 (2006) 255.
- [15] Salavati-Niasari M., Host (nanocavity of zeolite-Y)/guest ($[\text{Cu}([\text{R}]_2\text{-N}_2\text{X}_2)]^{2+}$ (R = H, CH₃; X = NH, O, S) nanocomposite materials: Synthesis, characterization and catalytic oxidation of ethylbenzene, *J Mol Catal A: Chem* 284 (2008) 102.
- [16] Islama S.M., Roy A. S, Mondal P., Mubarak M., Mondal S., Hossain D., Banerjee S., Santra S.C., Synthesis, catalytic oxidation and antimicrobial activity of copper(II) Schiff base complex, *J Mol Catal A: Chem* 336 (2011) 109.
- [17] Sarkar B., Bocelli G., Cantoni A., Ghosh A., Copper(II) complexes of symmetrical and unsymmetrical tetradentate Schiff base ligands incorporating 1-benzoylacetone: Synthesis, crystal structures and electrochemical behaviour, *27 (2008) Polyhedron* 695 - 696.
- [18] Marusak R. A., Doan K., Cummings S.D., *Integrated Approach to Coordination Chemistry: An Inorganic Laboratory Guide*, John Wiley & Sons (2007) 74.
- [19] Gangadharmath U.B, Revankar V.K, Mahale V.B, Synthesis and spectroscopic characterization of cationic mononuclear oxovanadium(IV) complexes with tetradentate Schiff bases as ligands, *Spectrochim Acta A* 58 (2002) 2654 -2655.

- [20] Kianfar A. H., Paliz M., Roushani M., Shamsipur M., Synthesis, spectroscopy, electrochemistry and thermal study of vanadyl tridentate Schiff base complexes, *Spectrochim Acta A* 82 (2011) 45
- [21] Bonadies J.A, Carrano C.J, Vanadium phenolates as models for vanadium in biological systems. 1. Synthesis, spectroscopy, and electrochemistry of vanadium complexes of ethylenebis[(*o*-hydroxyphenyl)glycine] and its derivatives, *J Am Chem Soc* 108 (1986) 4092.
- [22] Maurya M.R, Chandrakar A.K, Chand S., Oxidation of methyl phenyl sulfide, diphenyl sulfide and styrene by oxovanadium(IV) and copper(II) complexes of NS donor ligand encapsulated in zeolite-Y, *J Mol Cat A:Chem A* 278 (2007) 20.
- [23] Maurya M.R, Kumar M., Kumar A., Pessoa J.C, Oxidation of *p*-chlorotoluene and cyclohexene catalysed by polymer-anchored oxovanadium(IV) and copper(II) complexes of amino acid derived tridentate ligands, *Dalton Trans* (2008) 4229 - 4230.
- [24] Samanta S., Ghosh D., Mukhopadhyay S., Endo A., Weakley T. J. R., Chaudhury M., Oxovanadium(IV) and -(V) Complexes of Dithiocarbamate-Based Tridentate Schiff Base Ligands: Syntheses, Structure, and Photochemical Reactivity of Compounds Involving Imidazole Derivatives as Coligands, *Inorg Chem* 42 (2003) 1508-1517.
- [25] Maurya M. R., Saklani H., Agarwal S., Oxidative bromination of salicylaldehyde by potassium bromide/H₂O₂ catalysed by dioxovanadium(V) complexes encapsulated in zeolite-Y: a functional model of haloperoxidases, *Catal Commun* 5 (2004) 566.
- [26] Jacob C.R., Varkey S.P., Ratnasamy P., Selective oxidation over copper and manganese salens encapsulated in zeolites, *Micropor Mesopor Mat* 22 (1998) 469.
- [27] Salavati-Niasari M., Synthesis, characterization and catalytic epoxidation of styrene using molecular oxygen over “neat” and host-guest nanocomposite materials, *J Mol Catal A: Chem* 278 (2007) 25-26.
- [28] Kuz’niarska-Biernacka I., Biernacki K., Magalhães A.L., Fonseca A.M., Neves I.C., Catalytic behavior of 1-(2-pyridylazo)-2-naphthol transition metal complexes encapsulated in Y zeolite, *J Catal* 278 (2011) 106.

- [29] Varkey S.P., Ratnasamy C., Ratnasamy P., Zeolite-encapsulated manganese (III) salen complexes, *J Mol Catal A Chem* 135 (1998) 301.
- [30] Abraham R., Yusuff K.K.M., Copper(II) complexes of embelin and 2-aminobenzimidazole encapsulated in zeolite Y-potential as catalysts for reduction of dioxygen, *J Mol Catal A: Chem* 198 (2003) 177.
- [31] Jin C., Fan W., Jia Y., Fan B., Ma J., Li R., Encapsulation of transition metal tetrahydro-Schiff base complexes in zeolite Y and their catalytic properties for the oxidation of cycloalkanes, *J Mol Catal A : Chem* 249 (2006) 26.
- [32] Maurya M.R., Chandrakar A. K, Chand S., Oxovanadium(IV) and copper(II) complexes of 1,2-diaminocyclohexane based ligand encapsulated in zeolite-Y for the catalytic oxidation of styrene, cyclohexene and cyclohexane, *J Mol Cat A: Chem A* 270 (2007) 233 - 234.
- [33] Maurya M.R., Arya A., Pedro Adao J. C. Pessoa, Immobilisation of oxovanadium (IV), dioxomolybdenum(VI) and copper(II) complexes on polymers for the oxidation of styrene, cyclohexene and ethylbenzene, *Appl Catal A: Gen* 351 (2008) 250-251.
- [34] Maurya M. R., Sikarwar S., Kumar M., Oxovanadium(IV) complex of b-alanine derived ligand immobilised on polystyrene for the oxidation of various organic substrates, *Catal Commun* 8 (2007) 2022.
- [35] Maurya M.R., Sikarwar S., Oxidation of phenol and hydroquinone catalysed by copper(II) and oxovanadium(IV) complexes of N,N-bis(salicyledene) diethylenetriamine (H₂saldien) covalently bonded to chloromethylated polystyrene, *J Mol Catal A: Chem* 263 (2007) 183.

CHAPTER 5

5. CATALYTIC ACTIVITY STUDIES OF CU(II) CATALYSTS FOR OXIDATION REACTIONS

5.1 Introduction

Copper(II) complexes have been found to show excellent catalytic activity towards various oxidation reactions and have occupied a major place in oxidation chemistry due to their abundance in natural and biological media [1,2]. In recent years, considerable research has been dedicated to the preparation of different solid heterogeneous copper catalysts and their application in the oxidation of different organic substrates [3-8].

The Cu(II) complexes encapsulated in zeolite Y has also attracted considerable attention due to their remarkable activity in catalysis. Recent studies have shown that encapsulated zeolite Y copper(II) based catalytic systems displayed good activity and selectivity for the oxidation of styrene, phenol and various substrates when using H₂O₂ as oxidant [9-13].

The most typical oxidant used in oxidation reactions is hydrogen peroxide and alkyl hydroperoxides [14,15]. Advantages of hydrogen peroxide over other oxidants is its relative stability and being a relatively strong oxidant [16] and also provides an efficient route for epoxide preparation because it is easy to handle and the only by-product is water thus satisfying green chemistry requirements [17]. In zeolitic systems, hydrogen peroxide and oxygen are the preferred oxidants as they are highly mobile in the pores due their smaller size. They are also cheaper and sufficiently environment-friendly to be used on a commercial scale. However, aerobic oxidation is expected to occur at a slower rate as a result of the inability of molecular oxygen to be activated in comparison to peroxides which are highly reactive species [18]. The drawbacks of organic peroxides are that they may be explosive, corrosive, toxic and present extreme fire hazards. Many organic peroxides also give off flammable vapours when decomposing [19].

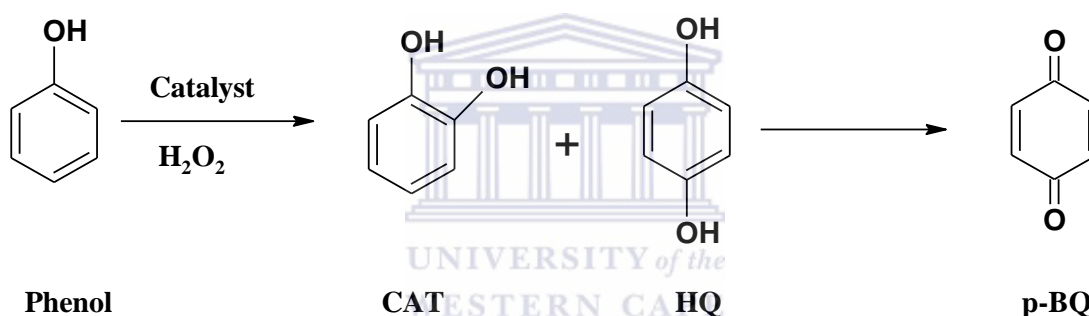
Results of the investigation of catalytic activity of Cu(L1)Cl and Cu(L2) complexes encapsulated in zeolite Y in the oxidation of phenol, benzene, styrene and cyclohexene using H₂O₂ as an oxidant are presented. The catalytic activity of neat complexes is also compared.

To find suitable reaction conditions in order to obtain maximum conversion of substrates, the effect of temperature, amount of catalyst, volume of solvent, concentration of H₂O₂ and the nature of solvent was investigated using Cu(L2)-Y as a representative catalyst. The optimized reaction conditions studied were only controlled to hydroxylation of phenol.

5.2 Oxidation reactions

5.2.1 Hydroxylation of phenol

The catalytic oxidation of phenol usually gives two products: catechol (CAT) and hydroquinone (HQ). In some cases, further oxidation may occur to form *para*-benzoquinone (Scheme 5.1). Numerous factors influence the catalytic activity of a reaction *viz.* H₂O₂/phenol molar ratio, temperature, amount of catalyst, type of solvent and volume of solvent.



Scheme 5.1 Oxidized products for the hydroxylation of phenol

The general reaction parameters discussed for phenol hydroxylation are:

5.2.1.1 Effect of H₂O₂/phenol molar ratio

5.2.1.2 Effect of temperature

5.2.1.3 Effect of solvents

5.2.1.4 Effect of volume of solvent

5.2.1.5 Effect of amount of catalyst

The percent substrate conversion and product selectivity were calculated from GC using the following formulae:

$$\% \text{ Conversion of substrate} = \frac{\text{Amount of products}}{\text{Amount substrate} + \text{Amount of products}} \times 100$$

$$\% \text{ Selectivity of a product} = \frac{\text{Amount of a product}}{\text{Total amount of products}} \times 100$$

The quantifications were made on the basis of the relative peak area of the substrate and their corresponding products.

5.2.1.1 Effect of H₂O₂/phenol molar ratio

In order to determine the effect of H₂O₂/phenol molar ratio on the oxidation of substrate, three different molar ratios (0.3:1, 1:1 and 2:1) were studied, whilst keeping a fixed amount phenol (0.025 mol) and catalyst (0.01g) in 3 ml MeCN at 70°C and running the reaction for 24h (Fig.5.1). It was found that on increasing the H₂O₂/ phenol ratio from 0.3:1 to 1:1, the conversion increased ~4 folds from 5.1 to 19.2 % and lead to a drop in catechol selectivity after 6h, yielding 75.3 %. The poor activity of the catalyst at low molar ratio could be as a result of significantly decreasing hydroxyl radicals generated from H₂O₂ that can react with excess of phenol to generate the intermediate [20].

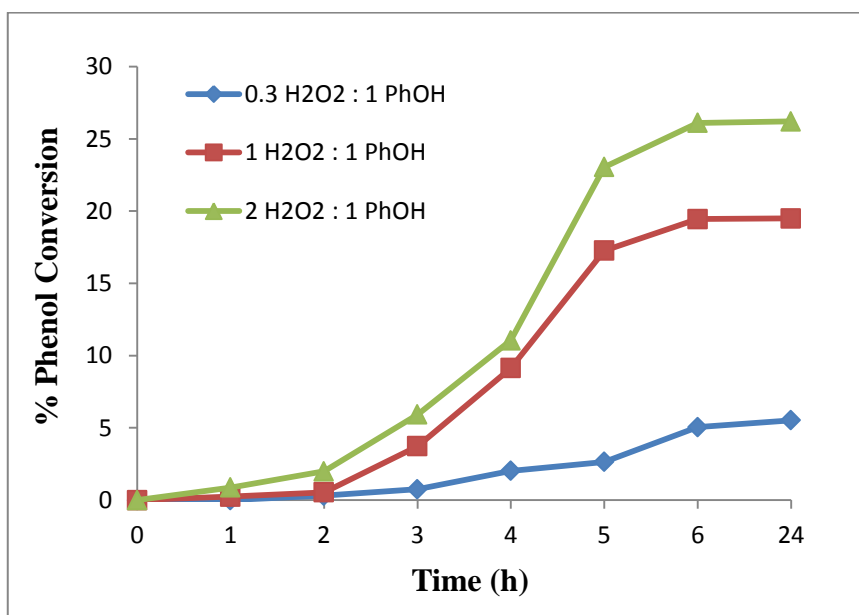


Figure 5.1 % Phenol conversion using different H₂O₂/PhOH molar ratios

When the amount of H₂O₂ was doubled, % conversion was increased by almost by 8 % but % catechol selectivity increased [9]. While, the effect of oxidant concentration had no influence on product selectivity. For this reason and in order to reduce oxidant consumption, it was decided that the best ratio to work with was 1:1. High selectivity to produce catechol was obtained for all ratios used (Table 5.1).

Table 5.1 Effect of H₂O₂/PhOH molar ratio on phenol hydroxylation^a and product selectivity

H ₂ O ₂ / PhOH (molar ratio)	% Phenol Conversion	% Product selectivity	
		CAT	HQ
0.3 : 1	5.1	100	-
1 : 1	19.2	75.3	24.7
2 : 1	27.1	78.1	21.9

^a Reaction conditions : phenol 2.35 g, Cu(L2)-Y 0.010 g, MeCN 3 ml, 70 °C, 6h

5.2.1.2 Effect of reaction temperature

The performance of the catalysts was investigated at three different temperatures, *viz.* 60, 70 and 80 °C whilst keeping all the other parameters constant over a period of 24h. Fig.5.2 illustrates the effect of temperature on the oxidation of phenol. At low temperature (60° C) the reaction show a very low activity with high selectivity to catechol formation. On increasing temperature to 70°C the % conversion increased 4-folds with a drop in CAT (75.3 %) selectivity. Further increasing the reaction temperature to 80 °C maximum conversion for phenol hydroxylation was observed. However, % catechol selectivity was decreased but still the predominant product.

It can be concluded that at higher temperature the reaction reached a maximum conversion, but with a decrease in product selectivity (Table 5.2).

A drawback at working at higher reaction temperatures the possibility of thermal degradation of the oxidant *i.e.* H₂O₂ [21]. This is as a result of H₂O₂ that is consumed in the parallel reaction of decomposition (H₂O₂ → H₂O + 1/2 O₂) [22]. For this reason and in order to work at lower temperature, it was decided that the best temperature to work with was 70°C.

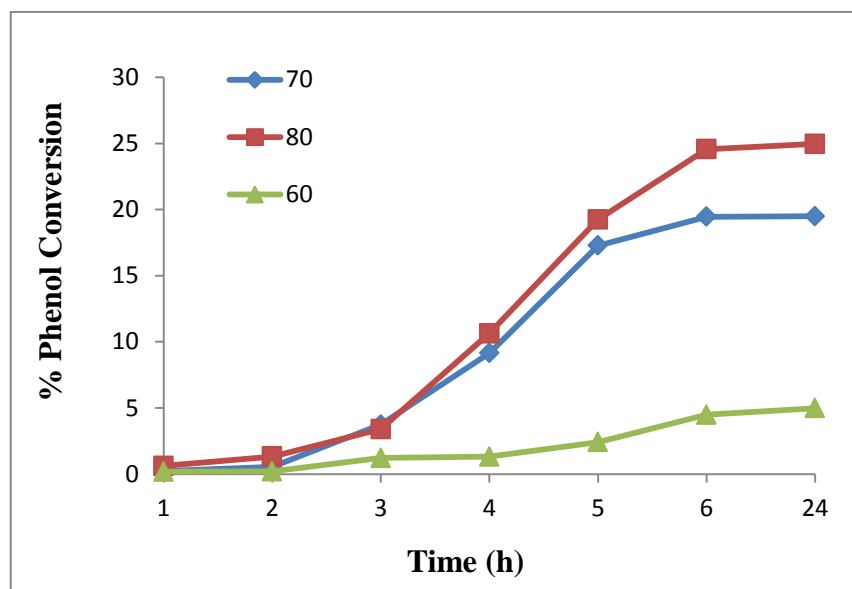


Figure 5.2 Effect of reaction temperature on % phenol conversion over time

Table 5.2 Effect of reaction temperature on phenol conversion^a and product selectivity.

Reaction Temperature (°C)	% Phenol Conversion	% Product selectivity	
		CAT	HQ
60	5.0	100	-
70	19.5	75.6	24.4
80	24.7	66.7	33.3

^a Reaction conditions : Phenol 2.35 g, H₂O₂ 2.83 g, Cu(L2)-Y 0.010 g, MeCN 3 ml, 6h

5.2.1.3 Effect of solvents

It is known that the nature of solvent has an important influence on the result of a reaction, i.e. on yields, products formation and reaction kinetics [23]. The influence of solvent on the catalytic activity for the hydroxylation of phenol was investigated using five different solvents ranging from polar, MeCN, ethanol and ethyl acetate to non-polar, i.e. DCM and n-hexane whilst keeping all the other reaction conditions constant.

Solvents influence reaction rates by competitive sorption/adsorptions in the supercages of zeolite, polarity, solvation power and the size of the solvent molecule [24]. The effect of different solvents on the oxidation of phenol is illustrated in Figure 5.3. From Table 5.3, it is clear that the nature of the solvent affects the rate of the reaction as well as the selectivity. Relatively low conversions were observed in n-hexane (1.81 %) and ethyl

acetate (2.90 %). Amongst all solvents, phenol conversion was the highest in MeCN, as it gave 19.45 % conversion after 6h reaction time. This could be explained that MeCN can coordinates better to the complex, hence, forming a five-coordinated complex with MeCN, where MeCN occupies one site [25].

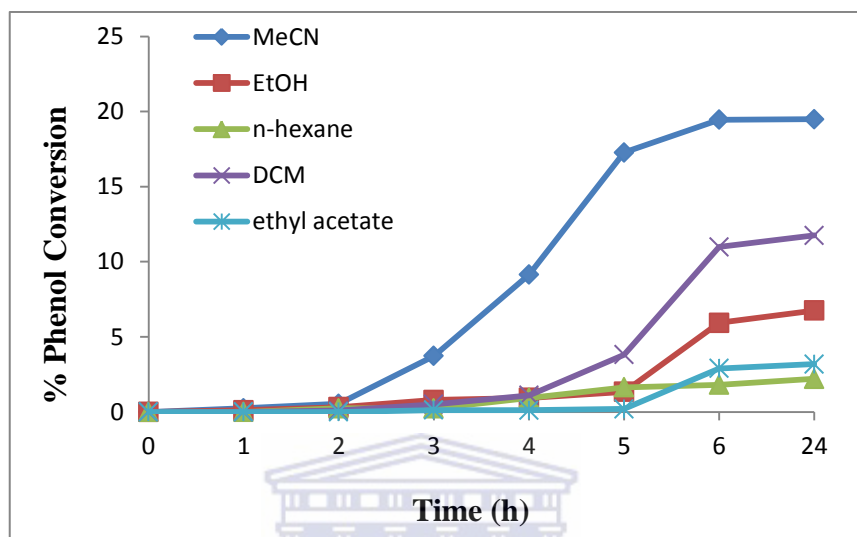


Figure 5.3 Effect of different solvents on the % phenol conversion over time at 70°C

UNIVERSITY of the
WESTERN CAPE

In DCM and n-hexane, the reaction mixture formed a non-homogeneous two-phase (bilayer) system and reaction occurred at the interface moving phenol to the organic layer whilst the catalyst caused the reaction to occur at the interface.

From these experiments for maximum % phenol conversion, the solvents can be rearranged as follows: MeCN >> DCM > ethanol > ethyl acetate > n-hexane. It can be concluded that MeCN was the best suited solvent for maximum % phenol conversion.

Table 5.3 Effect of solvents on phenol hydroxylation ^a, and product selectivity

Solvent	% Phenol Conversion	Product selectivity	
		CAT	HQ
MeCN	19.5	75.6	24.4
CH ₃ COOEt	2.9	80.9	19.2
n-hexane	1.8	90.7	9.3
DCM	11.0	100	-
EtOH	5.9	96.2	3.8

^a Reaction conditions: phenol 2.35g, 30 % H₂O₂ 2.83g, 0.010g [Cu(L2)]-Y, Solvent 3 ml, 70°C, 6h

5.2.1.4 Effect of volume of solvent

The volume of solvent plays an important role in the performance of a catalyst as represented in Fig.5.4 and Table 5.4. Three different volumes of MeCN 3, 5 and 7 were investigated to obtain the % conversion over time. An increase in volume of solvent by 2 ml (3 to 5 ml) led to a significant reduction in the overall catalytic performance by 11.59 % after 6h. Further increase by another 4 ml of solvent led to a considerable drop by 17.73 % in catalytic activity. It can be concluded that an increase in volume did not further improve the % phenol conversion.

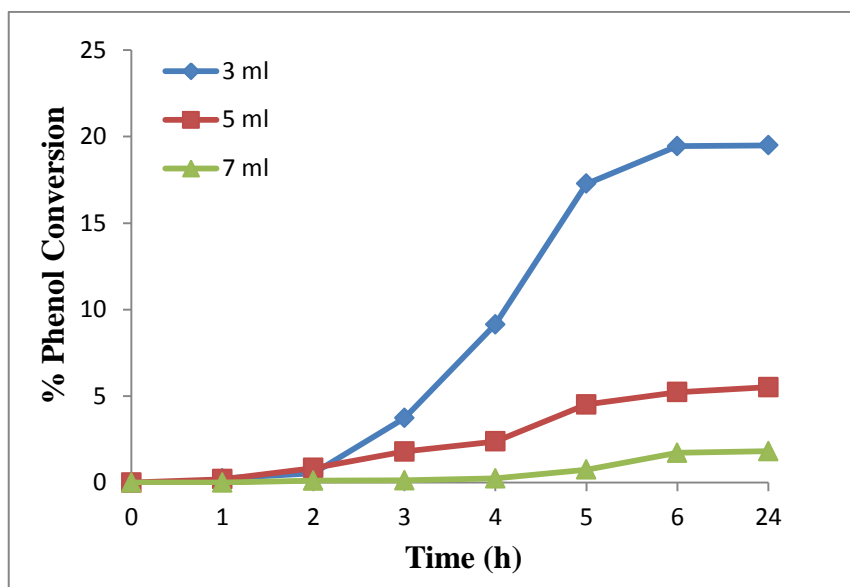


Figure 5.4 Catalytic performance under different volumes of solvent for phenol oxidation

This may be due to that increasing solvent volume will decrease reactant concentration in the reaction mixture which causes poor catalytic performance [26]. It was also noted that increasing the volume, leads to an increase in selectivity towards the formation of catechol. After 6h, no significant change in conversion and selectivity occurred for all reactions. Of the three different volumes of MeCN tested, the best volume to obtain maximum percentage conversion was 3 ml.

Table 5.4 Effect of volume of solvent on phenol conversion ^a and product selectivity

Volume (ml)	%Phenol Conversion	% Selectivity	
		CAT	HQ
3	19.5	75.6	24.4
5	7.9	94.9	5.1
7	1.7	100	-

^a Reaction conditions : phenol 2.35 g, H₂O₂ 2.83 g, 0.010 g Cu(L2)-Y, MeCN, 70 °C, 6h

5.2.1.5 Effect of amount of catalyst

The effect of the amount of catalyst on the catalytic performance for hydroxylation of phenol is represented in Fig.5.5. Three different amounts of catalyst were studied, 0.005, 0.01 and 0.02 g, whilst keeping the other parameters constant i.e. phenol (0.025 mol) and H₂O₂ (0.025 mol) in 3 ml MeCN at 70 °C.

Results indicate that additional amounts of catalysts enhanced the effect of phenol conversion.

As expected, increasing the amount of catalyst from 0.005g to 0.01g increased the conversion from 3.41 to 19.45 % after 6h giving an increase of 16 %. Further increment of amount of catalyst to 0.02 g, % conversion was increased to 26.94% i.e. the % conversion is increased only by 7 % (Table 5.5).

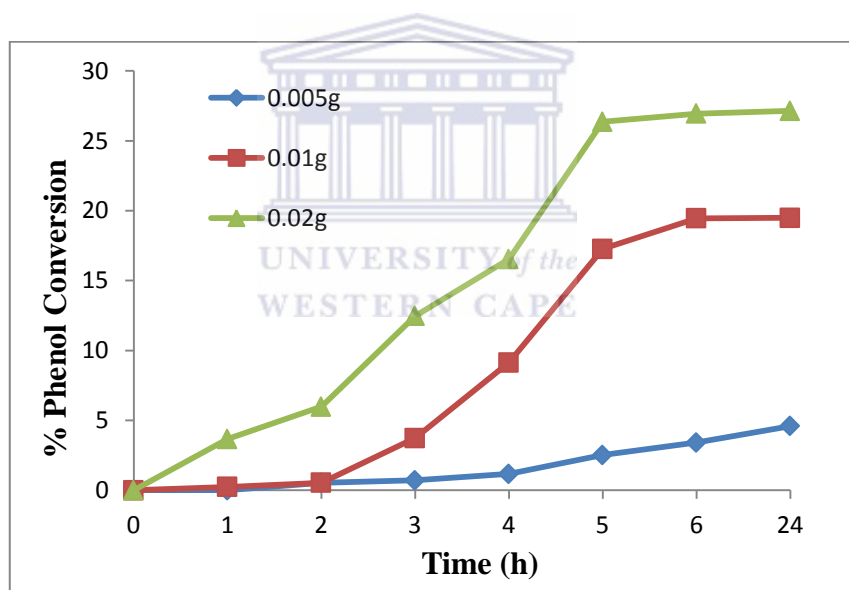


Figure 5.5 % Phenol conversion with increasing the amount of catalyst

The reason for the increase is due to the availability of large surface area and the acid sites, which favours the dispersion of more active species. Therefore, accessibility of large numbers of reactant molecules to the catalyst is favoured [28].

The enhancement of phenol conversion as a result of catalyst addition is due to the increase in efficiency of the decomposition rate of H₂O₂ in the presence of increased catalysts. Therefore, higher activity of organic substrates is expected [29].

The very slight increase in activity at higher amount of catalyst may possibly be due to adsorption or chemisorptions of two reactants on separate catalyst particles, thereby reducing the chance to interact [28].

Increasing the amount of catalyst also influenced the selectivity towards catechol. Selectivity of catechol was at a maximum at 0.005 g catalyst giving a yield of 100 % catechol whilst increasing the amount catalyst to 0.01g caused a drop in catechol selectivity (75.62 %). Upon further increase of catalyst to 0.02 g a further drop in catechol was noticed giving 68.34 %.

In order to reduce the amount of catalyst used and to accomplish higher catechol selectivity, it was decided that 0.01g catalyst was the appropriate amount for maximum conversion.

Table 5.5 Effect of volume of solvent on % phenol conversion ^a and selectivity

Catalyst weight (g)	% Phenol Conversion	% Product selectivity		
		CAT	HQ	BQ
0.005	3.4	100	-	-
0.01	19.5	75.6	24.4	-
0.02	27.0	68.3	8.5	23.2

^aReaction conditions : phenol 2.35 g, 30 % H₂O₂ 2.83 g, Cu(L2)-Y, MeCN, 70 °C, 6h

5.2.1.6 Comparison studies of different copper catalysts

Under the optimized reaction conditions, phenol (0.025 mol), H₂O₂/phenol molar ratio is 1:1, catalyst (0.01 g), CH₃CN (3 ml) and temperature (70 °C), the encapsulated copper complexes, ion exchanged zeolite along with its neat complexes were tested and the results are illustrated in Fig.5.6 and Table 5.6.

It was observed that the reaction was slow in the first 3h using the encapsulated Cu-catalysts (< 10 %) and improved afterwards. The neat Cu-complexes displayed a higher activity than their respective encapsulated analogues achieving maximum % conversion (22 - 23 %) after 1h. This can be attributed to the presence of more active metal centres than in encapsulated complexes using same amount of catalyst [35].

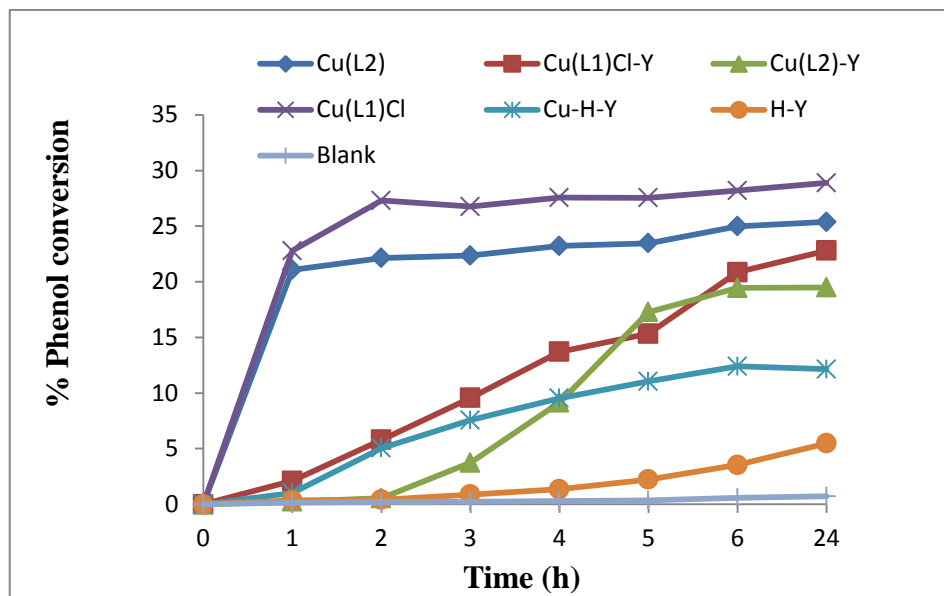


Figure 5.6 % Phenol conversion for catalysts over time

It is clear from Table 5.6 both encapsulated Cu-catalysts show higher % selectivity towards catechol than the corresponding neat complexes. Upon increasing the reaction time from 6 to 24h, only negligible change in % phenol conversion and product selectivity was observed. A blank reaction was carried out under the same optimum conditions which show no activity. On the other hand, the ion exchanged catalyst, Cu-H-Y, show a moderate activity compared to the respective encapsulated complexes, however, leaching of the Cu(II)-ion is always more likely for ion exchanged zeolite [36]. It can thus be concluded that the new encapsulated catalysts are more active and display almost similar selectivity when compared to the respective ion-exchange catalyst. The activity of these copper catalysts can be arranged in the following order: Cu(L1)Cl > Cu(L2) > Cu(L1)Cl-Y > Cu(L2)-Y.

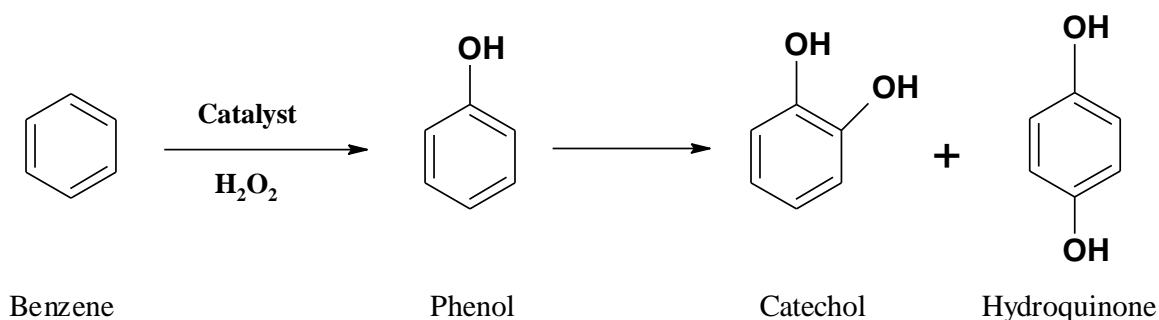
Table 5.6 % phenol conversion ^a and product selectivity

Catalyst	% Phenol Conversion	Selectivity (%)		
		CAT	HQ	BQ
Cu(L1)Cl	28.2	61.9	38.1	-
Cu(L2)	25.0	62.5	37.5	-
Cu(L1)Cl-Y	20.9	73.1	19.1	7.9
Cu(L2)-Y	19.5	75.6	24.4	-
Cu-H-Y	12.4	73.9	26.9	-
H-Y	3.9	95.8	4.2	-
Blank	0.6	94.2	5.8	-

^a Reaction conditions : Phenol 2.35 g, H₂O₂ 2.83 g, 0.010 g catalyst, Solvent 3 ml, 70°C, 6h

5.2.2 Hydroxylation of benzene

Hydroxylation of benzene was carried out under the same optimized conditions for phenol. The oxidation products for this reaction are presented in Scheme 5.2. Table 5.7 show under these reaction conditions, encapsulated complexes Cu(L1)Cl-Y and Cu(L2)-Y gave very low conversion (6.7 % and 5.6 %) after 6h respectively, yielding only phenol as product. The catalytic activity of the homogeneous complexes, Cu(L1)Cl and Cu(L2) was also tested under the same reaction conditions as the encapsulated complexes. It is observed that homogeneous Cu(II) complexes displayed higher activity in comparison to their encapsulated analogues. Fig.5.7 presents the catalytic comparison of the encapsulated and neat Cu(II) complexes as a function time.

**Scheme 5.2** Oxidized products for the oxidation of benzene

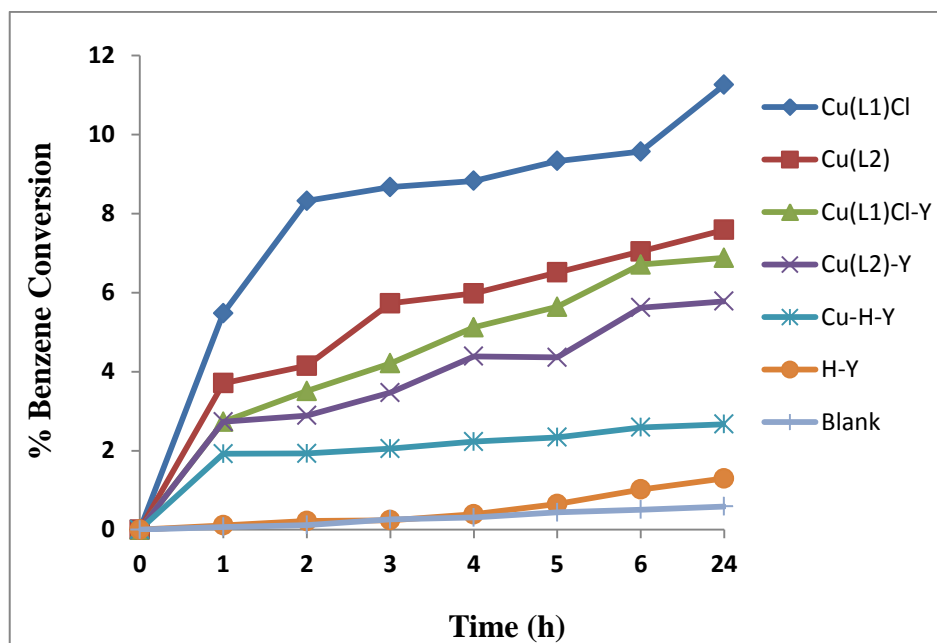


Figure 5.7 Benzene conversion for catalysts over time.

Table 5.7 % Benzene conversion^a and product selectivity

Catalyst	% Benzene conversion	% Selectivity		
		PhOH	CAT	HQ
Cu(L1)Cl	9.6	78.0	16.7	5.3
Cu(L2)	7.0	73.8	6.4	16.5
Cu(L1)Cl-Y	6.7	100	-	-
Cu(L2)-Y	5.6	100	-	-
Cu-H-Y	2.6	95.08	4.92	-
H-Y	1.0	100	-	-
Blank	0.5	100	-	-

^a Reaction conditions : benzene 1.93 g, H₂O₂ 2.83 g, catalyst 0.010 g, CH₃CN 3 ml, 70°C, 6h

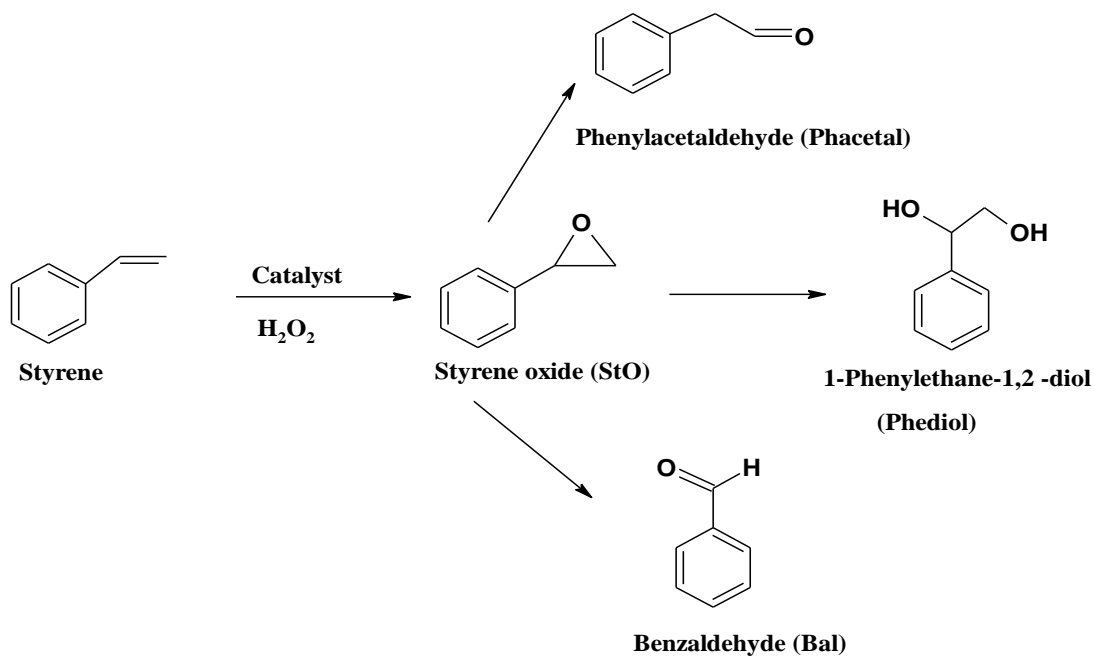
Table 5.7 shows % benzene conversion and product selectivity of the Cu-catalysts. It was observed that the neat complexes, Cu(L1)Cl and Cu(L2), further oxidation of phenol occurred i.e. formation of catechol and hydroquinone. This is due to the selectivity of the product (phenol) is more reactive than benzene [37]. It can be also concluded from the table that hydroxylation of benzene using the encapsulated complexes was less effective in comparison to their neat analogues. Other possible reasons that could contribute for the differences in the reactivity of the encapsulated complexes are steric effects, weak electrostatic interactions and the synergism as a result of the interactions with the zeolite framework [38].

Although, neat complexes displayed higher activity than encapsulated catalysts, the one-step hydroxylation conversion of benzene was still very low. This demonstrates the difficulty of C-H bond activation due to the resonance stability of benzene [39, 40]. Therefore, the one-step oxidation of benzene under Cu(II) systems showed low activity as exemplified by the low yield of phenol. Oxidation under Cu-H-Y, H-Y and blank (no catalyst) yielded very low conversion.

5.2.3 Oxidation of styrene

The catalytic oxidation of styrene using hydrogen peroxide (H_2O_2) as an oxidant can lead to various reaction products, depending on the catalyst and reaction conditions. The major products of the reaction are benzaldehyde, styrene oxide, phenylacetaldehyde, 1-phenylethan-1,2-diol and other unidentified oxidized products (Scheme 5.3).

The neat complexes and the encapsulated complexes analogues were also used and studied in the oxidation of styrene under the optimized reaction conditions. Fig.5.8 presents the profiles of conversion percentage of styrene as a function of time for these catalysts. It is clear from Table 5.8, that the performance of encapsulated catalysts, Cu(L1)Cl-Y and Cu(L2)-Y, were slightly lower than their neat analogues, Cu(L1)Cl and Cu(L2).



Scheme 5.3 The oxidized products for the oxidation of styrene

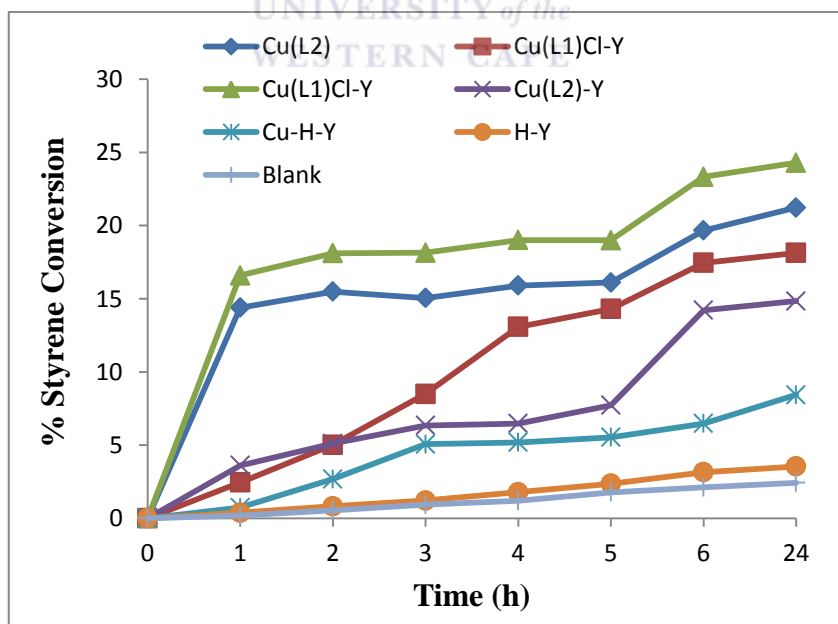
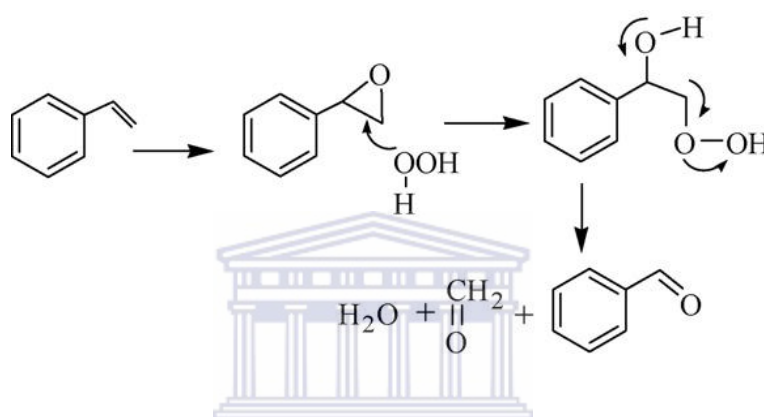


Figure 5.8 Styrene conversion for catalysts over time

Amongst products formed, benzaldehyde was the highest yield obtained (70-82%). This is possibly due to the conversion of most of the styrene oxide formed in the first step to benzaldehyde, which occurred *via* nucleophilic attack of H₂O₂ to styrene oxide followed by the cleavage of the intermediate hydroperoxystyrene (Scheme 5.4) [41]. Formation of benzaldehyde may also occur through direct oxidative cleavage of the styrene side chain double bond *via* the radical reaction mechanism [42]. The yields of all the other products are in low quantities and comparable. The formation of phenylacetaldehyde is very low for all catalysts and its formation is possible through isomerization of styrene oxide [43].



Scheme 5.4 Mechanism for the formation of benzaldehyde from styrene oxide [44].

The high amount of water present in H₂O₂ is partially responsible for the possible hydrolysis of styrene oxide to form 1-phenylethane-1,2-diol. The other unidentified products formed could be due further oxidation of benzaldehyde to form other oxidized products [45]. The neat complexes, Cu(L1)Cl and Cu(L2), show a conversion of between 18-20 % in the first 3h (Fig.5.8), whereas the activity of the encapsulated analogues was still very low (< 10 %) conversion. % Styrene conversion was improved after 3h using the encapsulated catalysts. The poor activity of Cu(L1)Cl-Y and Cu(L2)-Y may be understood to have originated from the diffusional resistance faced by styrene molecules in reaching the isolated catalytic centres in the cages of zeolite Y [46]. Therefore, less conversion is expected as one goes from smaller molecules to substrates having bulkier substituents making their entrance through the zeolite pore opening more difficult and ultimately resulting in lower activity [47,48]. From the results presented in Table 5.8, the percentage styrene conversion follows the order: Cu(L1)Cl > Cu(L2) > Cu(L1)Cl-Y > Cu(L2)-Y. The

selectivity of all Cu-systems are similar in trend for most cases and can be arranged as follows: benzaldehyde >> styrene oxide > 1-phenylethane-1, 2-diol > phenylacetaldehyde. Cu-H-Y, H-Y and blank were also tested under the same operating conditions but yielded poor activity.

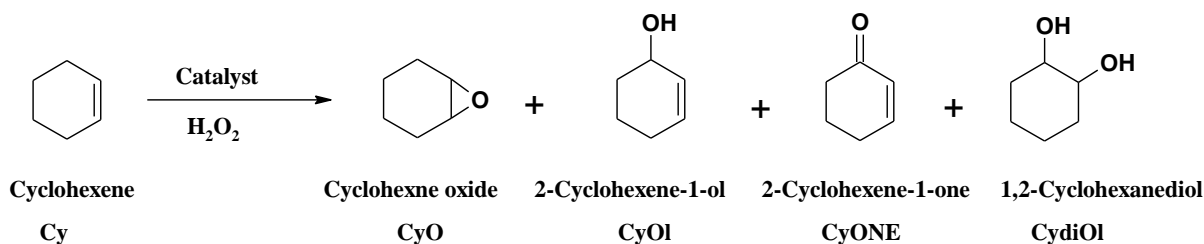
Table 5.8 The styrene conversion^a and product selectivity

Catalysts	% Styrene conversion	% Product selectivity				
		Bal	Phacetal	Sto	Phediol	Other
Cu(L1)Cl	23.3	70.6	6.7	7.7	7.5	7.6
Cu(L2)	19.7	72.9	4.9	8.2	7.2	7.1
Cu(L1)Cl-Y	17.5	79.8	3.7	8.5	5.6	2.5
Cu(L2)-Y	14.2	80.6	3.6	4.2	5.0	6.6
Cu-H-Y	6.5	73.1	4.3	2.8	4.3	15.4
H-Y	3.2	82.8	3.0	0.6	3.3	10.3
Blank	2.1	89.7	3.1	4.0	3.6	0.4

^a Reaction conditions: Styrene 2.60g, H₂O₂ 2.83g, 0.010 g catalyst, CH₃CN 3ml, 70°C, 6h

5.2.4 Oxidation of cyclohexene

Cyclohexene oxidation using H₂O₂ as an oxidant gives cyclohexene oxide, cyclohexene-1-ol, 2-cyclohexene-1-one and 1,2-cyclohexanediol as main products (Scheme 5.5). Fig.5.9 presents the conversion details as a function of time for these catalysts.



Scheme 5.5 The oxidized products for the oxidation of cyclohexene

The oxidation of cyclohexene was carried out under the same operating conditions optimized for phenol. Under these reaction conditions, the encapsulated complexes, Cu(L1)Cl-Y and Cu(L2)-Y gave ~67 and 65 % conversion, respectively, after 6h reaction time. The % conversion and product selectivity of the catalysts are represented in Table 5.9. In the first 4h, the % conversion for Cu(L1)Cl-Y and Cu(L2)-Y was very slow but gradually increased after longer reaction time. In contrast, neat analogues, Cu(L1)Cl and Cu(L2) were more reactive under the same operating conditions reaching maximum conversion after 5h.

In term of selectivity, % cyclohexene oxide obtained was good (29-43 %). This is may be due to the oxidation reaction occurs mainly on the double bond giving high yields of cyclohexene oxide [49].

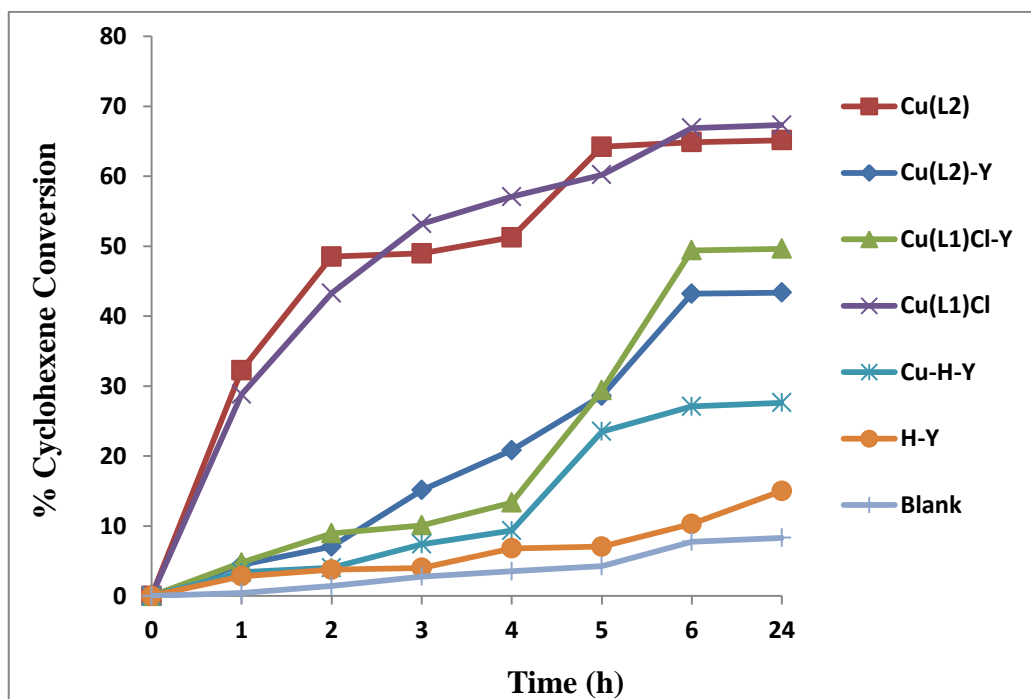


Figure 5.9 Cyclohexene conversion for catalysts over time

The two allylic products formed, cyclohexene-1-ol, 2-cyclohexene-1-one arises from the preferred attack of the activated C-H bond over the C-C bond. It was suggested by Valentine and co-workers [50] that the species responsible for cyclohexene oxidation is the product formed from the cleavage of the O-O bond, whereas the epoxide product is formed *via* the direct reaction of olefin with the coordinated HO_2^- ion. It is also known that the O-O bond of H_2O_2 is stronger than other oxidants (e.g. THBP) and an HOO^- complex is normally expected to having higher activation energy and ultimately has a long lifetime and higher probability of forming cyclohexene oxide [52].

The selectivity for the different reaction products for neat copper catalysts follows the order: cyclohexene-1-ol > cyclohexene oxide > 2-cyclohexene-1-one > cyclohexane-1,2-diol, while the encapsulated catalysts follow the order: cyclohexene oxide > cyclohexene-1-ol > 2-cyclohexene-1-one > cyclohexane-1,2-diol. From the results presented in Table 5.9, the percentage cyclohexene conversion using these catalysts decreases in the following order: $\text{Cu(L1)Cl} > \text{Cu(L2)} > \text{Cu(L1)Cl-Y} > \text{Cu(L2)-Y}$.

Table 5.9 The cyclohexene conversion ^a and product selectivity

Catalyst	% Cyclohexene conversion	% Product selectivity				
		CyO	CyOl	CyONE	CydiOl	Other
Cu(L1)Cl	66.9	29.3	45.5	10.2	1.0	13.9
Cu(L2)	64.9	27.9	50.8	12.2	0.5	8.6
Cu(L1)Cl-Y	48.2	32.1	28.6	19.3	13.2	6.7
Cu(L2)-Y	43.2	43.1	30.7	18.2	4.2	3.8
Cu-H-Y	27.1	33.1	20.1	8.9	2.9	35.1
H-Y	10.3	39.9	12.9	16.5	6.1	24.7
Blank	7.8	33.1	20.1	8.9	2.9	35.1

^a Reaction conditions : Cyclohexene 2.06 g, H₂O₂ 2.83 g, catalyst 0.010 g, CH₃CN 3 ml, 70°C, 6h

In Fig.5.9, Cu-H-Y and H-Y under the same experimental reaction conditions exhibit far lower conversions towards oxidation of cyclohexene. So it is quite evident that the presence of N and O donor ligands is relevant to improve conversion of cyclohexene. This also substantiates the presence of transition metal complexes that is the active site and not the copper ions in zeolite. Therefore, these results suggest these encapsulated and neat Cu(II) catalytic systems catalyses the conversion of cyclohexene very good giving high yield of cyclohexene oxide and cyclohexene-1-ol.

References

- [1] Roy P., Manassero M., Tetranuclear copper(II)–Schiff-base complexes as active catalysts for oxidation of cyclohexane and toluene, *Dalton Trans* 39 (2010) 1539.
- [2] Singh A.K., Singh M., Srivastava J., Rahmani S., Kinetics of the oxidation of lactose by copper(II) complexed with bipyridyl in alkaline medium using chloro-complex of rhodium(III) in its nano-concentration range as homogeneous catalyst: a spectrophotometric study, *Carbohyd Res* 354 (2012) 94.
- [3] Salavati Niasari M., Mirsattari N.S., Synthesis, characterization and catalytic oxyfunctionalization of cyclohexene with tert-butylhydroperoxide and hydrogen peroxide in the presence of alumina-supported Mn(II), Co(II), Ni(II) and Cu(II) bis (2-hydroxyanil)benzil complexes, *J Mol Catal A: Chem* 268 (2007) 50.
- [4] Gupta K.C., Suta A.K.R., Catalytic activity of polymer anchored N, N'-bis (o-hydroxy acetophenone) ethylene diamine Schiff base complexes of Fe (III), Cu(II) and Zn(II) ions in oxidation of phenol, *React Funct Polym* 68 (2008) 12.
- [5] Mukherjee S., Samanta S., Roy B.C., Bhaumik A., Efficient allylic oxidation of cyclohexene catalyzed by immobilized Schiff base complex using peroxides as oxidants, *Appl Catal A: Gen* 301 (2006) 79.
- [6] Mureseanu M., Pârvolescu V., Ene R., Cioatera N., Pasatoiu T.D, Andruh M., Cu(II) complexes immobilized on functionalized mesoporous silica as catalysts for biomimetic oxidations, *J Mater Sci* 44 (2009) 6795.
- [7] Karandikar P., Agashe M., Vijayamohanan K., Chandwadkar A.J., Cu²⁺ perchlorophthalocyanine immobilized MCM-41: catalyst for oxidation of alkenes *Appl Catal A* 257 (2004) 133.
- [8] (a) Koner S., Novel color isomerism and catalytic activities of Cu(salen) complex encapsulated in a zeolitic matrix, *Chem Commun* (1998) 593; (b) Sakthivel A., Sun W., Raudaschl-Sieber G., Chiang A.S.T., Hanzlik M., Kühn F.E., Grafting of a tetrahydro-salen copper(II) complex on surface modified mesoporous materials and its catalytic behaviour, *Catal Commun* 7 (2006) 302.
- [9] Salavati-Niasari M., Flexible ligand synthesis, characterization and liquid phase hydroxylation of phenol by H₂O₂ with host (nanopores of zeolite-Y)/guest [VO([R]₂-N₂X₂)]²⁺ (R = H, CH₃; X = NH, O, S) nanocomposite materials, *J Incl Phenom Macrocycl Chem* 65 (2009) 349 - 360.

- [10] Maurya M.R., Chandrakar A.K., Chand S., Zeolite-Y encapsulated metal complexes of oxovanadium(VI), copper(II) and nickel(II) as catalyst for the oxidation of styrene, cyclohexane and methyl phenyl sulphide, *J Mol Catal A: Chem* 274 (2007) 192 - 201.
- [11] Maurya M.R., Kumar M., Kumar U., Polymer-anchored vanadium(IV), molybdenum (VI) and copper(II) complexes of bidentate ligand as catalyst for the liquid phase oxidation of organic substrates, *J Mol Catal A: Chem* 273 (2007) 133-143.
- [12] Maurya M.R., Kumar U., Manikandan P., Synthesis and Characterisation of Polymer-Anchored Oxidovanadium(IV) Complexes and Their Use for the Oxidation of Styrene and Cumene *Eur J Inorg Chem* 16 (2007) 2303 –2314.
- [13] Maurya M.R., Sikarwar S., Kumar M., Oxovanadium(IV) complex of β -alanine derived ligand immobilised on polystyrene for the oxidation of various organic substrates, *Catal Commun* 8 (2007) 2017–2024.
- [14] Karakhanov E.A., Narin S.Y., Dedov A.G., On the mechanism of catalytic hydroxylation of aromatic hydrocarbons by hydrogen peroxide, *Appl Organomet Chem* 5 (1991) 445.
- [15] Shul'pin G.B., Hydrocarbon Oxygenations with Peroxides Catalyzed by Metal Compounds, *Mini-Rev Org Chem* 6 (2009) 95.
- [16] Mugo J.N, Mapolie S.F, Van Wyk J.L, Cu(II) and Ni(II) complexes based on monofunctional and dendrimeric pyrrole-imine ligands: Applications in catalytic liquid phase hydroxylation of phenol, *Inorg Chim Acta* 363 (2012) 2643.
- [17] Pavel O.D., Cojocaru B., Angelescu E., Parvulescu V.I., The activity of yttrium-modified Mg, Al hydrotalcites in the epoxidation of styrene with hydrogen peroxide *Appl Catal A: Gen* 403 (2011) 83.
- [18] Xavier K.O., Chacko J., K.K. Mohammed Yusuff, Zeolite-encapsulated Co(II), Ni(II) and Cu(II) complexes as catalysts for partial oxidation of benzyl alcohol and ethylbenzene, *Appl Catal A: Gen* 258 (2004) 256.
- [19] Noller. D, Mazurowski, S.G. Linden, De Leeuw F., Mageli O., A relative hazard classification of organic peroxides, *Ind Eng Chem* 56 (1964) 18.

- [20] Pardeshi S.K., Pawar R.Y., SrFe₂O₄ complex oxide an effective and environmentally benign catalyst for selective oxidation of styrene, *J Mol Catal A: Chem* 334 (2011) 40.
- [21] Liou R., Chen S., Hung M., Hsu C., Lai J., Fe (III) supported on resin as effective catalyst for the heterogeneous oxidation of phenol in aqueous solution *Chemosphere* 59 (2005) 121,124.
- [22] Hulea V., Dumitriu E., Styrene oxidation with H₂O₂ over Ti-containing molecular sieves with MFI, BEA and MCM-41 topologies, *Appl Cat: Gen* 277 (2004) 103.
- [23] Hulea V., Dumitriu E., Patcas F., Pot R., Graffin P., Moreau P., Cyclopentene oxidation with H₂O₂ over Ti-containing zeolites, *Appl Catal A* 170 (1998) 169.
- [24] Abbo H.S, Titinchi S.J.J, Synthesis and Catalytic Activity of Cu(II), Fe(III) and Bi(III) Complexes of Thio-Schiff Base Encapsulated in Zeolite-Y for Hydroxylation of Phenol, *Top Catal* 53 (2010) 262.
- [25] Abbo H.S, Titinchi S.J.J, Chand S., Prasad R., Investigation of [Ni{Me₄Bzo₂[14]aneN₄}]Cl₂ catalyzed selective hydroxylation of phenol to catechol by H₂O₂ in the homogeneous medium, *J Mol Cat A: Chem A: Chem* 218 (2004) 130.
- [26] Maurya M.R., Kumar M., Titinchi S.J.J, Abbo H.S, Chand S., Oxovanadium(IV) Schiff base complexes encapsulated in zeolite-Y as catalysts for the liquid-phase hydroxylation of phenol, *Cat Lett* 86 (2003) 103.
- [27] Maurya M.R, Chandrakar A.K., Chand S., Oxovanadium(IV) and copper(II) complexes of 1,2-diaminocyclohexane based ligand encapsulated in zeolite-Y for the catalytic oxidation of styrene, cyclohexene and cyclohexane, *J Mol Catal A: Chem* 270 (2007) 230.
- [28] Sherrington D.C., Kybett A.P., Supported Catalysts and Their Applications, *The Royal society of Chemistry* (2001) 178-181.
- [29] Molinari R., Poerio T., Argurio P., One-step production of phenol by selective oxidation of benzene in a biphasic system, *Catal Today* 118 (2006) 52.
- [30] Bennur T.H., Srinivas D., Sivasanker S., Oxidation of ethylbenzene over “neat” and zeolite-Y-encapsulated copper tri- and tetraaza macrocyclic complexes, *J Mol Catal A: Chem* 207 (2004) 169.

- [31] Adam F., Thankappan R., Oxidation of benzene over bimetallic Cu–Ce incorporated rice husk silica catalysts, *Chem Eng J* 160 (2010) 249.
- [32] Reis P.M., Silva J.A.L., da Silva J.J.R.F., Pombeiro A.J.L., Peroxidative oxidation of benzene and mesitylene by vanadium catalysts, *J Mol Catal A: Chem* 224 (2004) 189-195.
- [33] Maurya M.R, Kumar U., Manikandan P., Synthesis and Characterisation of Polymer-Anchored Oxidovanadium(IV) Complexes and Their Use for the Oxidation of Styrene and Cumene, *Eur J Inorg Chem* (2007) 2303.
- [34] Maurya M.R, Kumar U., Manikandan P., Polymer supported vanadium and molybdenum complexes as potential catalysts for the oxidation and oxidative bromination of organic substrates, *Dalton Trans* (2006) 3561.
- [35] Maurya M.R, Saini P., Haldar C., Avelicca F., Synthesis, characterisation and catalytic activities of manganese(III) complexes of pyridoxal-based ONNO donor tetradenatate ligands, *Polyhedron* 31 (2012) 718.
- [36] Maurya M.R., Chandrakar A.K., Chand S., Oxidation of phenol, styrene and methyl phenyl sulfide with H₂O₂ catalysed by dioxovanadium(V) and copper(II) complexes of 2-aminomethylbenzimidazole-based ligand encapsulated in zeolite-Y, *J Mol Catal A: Chem* 263 (2007) 235.
- [37] Marchetti F., Pettinari C., Di Nicola C., Pettinari R., Crispini A., Crucianelli M., Di Giuseppe A., Synthesis and characterization of novel oxovanadium(IV) complexes with 4-acyl-5-pyrazolone donor ligands: Evaluation of their catalytic activity for the oxidation of styrene derivatives, *Appl Catal A: Gen A* 378 (2010) 217.
- [38] Rao S.N., Munshi K.N., Rao N.N., Catalytic oxidation of styrene using cis-MoO₂(L)(solv) [L=salicylidene salicyloyl hydrazine) and its zeolite composite as catalysts in the presence of molecular oxygen, *J Mol Catal A: Chem* 156 (2000) 210.
- [39] Maurya M.R., Titinchi S.J.J., Chand S., Oxidation of phenol with H₂O₂ catalysed by Cr(III), Fe(III) or Bi(III) N,N-bis(salicylidene)diethylenetriamine (H₂saldien) complexes encapsulated in zeolite-Y, *J Mol Catal A: Chem* 193 (2003) 175.
- [40] Maurya M.R, Titinchi S.J.J., Chand S., Spectroscopic and catalytic activity study of N,N'-bis(salicylidene)propane-1,3-diamine copper(II) encapsulated in zeolite-Y, *Appl Catal A: Gen* 228 (2002) 186.

- [41] Maurya M.R, Kumar M., Kumar A., Pessao J.C, Oxidation of p-chlorotoluene and cyclohexene catalysed by polymer-anchored oxovanadium(IV) and copper(II) complexes of amino acid derived tridentate ligands, Dalton Trans (2008) 4227.
- [42] Nam W., Ho R., Valentine J.S, Iron-cyclam complexes as catalysts for the epoxidation of olefins by 30% aqueous hydrogen peroxide in acetonitrile and methanol, J Am Chem Soc 113 (1991) 7052-7054.
- [43] Koola J.D., Kochi J.K., Cobalt-catalyzed epoxidation of olefins. Dual pathways for oxygen-atom transfer, J Org Chem 52 (1987) 4545.
- [44] Chutia P., Kato S., Kojima T., Satokawa S., Synthesis and characterization of Co(II) and Cu(II) supported complexes of 2-pyrazinecarboxylic acid for cyclohexene oxidation, Polyhedron 28 (2009) 378.



CHAPTER 6

6. CATALYTIC ACTIVITY STUDIES OF OV(IV) CATALYSTS FOR OXIDATION REACTIONS

6.1 Hydroxylation of phenol

The coordination chemistry of vanadium is of great current interest due to its application of biological systems [1], catalytic [2], inhibitory [3], medicinal [4,5] and structural properties [6-8]. The catalytic efficiency of the neat oxovanadium complexes, the zeolite encapsulated complexes as well the ion-exchanged zeolites, was also tested for the hydroxylation of phenol. The catalytic results obtained for phenol hydroxylation under optimized conditions (Chapter 5 Section 5.2.1.6) are summarized in Table 6.1. Fig.6.1 compares the catalytic activity for phenol oxidation for these catalysts as well as in the absence of catalyst (blank). Fig.6.1 shows that % phenol conversion for the encapsulated catalysts, VO(L1)(acac)-Y and VO(L2)-Y, increases considerably within 2h reaching steady state after 3h reaction time. Under these reaction conditions, catalysts VO(L1)(acac)-Y and VO(L2)-Y gave ~ 24 and 21 % conversion, respectively, suggesting moderate activity. For comparison, their respective neat metal complexes, VO(L1)(acac) and VO(L2) have also been examined for their catalytic activities. However, conversion was considerably higher in comparison to that of encapsulated ones. VO(L1)(acac) was found to be more active giving ca. 35 % conversion, followed by VO(L2) which gave 30 %. In both homogeneous and heterogeneous catalysts, catechol was the major product. However, in terms of selectivity, the VO(L1)-Y is more selective for catechol formation (65%). Other oxidized product was also observed (*p*-benzoquinone) using all catalysts due to further oxidation of the products, *viz.* catechol and hydroquinone [9].

It was important to run proper blank experiments to establish the role of host and guest molecules in catalysis. Oxidation reactions carried out over parent H-Y zeolite exhibited only negligible conversion (~3%), showing the inability of zeolite framework to catalyze the reactions [10]. The V-exchanged zeolite shows distinctly higher catalytic activity than the parent H-Y zeolite. The results illustrated in Table 6.1, show that the neat and the encapsulated vanadium catalysts exhibit much higher activity in comparison to VO-H-Y. This confirms the role of the ligand which is an important factor to enhance the catalytic

activity over the activity of VO-H-Y alone. Also it confirms that the changes in electronic environment about the central vanadium ions drastically influences the catalytic performance. This also serves as another piece of evidence for the successful complexation of VO(IV) ions with the L1 or L2 ligands inside the zeolitic host [11].

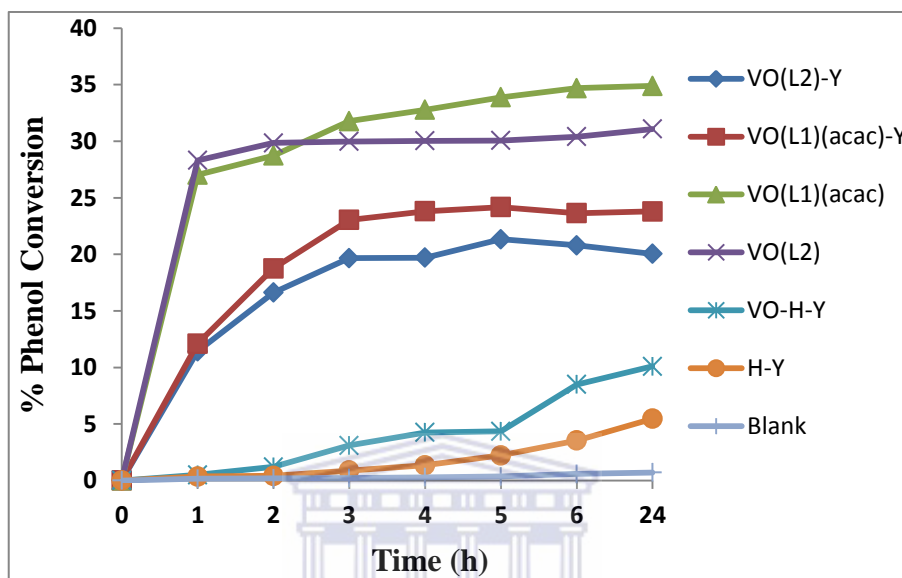


Figure 6.1 Phenol conversion for catalysts over time

The enhanced activity of the encapsulated catalysts could be due to the synergy between the catalytic behaviour of the metal complexes and the zeolite via the lattice oxygen of the zeolitic host [12,13]. A disadvantage of VO-H-Y, is leaching of the VO(IV)-ion which is always more likely [14]. Increasing the reaction time from 6 to 24 h does not show any significant change in either phenol transformation or catechol and hydroquinone formation. The activity of the catalysts may be arranged in the following sequence: VO(L1)(acac) > VO(L2) > VO(L1)(acac)-Y > VO(L2)-Y.

Table 6.1 % phenol conversion^a and product selectivity

Catalyst	% Phenol Conversion	Product selectivity (%)		
		CAT	HQ	Other
VO(L1)(acac)	34.7	50.7	43.9	5.4
VO(L2)	30.4	53.0	33.2	13.8
VO(L1)(acac)-Y	23.6	65.2	21.6	13.2
VO(L2)-Y	20.8	59.6	30.1	10.4
VO-H-Y	8.5	81.0	16.3	2.7
H-Y	3.9	95.8	4.2	-
Blank	0.6	94.2	5.8	-

^aReaction conditions : phenol 2.35 g, 30 % H₂O₂ 2.83 g, catalyst 0.010 g, Solvent 3 ml, 70°C, 6h

6.2 Hydroxylation of benzene

The catalytic activity results for the catalysts for benzene hydroxylation under the optimized conditions are shown in Fig.6.2 while Table 6.2 provides conversion and selectivity details. Only 10 - 12 % transformation of benzene has been achieved with the neat complexes and poor activity was observed for corresponding encapsulated ones. The catalytic performance of H-Y and reaction under no catalyst show no activity at all.

As can be concluded from Fig.6.2, VO(L1)(acac) and VO(L2) demonstrate a similar behaviour in oxidative transformations, suggesting that despite the differences in their structures, they have quite the same reactivity. In term of selectivity, these catalysts show 100 % phenol formation.

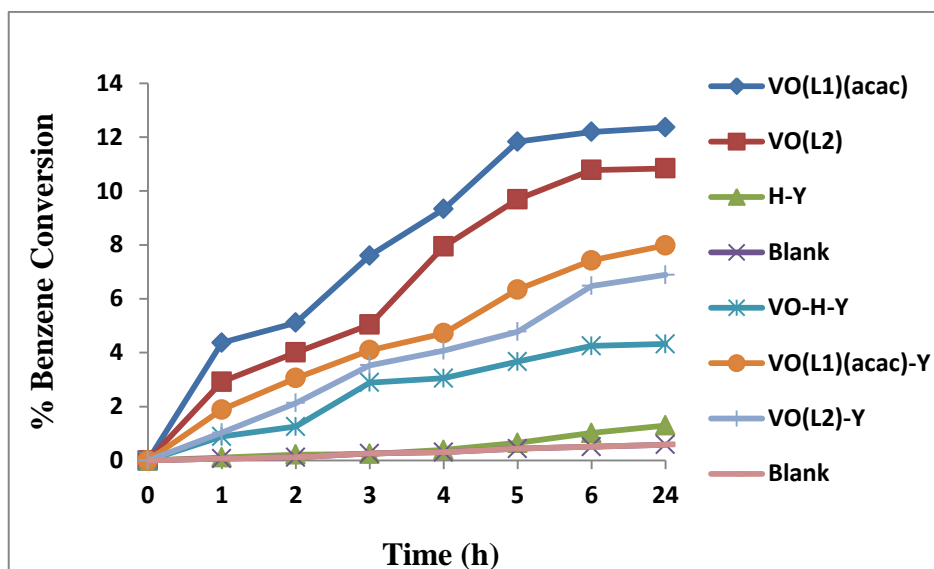


Figure 6.1 Benzene conversion for catalysts over time

Higher conversion with homogeneous catalysts should always be expected when compared to heterogeneous catalysts. This is in part due to the insolubility of the heterogeneous catalysts in acetonitrile which reduces their dispersion in solvent and thus availability of low surface area to interact with the oxidant [15]. Thus, VO(L1)(acac) and VO(L2) are better catalyst than their encapsulated analogues for the oxidation of benzene with high selectivity towards phenol.

Table 6.2 The % benzene conversion and product selectivity^a

Catalyst	% Benzene Conversion	% Product selectivity
		PhOH
VO(L1)(acac)	12.2	100
VO(L2)	10.8	100
VO(L1)(acac)-Y	7.4	100
VO(L2)-Y	6.5	100
VO-H-Y	4.3	100
H-Y	1.0	-
Blank	0.6	-

^a Reaction conditions : benzene 1.93 g, H₂O₂ 2.83 g, catalyst 0.010 g, Solvent 3 ml, 70°, 6h

6.3 Oxidation of styrene

The catalytic efficiency of VO(L1)(acac)-Y, VO(L2)-Y, VO(L1)(acac), VO(L2) and VO-H-Y was also tested for the oxidation of styrene under the optimized conditions. Results are illustrated in Fig.6.3 and Table 6.3. Under these optimized reaction conditions, VO(L1)(acac)-Y and VO(L2)-Y catalysts show a maximum of 12 - 15 % conversion after 6h. The low reaction rates obtained for the oxidation of styrene with the encapsulated complexes are probably due to diffusion resistance of styrene molecules through the porous support structure and the electronic changes induced in the metal centre through chemical modifications as a consequence of the ligand/metal centre of the immobilization methods employed. In term of selectivity, benzaldehyde (78 – 75 %) was observed as a major product. This may be due to the acidic nature of zeolite matrix that plays and leads to epoxide ring opening of styrene oxide [12].

The results also clearly indicate that neat oxovanadium complexes efficiently catalyse conversion of styrene giving 75-81 % conversion. The % selectivity towards the formation of benzaldehyde was (~ 50 %). The mechanism for formation of benzaldehyde and other products has already been discussed earlier (Chapter 5 Section 5.2.3).

The activity of the catalysts is as follows: VO(L1)(acac) > VO(L2) > VO(L1)(acac)-Y > VO(L2)-Y > VO-H-Y > H-Y counterparts. Therefore, the neat catalysts are better than their encapsulated analogues for the oxidation of styrene but with lower selectivity towards benzaldehyde

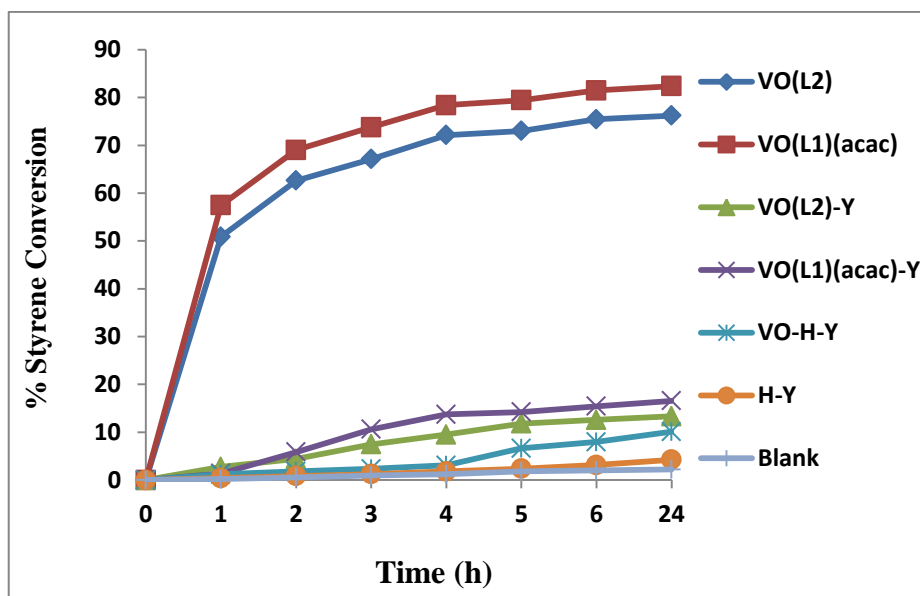


Figure 6.2 Styrene conversion for catalysts over time

The selectivity towards the products using the encapsulated and the neat VO(IV) catalytic systems are similar in the following order of: benzaldehyde >> styrene oxide > 1-phenylethane-1, 2-diol > phenylacetaldehyde.

Table 6.3 The styrene conversion^a and product selectivity

Catalyst	% Styrene Conversion	% Product selectivity				
		Bal	Phacetal	Sto	Phediol	Other
VO(L1)(acac)	81.5	51.7	12.2	16.5	11.0	10.6
VO(L2)	75.4	51.0	11.1	14.1	12.7	11.1
VO(L1)(acac)-Y	15.4	75.9	6.1	6.7	6.2	5.2
VO(L2)-Y	12.6	78.3	3.6	6.2	2.3	2.6
VO-H-Y	8.0	89.6	-	10.4	-	-
H-Y	3.2	82.8	3.0	0.6	3.3	10.3
Blank	2.1	89.7	3.1	4.0	3.6	0.4

^a Reaction conditions : styrene 2.60 g, H₂O₂ 2.83 g, 0.010 g catalyst, Solvent 3 ml, 70°C, 6h

6.4 Oxidation of cyclohexene

Fig.6.4 presents the % cyclohexene conversion details as a function of time in presence of various catalysts *viz.* VO-H-Y, H-Y, VO(L1)(acac)-Y, VO(L2)-Y, VO(L1)(acac), VO(L2) as well as in the absence of any catalyst. Table 6.4 illustrates the % conversion and selectivity after 6h reaction time.

These catalysts were tested under the optimized reaction conditions and both VO(L1)(acac)-Y and VO(L2)-Y gave nearly similar activity. As depicted in Fig.6.4, the cyclohexene conversion was very slow in the first three hours but gradually increased with time. On the other hand, the neat complex, VO(L1)(acac), shows 87 % conversion followed by VO(L2) yielding 82 %, whereas, VO(L1)(acac)-Y and VO(L2)-Y recorded conversions of about 64 and 58 %, respectively. It is clear that the homogeneous catalysts are more active than the heterogeneous ones.

After 6h, only small difference in the conversion and selectivity for the different reaction products was observed for all catalysts. The product selectivity of neat complexes follows the order : cyclohexene-1-ol > cyclohexene oxide > cyclohexene-1-one > cyclohexane-1,2-diol. The selectivity towards cyclohexene epoxide formation was high and the mechanism for the formation of reaction products was discussed earlier (Chapter 5 Section 5.2.4).

The oxidation of cyclohexene is negligible in the absence of catalysts, confirming that under the conditions of the experiments, the oxidation is indeed catalytic in nature whereas, the parent and ion-exchanged zeolites, H-Y and VO-H-Y, show poor activity.

Results in Table 6.4 illustrates that an enhancement in the conversion percentages in the presence of the neat and the encapsulated catalysts which confirm the determining role is played by metal complexes encapsulated in the zeolite [16].

It can be concluded that the vanadium based catalysts are more reactive than copper based catalytic systems in the oxidation reactions studied. This could be deduced due to the ready formation of peroxy complexes which transfers oxygen to substrates [17].

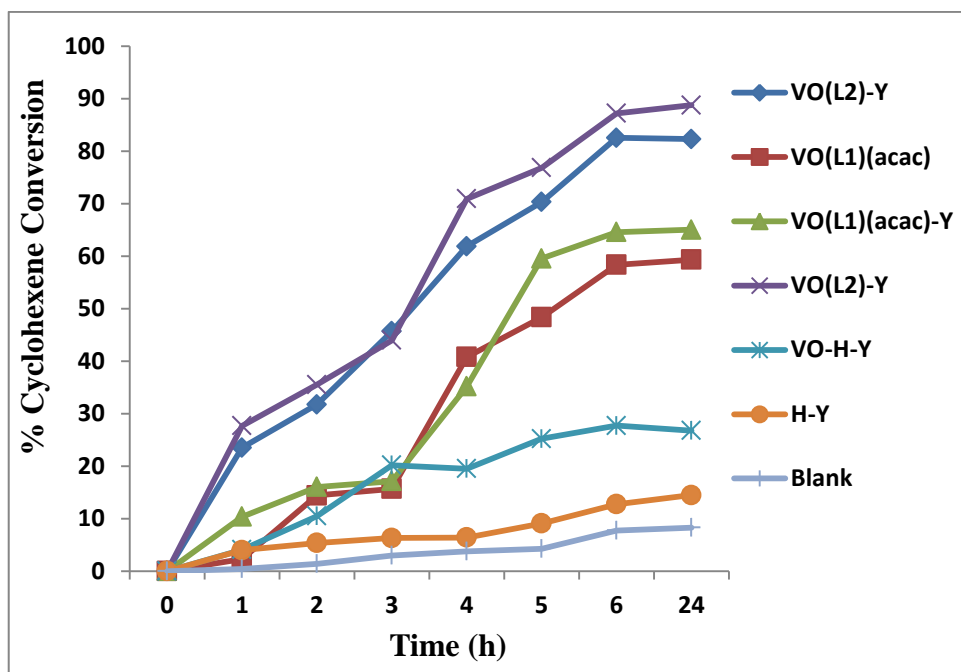


Figure 6.3 Cyclohexene conversion for catalysts over time

Table 6.4 Cyclohexene conversion^a and product selectivity

Catalyst	% Cyclohexene conversion	% Product selectivity				
		CyO	CyOI	CyONE	CydiOI	Other
VO(L1)(acac)	87.23	28.41	46.03	18.74	0.54	6.28
VO(L2)	82.57	28.95	34.62	24.39	1.29	10.75
VO(L1)(acac)-Y	64.59	25.44	24.77	48.29	1.65	0.15
VO(L2)-Y	58.38	32.63	26.22	35.15	6.00	-
VO-H-Y	27.73	25.44	24.77	48.29	1.65	0.15
H-Y	10.30	39.91	12.87	16.47	6.05	24.70
Blank	7.76	33.06	20.10	8.85	2.85	35.14

^a Reaction conditions : Cyclohexene 2.06 g, H₂O₂ 2.83 g, catalyst 0.010 g, Solvent 3 ml, 70°C

References

- [1] Rehder D., The coordination chemistry of vanadium as related to its biological functions, *Coord Chem Rev* 182 (1999) 297-322.
- [2] Ligtenbarg A.G.F, Hage R., Feringa B.L, Catalytic oxidations by vanadium complexes, *Coord Chem Rev* 237 (2003) 89-101.
- [3] Sakurai H., Kojima Y., Yoshikawa Y., Kawabe K., Yasui H., Antidiabetic vanadium(IV) and zinc(II) complexes, *Coord Chem Rev* 226 (2002) 187–198.
- [4] Rehder D., Santoni G., Licini G.M, Schulzke C., Meier B., The medicinal and catalytic potential of model complexes of vanadate-dependent haloperoxidases, *Coord Chem Rev* 237 (2003) 53-63.
- [5] Thompson K.H., Orvig C., Coordination chemistry of vanadium in metallo-pharmaceutical candidate compounds, *Coord Chem Rev* 219-221 (2001) 1033-1053.
- [6] Tsuchida E., Oyaizu K., Oxovanadium(III–V) mononuclear complexes and their linear assemblies bearing tetradentate Schiff base ligands: structure and reactivity as multielectron redox catalysts, *Coord Chem Rev* 237 (2003) 213–228.
- [7] Kojima M., Taguchi H., Tsuchimoto M., Nakajima K., Tetradentate Schiff base–oxovanadium(IV) complexes: structures and reactivities in the solid state, *Coord Chem Rev* 237 (2003) 183–196.
- [8] Maurya M.R., Development of the coordination chemistry of vanadium through bis(acetylacetonato)oxovanadium(IV): synthesis, reactivity and structural aspects, *Coord Chem Rev* 237 (2003) 163–181.
- [9] Ma N., Ma Z., Yue Y., Gao Z., Reaction testing of phenol hydroxylation and cyclohexane oxidation by gas chromatography: influence of residual hydrogen peroxide, *J Mol Catal A: Chem* 184 (2002) 361 – 370.
- [10] Xavier K.O., Chacko J., Mohammed Yusuff K.K., Zeolite-encapsulated Co(II), Ni(II) and Cu(II) complexes as catalysts for partial oxidation of benzyl alcohol and ethylbenzene, *Appl Catal A: Gen* 258 (2004) 257.
- [11] Chen P., Fan B., Song M., Jin C., Ma J., Li R., Zeolite-encapsulated Ru(III) tetrahydro-Schiff base complex: An efficient heterogeneous catalyst for the hydrogenation of benzene under mild conditions, *Catal Commun* 7 (2006) 971.

- [12] Kuz'niarska-Biernacka I., Fonseca A. M., Neves I.C., Manganese complexes with triazenido ligands encapsulated in NaY zeolite as heterogeneous catalysts, *Inorg Chim Acta* 394 (2013) 595.
- [13] Fan B., Li H., Fan W., Jin C., Li R., Oxidation of cyclohexane over iron and copper salen complexes simultaneously encapsulated in zeolite Y, *Appl Catal A: Gen* 340 (2008) 67–75.
- [14] Salvati-Niasari M., Ganjali M.R, Norouza P., Host (nanopores of zeolite Y) guest (oxovanadium (IV) tetradentate schiff-base complexes) nanocomposite materials: synthesis, characterization and liquid phase hydroxylation of phenol with hydrogen peroxide, *J Porous Mater* 14 (2007) 431.
- [15] Maurya M. R., Kumar M., Kumar U., Polymer-anchored vanadium(IV), molybdenum(VI) and copper(II) complexes of bidentate ligand as catalyst for the liquid phase oxidation of organic substrates, *J Mol Catal A: Chem* 273 (2007) 140.
- [16] Kuz'niarska-Biernacka I., Biernacki K., Magalhães A.L, Fonseca A.M., Catalytic behavior of 1-(2-pyridylazo)-2-naphthol transition metal complexes encapsulated in Y zeolite, *J Catal* 278 (2011) 102–110
- [17] Maurya M.R., Chandrakar A.K., Chand S., Oxovanadium(IV) and copper(II) complexes of 1,2-diaminocyclohexane based ligand encapsulated in zeolite-Y for the catalytic oxidation of styrene, cyclohexene and cyclohexane, *J Mol Catal A: Chem* 270 (2007) 234.

CHAPTER 7

7. CONCLUSION AND RECOMMENDATIONS

7.1 Conclusion

In this work, the encapsulation of copper(II) and oxovanadium(IV) complexes in zeolite-Y supercages was successful. The complexes derived from the ligands, L1 and L2 derived from acetylacetonate and ethylene diamine in 1:1 and 2:1 molar ratios, respectively were synthesized and their structures established by various physico-chemical techniques. FT-IR and XRD confirmed that the zeolite framework was not affected upon encapsulation of the complex inside the zeolite cage. With the development of these complexes their catalytic activity and selectivity for various oxidation reactions was demonstrated. Results allowed one to conclude that these catalysts were successfully synthesised for oxidation reactions of, benzene, phenol, cyclohexene and styrene. The homogeneous catalysts proved to be more favourable with higher conversions with shorter reaction times than the heterogeneous catalysts. However, the high selectivity and stability of encapsulated catalysts make them more feasible for the industry. In this study it was found that the differences associated with the use of bulky substrates by zeolite encapsulated complexes are rather unfavourable giving poor catalytic activity. This can be ascribed to a large extent as being caused by shape selective effects in zeolite pores making diffusion of larger substrates through the zeolite pores difficult. Therefore, the smaller cyclohexene molecules exhibited higher conversion rates as compared to bulkier styrene molecules. In general, the oxovanadium(IV) encapsulated and neat catalytic systems were more active than the corresponding copper-based systems. The activity of the encapsulated complexes was only improved over longer reaction time.

The activity of the oxovanadium based catalysts is as follows: $VO(L1)(acac) > VO(L2) > VO(L1)(acac)-Y > VO(L2)-Y > VO-H-Y > H-Y$ counterparts. While the activity of copper based catalysts follow the order: $Cu(L1)Cl > Cu(L2) > Cu(L1)Cl-Y > Cu(L2)-Y$.

Although homogeneous catalysts gave higher activity, in certain cases there were only small differences in catalytic activity for specific reactions between homogeneous and heterogeneous catalysts thus showing the potential activity of the heterogeneous catalysts. The possible reaction pathway of the catalysts in the oxidation reactions was determined

by UV-vis spectroscopy studies of the neat complexes which proved the generation of peroxovanadium(IV) or hydroperoxide-copper(II) intermediate species. These intermediates were found to be the active species for the various catalytic oxidation reactions responsible for transfer of oxygen atom to the substrates. This finding explains the reaction mechanism in free metal and zeolite encapsulated complexes.

7.2 Future work and recommendations

The future work is to investigate the effect of different β -diketones with electron withdrawing or electron rich groups on the catalyst activity. This will be a step towards understanding how certain substituents influence the catalytic activity and selectivity. The study can be extended using different metals to study the effect of the active sites on the catalytic activity. Also the catalysts prepared in this study could be tested for other important oxidation reactions, such as benzoin and methyl phenyl sulphide oxidation reactions.

